Sediment Pathways in San Francisco South Bay

Michelle Gostic

TU Delft

SFEI AQUATIC SCIENCE CENTER
SAN FRANCISCO ESTUARY INSTITUTE & THE AQUATIC SCIENCE CENTER

Deltares
Enabling Delta Life

UNESCO-IHE
Institute for Water Education

USGS
science for a changing world

CoMEM

Front cover: San Joaquin and Sacramento rivers deliver large pulse of sediment to San Francisco Bay [Image courtesy of NASA Earth Observatory].

Back cover: High-resolution digital elevation model of the Sacramento-San Joaquin River Delta and San Francisco Bay created by USGS and the California Department of Water Resources [see Fregoso et al. (2017)].

Sediment Pathways in San Francisco South Bay

by

Michelle Gostic

as a requirement to attend the degree of:

Master of Science
Coastal & Marine Engineering and Management

CoMEM

Erasmus+: Erasmus Mundus Mobility Programme

Taught at the following educational institutions:

Norges Teknisk- Naturvitenskapelige Universitet (NTNU)
Trondheim, Norway

Technische Universiteit Delft (TU Delft)
Delft, The Netherlands

University of Southampton
Southampton, United Kingdom

at which the student has studied from August 2016 to July 2018

to be defended publicly on Tuesday July 16, 2018 at 10:30 AM
at the Delft University of Technology

under supervision of:	Prof. dr. ir. W. S. J. Uijttewaal,	TU Delft
	Dr. ir. M. van der Wegen,	Deltares; UNESCO IHE
	Dr. ir. B. C. van Prooijen,	TU Delft
	Dr. ir. D. J. R. Walstra,	Deltares
	Ir. S. G. Pearson,	TU Delft; Deltares

An electronic version of this thesis is available at http://repository.tudelft.nl/.

UNESCO-IHE Institute for Water Education · TU Delft Delft University of Technology · SFEI San Francisco Estuary Institute & the Aquatic Science Center · Aquatic Science Center · Deltares Enabling Delta Life · USGS science for a changing world

The Erasmus+: Erasmus Mundus MSc in Coastal and Marine Engineering and Management is an integrated programme including mobility organized by five European partner institutions, coordinated by Norwegian University of Science and Technology (NTNU).

The joint study programme of 120 ECTS credits (two years full-time) has been obtained at two or three of the five CoMEM partner institutions:

- Norges Teknisk- Naturvitenskapelige Universitet (NTNU), Trondheim, Norway
- Technische Universiteit (TU), Delft, The Netherlands
- Universitat Politècnica de Catalunya (UPC) BarcelonaTech, Barcelona, Spain
- University of Southampton, Southampton, Great Britain
- City University London, London, Great Britain

During the first three semesters of the programme, students study at two or three different universities depending on their track of study. In the fourth and final semester an MSc project and thesis has to be completed. The two-year CoMEM programme leads to a multiple set of officially recognized MSc diploma certificates. These will be issued by the universities that have been attended by the student. The transcripts issued with the MSc Diploma Certificate of each university include grades/marks and credits for each subject.

Information regarding the CoMEM programme can be obtained from the programme coordinator:

Øivind A. Arntsen, Dr. ing.
Associate Professor in Marine Civil Engineering
Department of Civil and Transport Engineering
NTNU Norway
Mob: +4792650455 Fax: + 4773597021
Email: oivind.arntsen@ntnu.no

CoMEM URL: https://www.ntnu.edu/studies/mscomem

Acknowledgements

This thesis reflects the knowledge and skills I've developed over the past two years in pursuit of a Master of Science degree in Coastal and Marine Engineering and Management (CoMEM), and it would not be complete without acknowledging all of the people whose support I have to owe for this achievement.

To start, I want to thank the CoMEM founders and current administrators for creating this opportunity and for continually fighting to sustain and improve such an incredible program. Øivind and Sonja- thanks for making us feel at home in Trondheim and for your continued support over the last two years.

I would like to thank my thesis committee - Wim Uittewaal, Mick Van der Wegen, Dirk-Jan Walstra, Bram van Prooijen, and Stuart Pearson - for your insightful comments and thoughtful feedback over the past five months. Mick - thanks for taking me on as a student despite my restricted timeline and for your patience and guidance as my supervisor. Most of all, thanks for always asking if I was "having fun."

Stuart - thanks for the constant support and encouragement (on thesis-related topics and otherwise). I am stunned by your mental library of publications and feel lucky to have had access to it. Thanks for being so willing to share your codes, templates, and new ideas. Your enthusiasm is contagious. I would also like to thank Ermano de Almeida and Irene Rivera Arreba for their encouragement and technical support while getting started with LaTex.

To Deltares staff - I am endlessly grateful for the opportunity to work in such a positive and inspiring environment. Thanks for being so welcoming to myself and other students. A special thanks to Arjen Markus for being incredibly generous with his time and for helping me to learn and work with DELWAQ. This project would not have been possible without your clear and thorough explanations and help tackling DELWAQ-related challenges. I would also like to thank Thijs van Kessel, Fernanda Achete, and Katherine Cronin for their help understanding and implementing the buffer layer concept in DELWAQ.

My experience at Deltares would not have been the same without my fellow students. I will sincerely miss keeping up with the coot drama (by the way, have you seen Jaime?), and seeing your bright smiling faces every day.

To my fellow CoMEMbers - you. guys. are. the. best. My appreciation for your friendship and support goes well beyond what I can write here, and I feel incredibly lucky and humbled to have shared the past two years with such passionate, caring, smart, beautiful, and interesting people. I am better for having known each one of you, and I really look forward to seeing what wonderful things you all go on to accomplish. Cheers to seeing you all very soon.

Lastly, none of this would have been possible without the love and support of my friends and family back home, who encouraged me to embark on this adventure. Mom and Dad, thanks for your unwavering support as I decided to move an ocean away and for instilling in me a love for science and an appreciation for the natural world. With these gifts, there will always be something new to explore.

Michelle Gostic
Delft, July 2018

Executive Summary

San Francisco Bay is the largest estuary on the west coast, and it supports a surrounding population of over 7 million people. Human developments have reduced the amount of fine sediments delivered to the Bay-Delta system in recent years, which threatens habitat restoration initiatives and suitable water quality in the southern reach of the Bay (South Bay), where an ample supply of fine sediments is needed to support tidal flat development and to maintain conditions that limit the excessive growth of algae populations. A better understanding of how sediments enter and are redistributed within South Bay is needed to anticipate how the dynamics and supply of fine sediments will change under future conditions.

In this study, a pair of process-based numerical models was applied to investigate fine sediment pathways in San Francisco Bay. An offline coupling between a DELWAQ water quality model and a Delft3D FM hydrodynamics model provides an efficient method to study suspended sediment transport in large, complex systems. The DELWAQ model was forced with high frequency river discharge and suspended sediments data at the primary river boundaries, and the initial sediment condition was determined through a Bed Composition Generation (BCG) simulation. A buffer layer bed model was implemented to describe deposition and resuspension, and the model was calibrated using measured suspended sediment concentration data.

The DELWAQ model was applied to various hydrodynamic scenarios to better understand the effects of wind, density-driven flows, and freshwater discharge on sediment dynamics in San Francisco Bay. The results suggest that sediment import and export at the mouth of South Bay is linked to density-driven circulation induced by horizontal salinity gradients between South Bay and Central Bay. During years with particularly high volumes of freshwater discharge from the Sacramento and San Joaquin Rivers, South Bay is more likely to import sediments, and extreme pulses of freshwater were shown to enhance sediment connectivity between North Bay and South Bay. Sediment exchange between the channel and the flats in South Bay is facilitated by the tide, and wind wave resuspension influences the magnitude of sediment fluxes into and within the southern reach.

This study advances our understanding of sediment dynamics in the complex San Francisco Bay estuary. With further validation, the DELWAQ model developed in this research can be used as a tool to predict system response to future conditions brought on by climate change and human-induced alterations to the watershed. Large-scale management decisions regarding the Bay Area and the Central Valley could alter the long-term trajectory of the estuary and determine whether it will maintain ecological viability while adapting to changing hydrodynamic and environmental conditions. Insights learned from sediment transport modelling can adequately capacitate the Bay's leadership as well as countless population-dense estuaries around the world confronting analogous challenges.

Preface

For over a decade, the US Geological Survey and Deltares have been collaborating to better understand how the Sacramento-San Joaquin Bay-Delta system will respond to changing conditions brought on by climate change as part of the CASCaDE (Computational Assessments of Scenarios of Change for the Delta Ecosystem) Project. Of special concern was the impact of potential climate scenarios on ecosystem functions and water quality. The CASCaDE project has nominally ended, but the research and exploration into the San Francisco Bay system provided a strong foundation for continued research. The San Francisco Estuary Institute, interested in understanding the controlling factors of water quality and phytoplankton blooms, became invested in suspended sediments modelling initiatives that were part of the Deltares-USGS partnership. This study is motivated by the goals of the Deltares-USGS-SFEI collaboration and advances the development of a sediment transport model of San Francisco Bay.

The hydrodynamic San Francisco Bay-Delta community model, which was developed with contributions from UNESCO-IHE, USGS, Deltares, California Landscape Conservation Cooperative, San Diego Supercomptuer Center, Berkeley University of California, SFEI, and Stanford University is open source and available at: http://www.d3d-baydelta.org/.

List of Figures

List of Tables

List of Abbreviations

Abbreviation	Description
ATF	Aquatic Transfer Facility
D-FLOW	Flow engine of Delft3D FM Suite, compatible with Delta Shell framework
DELWAQ	D-Water Quality engine of Delft 3D FM Suite, compatible with Delta Shell framework
DEM	digital elevation model
DMB	Dumbarton Bridge
EPS	extracellular polymeric substances
FM	flexible mesh
g	gram
GHG	greenhouse gas
IPCC	Intergovernmental Panel on Climate Change
kg	kilogram
kT	kiloton (equivalent to $1x10^9$ grams)
LLS	local land subsidence
m	meter
Mg	megagram
MSL	mean sea level
NB	North Bay
Pa	pascals
Q_{Delta}	Delta discharge; combined discharge from Sacramento & San Joaquin Rivers
RCP	representative concentration pathway (GHG concentration trajectory adopted by IPCC)
RMSE	root mean square error
rSLR	relative sea level rise
s	second
SB	South Bay
SFB	San Francisco Bay
SFEI	San Francisco Estuary Institute
SFSB	San Francisco South Bay
SLR	sea level rise
SMB	San Mateo Bridge
SPM	suspended particulate matter
SSC	suspended sediment concentration
SSF	suspended sediment flux
USGS	United States Geological Survey
WQ	water quality
WWTP	waste water treatment plants
WY	water year

Contents

1

Introduction

Estuaries are coastal areas where freshwater draining from inland watersheds meets the sea. Receiving inputs from both marine and riverine sources, estuaries provide unique and valuable habitat for a diverse assemblage of plant and animal populations that thrive in such dynamic conditions. Many estuaries are highly developed and subject to anthropogenic pressures that have significant impacts on a system's hydrodynamics and ecological health. Suspended sediment is an important ecological indicator in estuaries, and the net transport of fine material serves as a proxy for the fate and transport of many harmful pollutants. An ample supply of fine sediment is needed to maintain tidal flat elevations that sustain intertidal communities and provide natural forms of flood protection and storm mitigation. SFB is one of many estuaries subject to high levels of anthropogenic influence, and human activity has shaped its evolution over the past 150 years. The southern reach of the bay (South Bay) is susceptible to water quality issues due to elevated contamination levels from runoff and sewage discharge combined with high water residence times. To properly manage such a densely populated area without threatening the future viability of the system, a thorough understanding of the sediment dynamics in South Bay is needed.

1.1. Motivation

San Francisco Bay (SFB) is the largest estuary on the west coast, and it supports a surrounding population of over 7 million people; by 2040 this number is projected to grow by 30% (Metropolitan Transportation Commission 2017). Human developments in the Bay Area and throughout the SFB watershed influence the amount of sediment delivered to the system, thus threatening the estuary's ecological health and shaping its morphological development.

1.1.1. Fine Sediments in San Francisco Bay

Each year rivers deliver 2.28 million metric tons of suspended fine sediment to SFB (McKee et al. 2013). These sediments provide material needed to maintain saltmarsh elevations, enabling the viability of valuable intertidal habitats. Alternatively, sediment can settle in harbours and navigation channels, requiring expensive and environmentally disruptive dredging operations. Approximately 20 million USD of cargo is handled by San Francisco ports annually, and between 1995 and 2002 an average of 3.1 million m^3 of sediment was dredged from navigation channels annually (Barnard et al. 2013, Mckee et al. 2006). A better understanding of the forces governing sediment transport can inform more educated decisions regarding sediment management on a system-wide scale, providing opportunities to work together with natural processes to strategically deliver sediment to targeted (e.g. wetland restoration) areas. Changing climate and regional weather patterns are likely to alter the hydrodynamics of estuaries, which raises important questions about how these systems will respond. A deeper knowledge of the forces driving sediment transport is essential to predicting how estuaries will react to future changes in water levels, sediment supplies, and weather patterns.

Figure 1.1: An overview of SFB. The estuary can be discretized into two distinct sub-embayments: North Bay, extending from the Golden Gate up to the confluence of the San Joaquin and Sacramento Rivers, and South Bay, extending south from Oakland Bridge to San Jose. The focus of this study is how sediment enters and is redistributed within the main body of South Bay (between Bay Bridge and Dumbarton Bridge). Most freshwater delivered to the system enters via the Sacramento-San Joaquin River Delta at the northern boundary. Spatial data sources: SFB DEM - Fregoso et al. (2017); Central Pacific DEM - National Geophysical Data Center (2003); WWTP locations - Heberger et al. (2009).

1.1.2. Water Quality

San Francisco Bay consists of two sub-embayments - North Bay and South Bay - which are characterized by distinct hydrodynamic forcings. North Bay receives large inputs of freshwater from the Sacramento and San-Joaquin River systems, which together deliver over 90% of freshwater input to SFB (Conomos et al. 1985). The area where these two rivers converge before draining into the estuary is referred to as the Delta (see Figure 1.1). Unlike North Bay, South Bay lacks a significant freshwater source at its landwards boundary, meaning that it is not flushed as regularly. The longer hydraulic residence time in South Bay leads to water quality issues, which are compounded by the high number of sewage

outfalls from waste water treatment plants that discharge nutrients into South Bay (see Figure 1.1). In dry summer periods, sewage discharge volumes can actually exceed freshwater inputs into South SFB (Conomos 1979). Agricultural and urban runoff, atmospheric deposition, and pesticides applied to control invasive species also contribute to elevated contamination levels in South Bay (Fong et al. 2016).

Fate and Transport of Contaminants

The adsorptive properties of fine sediments makes them particularly effective carriers of contaminants, so the transport and distribution of pollutants is linked to that of fine material. An understanding of trends in sediment transport and SPM dynamics can reveal information about sediment-associated contaminants. Collecting sediment flux and suspended sediment concentration data is often cheaper and easier than directly measuring the transport and concentration of pollutants themselves (Schoellhamer et al. 2007). Of special concern in SFB are Mercury, PCBs, and organichloride pesticides that enter South Bay attached to suspended sediments from the Central Valley (Mckee et al. 2006). If a contaminant-containing particle settles on the bed, the pollutant and its harmful effects are effectively removed from the aquatic system until sufficiently high bed shear stresses re-entrain them in the water column.

The amount of sediment delivered to SFB has been increasingly reduced by the construction of dams, reservoirs, hydroelectric power facilities, and local irrigation systems throughout the watershed (Conomos et al. 1985, Mckee et al. 2006). A continued trend of decreasing sediment supply could offset South Bay's sediment budget, causing erosion and threatening existing tidal flats. Evidence of such a trend has already been observed in South Bay (Foxgrover et al. 2004). Erosion of previously immobile sediments could reintroduce pollutants contained in the benthic layer back into the environment (Mckee et al. 2006). This raises concerns about the potential for legacy contamination from historical hydraulic mining activities to re-enter the SFB system. Harmful byproducts of mining activities, including mercury, made their way to SFB during the California Gold Rush and still pose a threat to human and ecological health (Alpers et al. 2005). Sediment cores extracted in 1990 revealed that 43% of surface material in SFB contained mining debris, suggesting that these sediments remain active in the system (David et al. 2009). For further explanation of the legacy of hydraulic mining activities in the Sierra Nevadas and the impact on SFB, see Section 2.1.1.

Harmful Algae Blooms

Another way that fine sediments impact estuarine water quality is their effect on the aquatic light climate. Suspended sediment concentrations are closely related to turbidity, an important ecological indicator that governs light availability and regulates primary production rates.

High inputs of sewage discharge and runoff combined with a relatively low degree of flushing make South Bay highly susceptible to water quality issues. The nutrient concentrations observed in South Bay are characteristic of eutrophic ecosystems that are typically vulnerable to algae blooms. Algae blooms are known to cause hypoxic conditions, which can result in large-scale die-offs of fish and other aquatic species. However, such bursts of algal growth are not common in South Bay due to historically high turbidity levels. Fine sediment suspended in the water column limits the light penetration depth, which regulates rates of primary productivity and limits the growth of algae populations (Cloern 1987).

The high turbidity levels observed in South Bay are believed to regulate the frequency and magnitude of harmful algae blooms; however, it is unclear whether these turbidity levels will be sustained if the ongoing trend of decreasing sediment loads to SFB continues (Ganju et al. 2008, Krone 1979). Krone (1979) predicted that reduced sediment supply caused by water diversion and other anthropogenic alternations to the SFB watershed would lead to lower turbidity levels, thus increasing the likelihood of harmful phytoplankton blooms in the future. Analysis by Schoellhamer (2011) revealed a 36% step decrease in measured SSC values in SFB between the periods 1991-1998 and 1999-2007, which he associated with a shift towards sediment supply-controlled transport.

1.1.3. Habitat Restoration

Over the last 150 years San Francisco South Bay has lost more than 80% of its tidal marshes due to diking for industrial salt ponds, agriculture, and urbanization (Foxgrover et al. 2004). The South Bay

Salt Pond Restoration Project aims to restore over 15,000 hectares of salt ponds to tidal wetlands. The goals of the initiative are to return saltmarsh habitats to native plant and animal species, to provide wildlife and outdoor recreation opportunities to residents of the bay area, and to contribute to flood management strategies in South Bay (Valoppi 2018). The decreasing trend in SSCs observed by Schoellhamer (2011) threatens tidal marsh restoration in that it increases the time needed to restore vegetation and reduces the likelihood that natural sedimentation will keep pace with sea level rise. Based on a sediment budget constructed by Shellenbarger et al. (2013) between 29-45 million m^3 of sediment is needed to elevate restoration areas to levels needed to support salt marsh vegetation. Foxgrover et al. (2004) found that from 1858 to 1983 South Bay has experienced a net loss of sediment, having undergone both erosional and depositional periods. A better understanding of how much sediment is imported into South Bay and when this import occurs is needed to determine the required balance between natural sedimentation and artificial nourishment to provide an adequate sediment supply for tidal flat development. Further, such knowledge could help to time the dike breachings such that they correspond to periods of net sediment import into South Bay, thus utilizing natural processes to deliver sediment to restoration areas (Shellenbarger et al. 2013).

1.2. Existing Theory

The governing processes causing sediment import into SFSB are not well understood. Conventional wisdom is that sediment enters via the deep channel during periods of high Delta discharge and is redistributed on the shoals by wind waves in the summer (Brand et al. 2010, Carlson & McCulloch 1974, Conomos et al. 1985, Shellenbarger et al. 2013). Water exchange at the mouth of South Bay is driven by the tide and density-driven circulation (Conomos 1979, McCulloch et al. 1970, Pubben 2017), but the degree to which these processes impact residual sediment transport has not been extensively studied.

Figure 1.2: Satellite image of SFB showing a plume of sediments entering the system via the San-Joaquin Sacramento River Delta. [Photo from dredgeresearchcollaborative.org]

Recent research has challenged existing theories about the relative contributions of sediments from far-field (the Delta) and local sources to sediment import in South Bay. McKee et al. (2013) compared the supply of sediment to SFB from the Central Valley to that from the small tributary watersheds surrounding the estuary. The hundreds of small tributaries that drain into the Bay account for only

5% of the total watershed area that feeds the bay and just 7% of the annual freshwater discharge; however, the study found that these local sources provided 61% of the suspended sediment load to SFB. This could be attributed to the opposing effects of anthropogenic impacts in the Central Valley watershed and in the area adjacent to the bay. Approximately 48% of the San-Joaquin-Sacramento Delta watershed is blocked by dams, as shown in Figure 1.3b (Minear 2010). River damming and water diversion throughout the Central Valley watershed have reduced sediment loads delivered to SFB via the Delta, but in the steep local watersheds in the direct vicinity of the estuary, construction and hydromodification activities enhance rather than hamper precipitation-discharge events. With decreasing sediment input from the San Joaquin-Sacramento rivers system and further urbanization of the area surrounding South Bay, the effects of local tributaries on sediment supply and transport in South Bay may become increasingly significant.

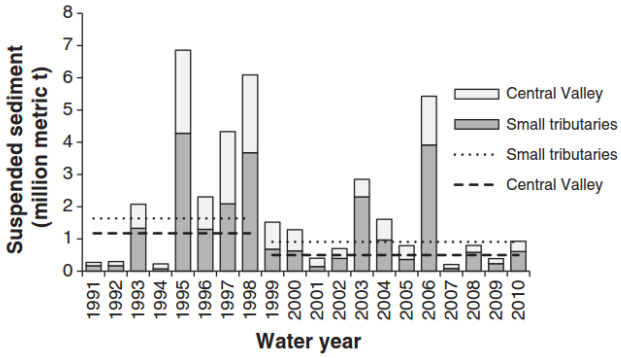

(a) Changes in suspended sediment loads entering SFB from the Sacramento-San Joaquin river system and local tributaries in the Bay Area. Note a change after 1999 following four consecutive wet years. [Image: (McKee et al. 2013)]

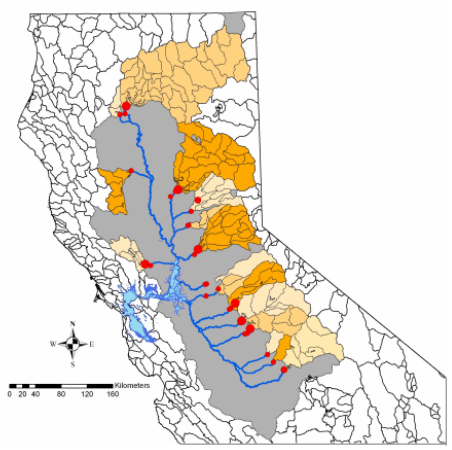

(b) Dammed sections of San Joaquin-Sacramento watershed. Areas shaded with orange and yellow are upstream of dams, and the grey area covers the undammed portion of the watershed. [Image: (Minear 2010)]

Figure 1.3: Recent trends in sediment load delivery to SFB (left), partially due to the damming of rivers draining from the SFB watershed (right).

Shellenbarger et al. (2013) created a sediment budget for San Francisco South Bay based on measured suspended sediment flux crossing system boundaries at the two main tributaries - Guadalupe River and Coyote Creek - and at Dumbarton Narrows (see Figure 1.1). He found that there was a large variability in net sediment import or export at Dumbarton Bridge, which is largely controlled by the highly variable springtime sediment flux. Net zero sediment flux values at Dumbarton Bridge were measured during the summer. He also concluded that peak SSC values were decoupled from peaks in local tributary discharge, indicating that the bulk of sediment contributing to peak SSC values does not come from local tributaries (Shellenbarger et al. 2013).

Along with the processes facilitating sediment import across Bay Bridge, this study concerns the redistribution of sediment within South Bay. Within South Bay, tidal advection, seasonal winds, and density-driven flows influence SSCs and sediment fluxes (Schoellhamer et al. 2007). Half of the variation in SSCs in the channel are attributed to changes in energy associated with the neap-spring tidal cycle. During spring tides, increased resuspension and increased advective transport of highly concentrated shallow water influence the SSC signal. Short slack water periods don't allow for the deposition of all suspended sediments that have been entrained since the previous slack. As a spring tide is approached, the minimum SSC observed over each flood-ebb cycle increases, and as neap is approached, the maximum SSC observed over a tidal cycle decreases. The result is a tidally averaged SSC signal that follows the spring-ebb cycle (Schoellhamer 1996).

Suspended sediment concentrations on the flats are influenced by wind speed (Lacy et al. 1996, Schoell-

hamer 1996). During spring tides, advective transport brings sediments suspended on the shoals due to wind waves into the main channel; this advective transport is less significant during neap tides, resulting in a SSC signal in the channel that is well correlated with seasonal variation in wind shear stress (Schoellhamer 1996). Brand et al. (2010)'s investigation into the driving forces of sediment dynamics on shoals throughout SFB concluded that large sediment fluxes are caused by the nonlinear interaction of wind waves and tidal currents. High SSCs were observed on tidal flats during a flood tide following wave events during ebb. Lacy et al. (1996) reports similar observations of high SSCs during flood due to wave re-suspension on the shoals at low water. During periods of calm wind, Brand et al. (2010) observed higher SSC concentrations during low water.

The literature suggests that sediments enter South Bay during periods of high Delta discharge, and that wind wave resuspension facilitates sediment exchange within South Bay; however, the pathways taken by fine sediments into and within South Bay are not well understood. The goal of this thesis is to develop a model as a tool that can be used to study how sediments are imported and redistributed within South Bay, and to apply the model to determine how these transport pathways change under different conditions.

1.3. Project Scope

As a highly complex and dynamic system, there remains much to be learned about the processes governing sediment transport in South Bay. This section outlines the targeted goals and aims of this research and the steps taken to achieve them.

1.3.1. Goals

This study seeks to answer the following questions:

Research Questions:

1. *What are the processes controlling sediment exchange between South Bay and Central Bay?*
2. *How are sediments redistributed within South Bay, and what processes facilitate sediment exchange between the channels and the shoals?*
3. *What pathways do sediments entering from local tributaries follow, and on what timescales does this occur?*
4. *By which pathways do sediments delivered by the Sacramento and San Joaquin Rivers enter South Bay?*

In which the following are defined:

Sediment - considering only fine sediments

South Bay - stretch of SFB between Oakland Bay Bridge and Dumbarton Bridge

Objectives:
To answer the defined research questions, the following objectives were set:

- Determine the pathways by which sediments from the San-Joaquin and Sacramento Rivers enter South Bay.
- Investigate how density-driven flows, wave resuspension, and tidal asymmetry impact residual sediment transport.
- Assess how sediment transport patterns in South Bay change under different hydrodynamic scenarios.

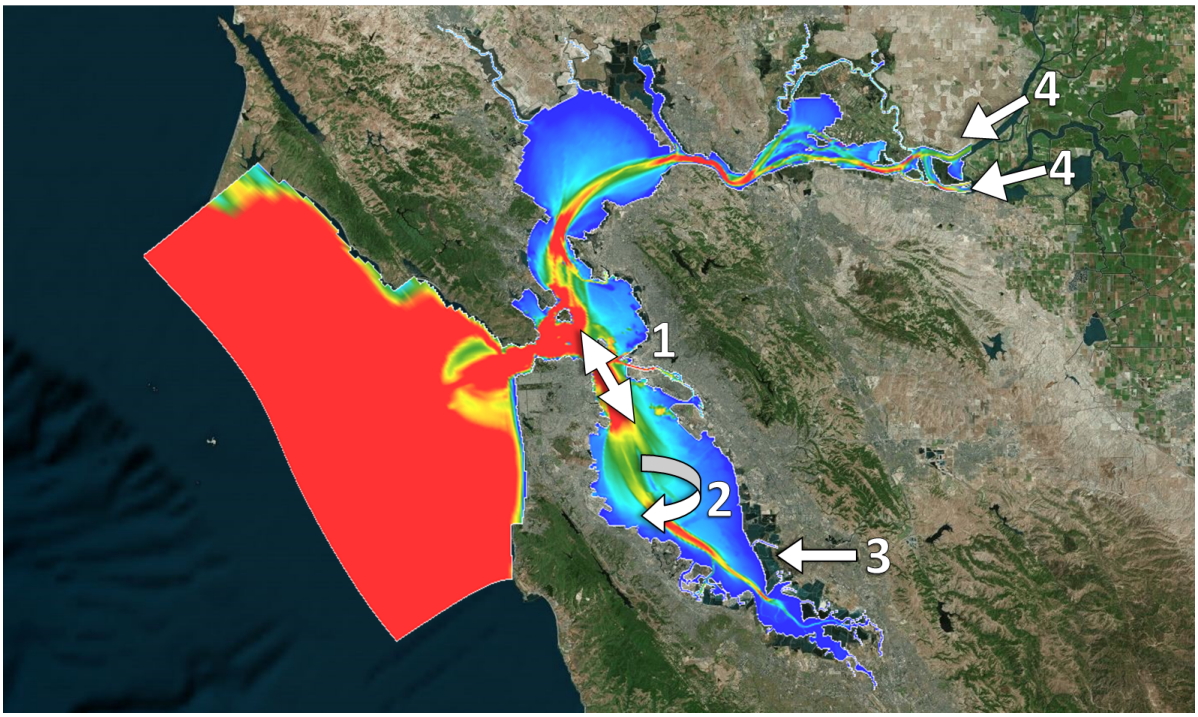

Figure 1.4: Model bathymetry overlaid on satellite imagery of the SFB region. The numbers and arrows correspond to each of the four research questions posed in this section.

1.3.2. Research Approach

Studies based on data measurements and conceptual models have provided valuable insight into sediment transport patterns in South Bay, but the interpretation of these findings is limited to the spatial and temporal range of data available. The application of a 3D numerical model to investigate sediment pathways in South Bay provides an opportunity to examine processes occurring throughout the entire embayment - not only in the areas where data measurements are collected. Further, a numerical model allows for various scenarios and conditions to be explored whether or not they have been observed in reality, providing a tool to predict system response to projected future conditions or large-scale management decisions.

The water quality of South Bay is of special concern due to the high potential of phytoplankton blooms which are believed to be regulated by high turbidity levels (Cloern 1987). Ample fine sediment availability is needed to support tidal habitat restoration projects, especially given recent trends in the decreasing sediment load delivered to SFB. The demand for a better understanding of the sediment dynamics in South Bay has led to recent progress in modelling the hydrodynamics and sediment transport in the southern reach of SFB (Pubben 2017, van Kempen 2017). This study builds upon these developments to further our understanding of sediment pathways in South Bay.

A validated and tested Delft3D Flexible Mesh D-FLOW model describes the hydrodynamics of the South Bay system, including density-driven currents induced by horizontal temperature and salinity gradients (Pubben 2017). An offline coupling of a DELWAQ model with the D-FLOW hydrodynamics allows an efficient way to study sediment transport patterns under different scenarios. Figure 3.1 shows the flow of information between the hydrodynamic and sediment transport models. The DELWAQ model reads in the system hydrodynamics as input and simulates sediment transport based on the bed shear stresses, flow velocities, and vertical dispersion computed in the D-FLOW model.

van Kempen (2017) began to develop a DELWAQ model to observe the effects of wind-induced currents and baroclinic flows on advective and dispersive transport in SFB (van Kempen 2017). The previous model version did not include sediment exchange between the bed and the water column; no sedi-

ments were initialized in the bed, so SFB is represented as a concrete basin. Sediments enter the model through river boundaries. In this model, under calm conditions with low bed shear stresses, particles settle low in the water column but are never deposited on the bed, so near-bed sediment fluxes are overestimated. This study aims to improve the previously existing model by incorporating the vertical exchange of sediments between the bed and the water column. Describing erosional and depositional processes in the DELWAQ model will provide a tool with which the effects of tidal asymmetry and wave resuspension on sediment pathways can be studied. A further description of the D-FLOW and DELWAQ models is provided in chapter 3.

In this study, the DELWAQ model was calibrated and validated for one year representing baseline conditions, and then applied to other hydrodynamic scenarios to evaluate the impact of wind, estuarine circulation, and river discharge on sediment pathways in South Bay.

The following outlines the approach taken to meet the goals and objectives set for study.

PHASE 1

1. Develop DELWAQ model
   - Implement bed model (erosion and resuspension)
   - Define initial sediment condition
   - Calibrate model to determine appropriate & realistic sediment parameters

PHASE 2

2. Sediment tracer analysis
   - Label sediments starting in different areas of SFB and trace their pathways.

3. Apply calibrated DELWAQ model to different hydrodynamic scenarios
   - Turn off baroclinic flows to evalute impact of density-driven circulation.
   - Turn off wind to evaluate impact of wind-induced currents and wave resuspension.
   - Consider wet year to evaluate impact of extreme freshwater discharge rates.

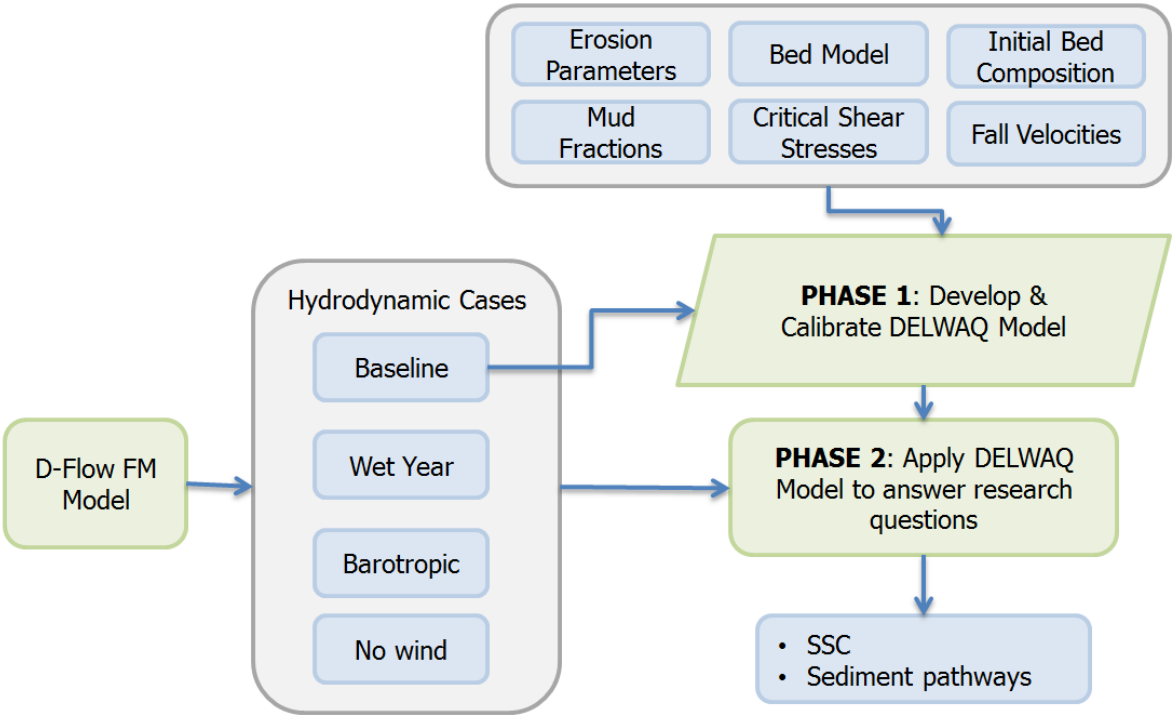

Figure 1.5: Work flow diagram.

2

Background

This chapter provides the information needed to study sediment pathways in SFB. An overview of the processes and environmental conditions that shape the estuary is given in Section 2.1, with special attention to South Bay. In a tidally influenced environment, the net transport of fine sediments is often small compared to the magnitude of sediment fluxes. It is therefore important to properly describe erosion and deposition to simulate and predict sediment transport on a system-wide scale. Relevant theory regarding the physics of cohesive sediments and fine sediment transport is provided in Section 2.2, and the ways that relevant processes are represented in a numerical model are introduced.

2.1. System Overview

To be more conclusive about sediment pathways in South Bay and to achieve the goals outlined in Section 1.3, a comprehensive understanding of the SFB system is needed. Here, the factors shaping the development of the estuary and the dominant processes controlling sediment dynamics throughout the Bay are described.

2.1.1. History

The Bay-Delta system has been subject to human influences since California experienced its first major population boom during the Gold Rush. Moftakhari et al. (2015) estimated that anthropogenic alterations to the SFB watershed are responsible for about 55% of the sediment delivered to the estuary between 1849 and 2011. In the mid 1850's, people rushed to capitalize on lucrative mineral deposits in the Sierra Nevada mountains. Hydraulic mining activities generated lots of loose sediment and debris, which were carried downstream by the Sacramento and San Joaquin rivers and ultimately delivered to the Bay. The rich sediment supply resulted in sedimentation and shoreline progradation throughout the estuary, which saw over 350 million m^3 of net sediment deposition between 1856 and 1887 (Capiella et al. 1999, Foxgrover et al. 2004, Fregoso et al. 2008, Jaffe et al. 2007).

Hydraulic mining ceased after a court case ended the practice in 1884, but since then, anthropogenic activity throughout the watersheds draining into SFB have continued to impact the amount of sediment delivered to the estuary. The construction of dams, reservoirs, hydroelectric power facilities, and local irrigation systems along the major rivers feeding into SFB have lowered freshwater and sediment yields from the Central Valley (Conomos et al. 1985, Mckee et al. 2006). As a result, the fraction of the sediment load contributed by local tributaries compared to that from the Sacramento-San Joaquin Delta has increased over time. The combination of reduced flow and lower sediment supply has resulted in a 50% overall reduction in annual sediment delivery to the bay (Moftakhari et al. 2015). Understanding the impacts of these human-induced fluctuations in sediment supply from far-field and local sources can help to anticipate system response to future changes and inform management and policy decisions.

2.1.2. Geometry

San Francisco Bay is characterized by a channel-shoal morphology in which deep, narrow channels maintained by tidal currents are flanked by shallow mudflats (Conomos et al. 1985). The bay consists

of two sub-embayments with distinct hydrological properties. The northern reach (North Bay) extends from the confluence of the Sacramento and San Joaquin rivers ("The Delta") south to the Golden Gate Bridge. North Bay is about 75km long and contains three smaller embayments (Suisun Bay, San Pablo Bay, and Central Bay) that are separated by narrow straits (Carquinez and San Pablo Straits). North Bay can be characterized as a partially mixed estuary. Ninety percent of freshwater delivered to SFB enters through its northern boundary, the Sacramento-San Joaquin River Delta, and from the south a progressive tidal wave delivers saltwater and provides energy for mixing (Conomos et al. 1985).

South Bay extends from the Oakland Bay Bridge to the southern tip of the estuary at San Jose (though this study focuses on the area between Bay Bridge and Dumbarton Narrows). It was defined by Walters et al. (1985) as a tidally oscaillating lagoon with density-driven exchanges with the northern reach. The average water depth in South Bay is 2.6m with a maximum depth of 20m at mean water tide level (Hager & Schemel 1996). A narrow channel with a depth of 13-15 meters longitudinally traverses the embayment. The channel is bounded on both sides by shallow mudflats of 2-4 m depth. Flow velocities in the channel commonly exceed 1m/s, whereas currents over the shoals are much slower, around 0.4m/s (Brand et al. 2010). The bay is characterized by fine sediments with a mean grain size of 52 μm, and the bed is composed of 75% silt and 25% silt and clay (Cloern & Schraga 2017).

2.1.3. Climate

San Francisco Bay experiences a Mediterranean climate with cool, wet winters and warm, dry summers. The North Pacific high pressure system hovers over California in the summer, thus deflecting storms away and creating dry conditions. Summers in SFB are dominated by westerly/northwesterly winds. Prevailing westerlies are superimposed with local winds generated by pressure gradients caused by the differential heating of land and water masses. Together, this leads to a strong diurnal wind forcing in the summer that can generate wind waves with 2-3 second periods and wave heights exceeding 1m (Conomos 1979).

In the winter, once the high pressure system has migrated south towards the equator, storms bring heavy rain and gale winds (Conomos 1979). These storms can generate winds from the east and southeast, contrary to prevailing wind patterns. Most rainfall in SFB occurs between October and April (Shellenbarger et al. 2013).

2.1.4. Hydrodynamics

As an estuary, South Bay is subject to the effects of both freshwater and saltwater influences. The currents and circulation patterns observed in South Bay are a function of the tide, freshwater inflow, basin geometry, and wind stresses.

Freshwater Inflow

About 90% of freshwater input to SFB is delivered via the Delta, and the remaining 10% enters through over 450 smaller tributaries surrounding the Bay (Conomos 1979, McKee et al. 2013). Freshwater reaches South Bay from far-field sources via its northern boundary and from local sources that drain directly into South Bay. The Sacramento-San Joaquin river systems typically experience two high discharge periods each year - one between December and February due to winter storms and one between March and June due to snowmelt in the Sierras (McCulloch et al. 1970). Local tributaries draining directly into South Bay experience the first discharge peak due to winter storms but are not affected by snowmelt. The three main tributaries delivering freshwater to South Bay are Guadalupe River, Coyote Creek, and Alameda Creek (see Figure 1.1).

In addition to freshwater inputs from The Delta and from local watersheds, wastewater treatment plants contribute freshwater (but no sediments) to the Bay. Although South Bay receives only about 10% of freshwater inputs into SFB, 76% of all wastewater discharged into the estuary enters South Bay. During dry periods, sewage discharge can actually exceed natural inflows into South Bay (Conomos 1979).

Looking ahead, changing precipitation patterns could change the timing and magnitude of freshwater inputs to SFB. Large pulses of freshwater entering through the Delta are likely to come earlier in the

year due to the earlier onset of snowfall and precipitation falling as rain rather than snow (Dettinger et al. 2004, Miller et al. 2004, van Rheenen et al. 2004). Freshwater inputs during the dry season are projected to decline over the next century. These projected changes are likely to result in wetter springs and drier summers in SFB (Grenier & Davis 2010).

Circulation

Currents induced by wind shear stress on the water surface and density gradients due to spatially and temporally varying salinity and temperature fields are superimposed on tidal currents to create the complex 3D circulation patterns observed in South Bay.

Tide

The tide in SFB is characterized as mixed semidiurnal, meaning it experiences two high and two low waters of varying magnitude each day. The tidal wave propagates down through South Bay, and much of the energy is reflected at the southern boundary, resulting in a tidal signal of standing character. The mean tidal range at Golden Gate is 1.7m. Due to the standing nature of the tidal wave, the range increases along the axis of the embayment from 2m at Dumbarton Bridge to 2.6m at the southern tip of South Bay (Conomos 1979, Walters 1982). The horizontal tide (current velocity) leads the vertical tide (water level elevation) by a quarter of a tidal period, so low water slack and high water slack correspond to high and low water. Tidal currents provide energy for mixing in estuarine systems, so the marked spring-neap variations observed in SFB create fortnightly varying currents that are inversely linked to stratification in the water column (Walters et al. 1985).

Unlike in South Bay, the tidal wave in North Bay is progressive. The difference in tidal character between the two reaches of SFB impacts tidally driven exchanges between the northern and southern reach. The phase shift between flow velocity and water level varies in different parts of the Bay, and the progressive tide in the northern reach propagates slower than the standing wave in the southern reach. The result is that water in the southern reach ebbs while water in North Bay floods, and vice versa (Conomos 1979). Aerial observations during a winter storm show a sediment plume from the Delta that moves across Central Bay when North Bay is in the last stages of ebb and South Bay is beginning to flood (Carlson & McCulloch 1974). Understanding these tidal-phase differences is essential to investigating the mechanisms that lead to sediment exchange between North and South Bay.

Wind Shear

When wind blows over a body of water it exerts shear stress on the surface, which can generate waves and initiate currents. The shear force exerted on the surface is proportional to the square of the wind speed (Walters et al. 1985). The extent to which such stresses generate circulation patterns is dependent on wind fetch and bay morphology. Winds in South Bay are strongest during the summer and during winter storms. Due to the configuration of South Bay, the wind direction determines the character of resulting circulation currents. Northerly and northwesterly winds generate wind set-up along the channel, driving a strong return flow. Southeasterly winds generate a strong flow northwards up the channel. If winds from the north, northwest, or southeast are strong enough their effects can dominate tidally driven flows. However, westerly winds flowing normal to the main channel in South Bay are only capable of creating weak return flows across the shoals (Walters et al. 1985).

Density-Driven Flows

Since estuaries receive inputs from both marine and riverine sources, water entering the system varies greatly in terms of salinity and temperature. As the density of water is dependent on these properties, horizontal density gradients are often generated in estuaries in cases where freshwater is discharged at its landward boundary. Denser, more saline water from the sea travels landwards underneath seaward-moving freshwater, inducing a classic gravitational circulation pattern with bottom currents directed landwards and surface currents directed seawards.

Unlike North Bay, South Bay lacks a significant source of freshwater at its head. As a result the water properties in the southern reach are controlled by tidal and density-driven exchanges with

Central Bay. Pubben (2017) found that salinity differences dominate over temperature in determining density gradients in South Bay. The salinity field varies seasonally and is influenced by water exchanges with Delta discharge and the Pacific. Both classic estuarine and reverse estuarine circulation patterns are observed in South Bay throughout the year, and the nature of this circulation is linked to the magnitude of river discharge from the Delta (Conomos 1979, McCulloch et al. 1970, Walters et al. 1985).

Horizontal temperature and salinity differences in South Bay generate density-driven currents, which vary proportionately with density gradients and inversely with the intensity of vertical mixing (Walters et al. 1985).

Near-oceanic salinity values are observed in South Bay during most of the year, but during periods of high Delta discharge, influxes of freshwater lower salinity values in the southern reach of SFB. Salinity values increase in the summer due to higher evaporation rates (brought on by higher wind speeds, temperature, and solar radiation) and lower freshwater discharge volumes. About 120 cm/year of water evaporates from South Bay, which is enough to support industrial salt production. On occasion, the salinity in South Bay can exceed that in the Gulf of the Farallones, seaward of the Golden Gate. (Conomos et al. 1985).

Over the course of year, the salinity field in South Bay can be characterized in one of three ways, each of which is linked to a certain level of Delta discharge. McCulloch et al. (1970) described these three scenarios as idealized periods throughout the year, which are summarized here:

1. Low Delta discharge: June-November; highest salinity values observed in South Bay; reverse estuarine circulation gives way to weaker summer flows driven by tidal and wind forces, and stirring by wind waves creates nearly isohaline conditions (Walters et al. 1985); both South Bay and Central Bay salinities are near oceanic values.

   In this study, low Delta discharge is defined as $Q_{Delta} < 800\ m^3\ s^{-1}$.

2. High Delta discharge: December-February; low salinity in Central Bay. Conomos (1979) reported a time lag of 6 days between peak Delta discharge and minimum salinity observed in Central Bay; South Bay salinity exceeds that in Central Bay, and water exchanges between South Bay and Central Bay dilute South Bay. Results in reverse estuarine circulation pattern with bottom currents directed seawards and surface currents directed landwards.

   In this study, high Delta discharge is defined as $Q_{Delta} > 800\ m^3\ s^{-1}$, and extreme Delta discharge is defined as $Q_{Delta} > 10{,}000\ m^3\ s^{-1}$.

3. Reducing Delta discharge: March-May; increasing salinity in Central Bay; salinity increases in northern end of South Bay resulting in classic estaurine circulation with bottom currents directed landwards and surface currents directed seawards.

   In this study, reducing Delta discharge is defined as the period following high Delta discharge when the horizontal salinity gradient along the longitudinal axis of South Bay exceeds the baseline gradient observed during periods of low Delta discharge.

The direction and magnitude of density-driven circulation has large implications on net sediment transport. As density-driven circulation drives flows in different directions near the surface and near the bed, the sediment concentration profile across the vertical dimension is important to determining the net effect of baroclinic flows.

The strength of density-driven currents is a function of freshwater inflow and the magnitude of vertical mixing. Energy for mixing comes from tidal forces, thus the degree of stratification in South Bay can be linked to the tidal amplitude following a neap-spring cycle (Walters et al. 1985). In the same way that salinity corresponds to Delta discharge, flushing and water quality in South Bay is also linked to freshwater flows from the Sacramento-San Joaquin river system. During periods of large Delta discharge, South Bay experiences a high degree of flushing, with a residence time on the order of 1-2 weeks. During dry periods, the residence time approaches 5 months and water exchange is dominated by wind and tidal mixing (Conomos 1979).

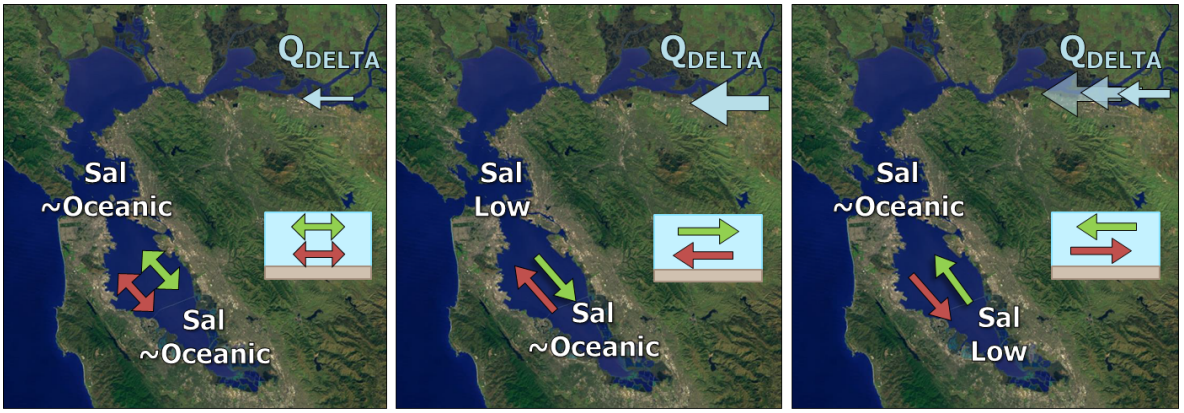

Low Delta Discharge
SB: Well-Mixed

High Delta Discharge
SB: Reverse Estuarine Circulation

Reducing Delta Discharge
SB: Classic Estuarine Circulation

Figure 2.1: Three stages of salinity gradients and induced circulation patterns observed in South Bay. From left to right, these scenarios describe circulation during periods of 1) low Delta discharge, 2) high Delta discharge, and 3) recovery after high Delta discharge.

2.2. Cohesive Sediments

One of the objectives of this study is to examine the effects of tidal asymmetry, baroclinic flows, and wave resuspension on net sediment transport in South Bay using a numerical model. This can only be accomplished by implementing bed exchange in teh model. This section gives an overview of the processes relevant to understanding the vertical exchange of fine sediment between the bed and the water column and the horizontal movement of sediments resulting in net transport.

Fine sediments are composed of particles finer than 63 μm, and exhibit different properties and behavior than non-cohesive sediments. Fine grains are generally plate-like in shape with ionic charges, causing them to have strong cohesive (ability to bond with similar substances) and adhesive (ability to bond with different substances) properties. The degree of charge or attraction of a particle depends on the mineralogy of the source rock from which the sediment originated. Due to their ability to bond with other matter, fine sediments are effective transporters of contaminants and pollutants (Thompson et al. 2017).

The nature of the exchange of sediments between the bed and the water column is fundamentally different for sand and for mud. Non-cohesive sediments will be eroded nearly instantaneously once the bed shear stress exceeds a critical value and deposited once the bed shear stress drops below a critical value (van Maren 2013). The case for fine grains is more complex, since the amount of energy required to entrain a particle is greater than that needed to keep it in suspension (Winterwerp & van Prooijen 2016). Cohesive sediments are subject to a number of processes that together determine whether grains will settle or remain in suspension.

Table 2.1: Sediment characterization based on grain size. Mud is the term used to collectively refer to clay and silt.

Sediment Class	**Min Diameter,** μm	**Max Diameter,** μm
Sand	63	2000
Silt	2	63
Clay	0	2
Mud	0	63

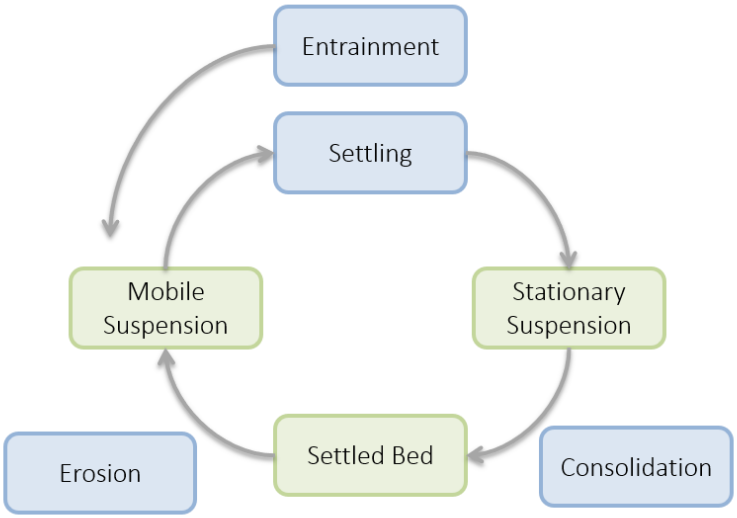

Figure 2.2: The cycle of fine grained sediments. Processes are shown in blue and the resulting states are shown in yellow. [Image: Redrawn from Thompson et al. (2017)]

2.2.1. Bed Exchange

The vertical exchange of fines is governed by the settling velocities of matter in suspension, the nature of the bed, and the hydrodynamic forcings at work (Winterwerp & van Prooijen 2016). Detail into how these factors impact the mechanisms driving the cycle of fine grained sediments is provided here.

Flocculation

Due to their cohesive properties, fine grains in suspension tend to form aggregates, or flocs. Floccules are much larger than individual particles, but their density is much lower due to high water content. Unlike individual grains of mud, which are usually flat, flocs are spherical in shape. Floc size is determined by a balance between break-up and formation and is governed by the Kolmogorov microscale (η), a measure of the size of the smallest dissipating turbulent eddies in a flow. When η is much smaller than the existing flocs, inertial effects dominate, and flocs will break up. Conversely, when η is much larger than existing floc diameters, viscous effects dominate, and floc formation will persist (Thompson et al. 2017). As shown in Equations 2.1 and 2.2, the Kolmogorov microscale is related to shear stress through the rate of energy dissipation. Therefore, changes in shear stress impact the scale of turbulent eddies, which in part controls the nature of floc break-up and dissipation.

$$\eta = \left(\frac{\nu^3}{\varepsilon}\right)^{0.25} \tag{2.1}$$

$$\varepsilon = \frac{U_*^3}{\kappa\delta} \tag{2.2}$$

with:

ν = kinematic viscosity $[m^2 s^{-1}]$

ε = energy dissipation rate $[Nms^{-1}kg^{-1}]$

U_* = friction velocity $[ms^{-1}]$

κ = von Karman's constant (0.41)

δ = boundary layer thickness $[m]$

Floc size is related to the sediment concentration in the water column, in that higher sediment concentrations offer more opportunities for particles to collide and aggregate together. The temperature, pH, and salinity of the surrounding fluid also controls flocculation rates (Thompson et al. 2017). Due to the influence of flow velocity (turbulent stresses), water depth, sediment concentration, and water properties, floc size varies over tidal, spring-neap, and seasonal timescales (Winterwerp & van Prooijen 2016). The complex temporal variation in floc size and the dependence of floc formation on local water properties makes explicitly describing the settling velocity of cohesive sediments difficult.

Settling

The settling velocity of spherical particles is often described by Stoke's law, where the fall velocity is derived from a balance between the drag and gravity forces acting on a grain in a viscous fluid. According to Stoke's law, the speed at which a particle settles towards the bed is a function of the diameter and density of individual grains and the dynamic viscosity and density of the surrounding fluid. Sediment samples providing the size distribution of non-cohesive sediments, therefore, provide information about the sediment fall velocity.

However, determining the fall velocity of cohesive particles is more complicated, due to their tendency to form flocs with distinct properties in the water column. The fall velocity of flocs depends on the size, shape, and density of the floc, sediment concentration, and also on the salinity, temperature, and turbulence of the surrounding water. The settling rate of cohesive sediments is dependent on a number of temporally and spatially varying parameters, and thus is difficult to describe. Floc cameras can directly measure settling velocities in-situ, and LISST devices can be used to measure floc sizes; however floc densities are also needed to describe floc fall velocities accurately (Winterwerp & van Prooijen 2016). In numerical models, the fall velocities of cohesive sediments are often calibrated to determine an appropriate value, because data on floc settling velocity is rarely available, hard to obtain, and only representative of the conditions under which the data was collected.

Bed Development

The sediment-water interface is characterized by layers of individual grains, flocs, and biological matter that increases in density with depth. The structure of the sediment-water interface depends on the sediment composition and the amount of time allowed for settling. As particles settle on the bed, they are subject to consolidation and compaction if hydrodynamic conditions allow time for these processes to occur (Thompson et al. 2017).

Under calm conditions, the bed may progress through a number of stages after new sediments are deposited, the first of which is lutocline development. A lutocline is a horizontal interface near the surface of the bed at which a sharp increase in sediment concentration takes place. The presence of a lutocline promotes the formation of a mobile (fluid) mud layer, which is common when the rate of sedimentation exceeds that of consolidation (Winterwerp & van Prooijen 2016). As the concentration of sediment increases, a non-Newtonian stationary mud layer can form as the mud-fluid mixture builds resistance to shear stresses. Once the bulk density exceeds 1200 kg m^{-3}, the sediment is considered to be part of a deforming cohesive bed. Flocs are compressed and consolidation expels excess pore water. At this stage, elastic behavior is observed; induced stresses result in changes in viscosity in the bed material, but it does not yet exhibit plastic properties. Further consolidation and compaction leads to the formation of a stationary cohesive bed that possesses yield strength and undergoes irreversible deformation (Thompson et al. 2017).

During each of these stages, the bed assumes different properties that determine how it responds to stresses. In this way, the local critical threshold for erosion and sediment resuspenison rates are influenced by the history of bed sediments.

Erosion

Unlike sandy beds, where the threshold of erosion is related to the size of individual grains, the threshold of erosion for muddy beds is linked to the cohesive (shear) strength of the bed. The bulk density of bed material can be used as a proxy for mud or clay content, and generally, the threshold of erosion increases with increasing mud content (Thompson et al. 2017). Bed cohesion typically increases with

depth, and the relationship between the sediment shear strength and depth can be described with Mohr-Coulomb theory. The ratio of the shear stress at a certain depth to the effective strength at a certain depth is constant.

$$tan(\phi) = \frac{\partial \tau_C}{\partial \sigma} = constant \tag{2.3}$$

$$\tau_C(z) = \tau_C(0) + \sigma tan(\phi) \tag{2.4}$$

with:

ϕ = friction angle
τ_C = critical shear stress $[Pa]$
z = depth [m] increasing downwards

The effective stress is defined as the buoyant geostatic and hydrostatic pressures within the sediment column, and accounts for the weight of everything above it, without pore pressure (Thompson et al. 2017).

Wave Resuspension
As waves induce oscillatory motions, the wave boundary layer is thin compared to that generated by a unidirectional current. As a result, the vertical velocity gradient in the wave boundary layer (and thus shear stresses) are large, making waves very effective at stirring up bed sediment ($\tau_b \propto \frac{\partial u}{\partial z}$). Turbulent mixing by waves is limited to the near-bed wave boundary layer. In terms of fine sediment transport, waves re-suspend sediment while currents are responsible for vertical mixing throughout the water column and horizontal transport (Bosboom & Stive 2013, Thompson et al. 2017, Winterwerp & van Prooijen 2016).

Effects of Biology

Plants and animals can enhance or reduce sediment transport rates via bioturbation and biostabilization, respectively. The net impact of biology on sediment dynamics is a balance between effects that increase and those that lower the erosion threshold of the bed. The presence of biologic matter including biofilms (Iglecia et al. 2011, Ketron et al. 2011), diatoms (Cloern et al. 1983), clams (Nichols et al. 1990), benthic invertebrates (Nichols 1985), sea grasses (Zimmerman et al. 1995), and lugworms (Wells 1962) in SFB could influence the sediment dynamics of the system. Table 2.2 provides examples of how biology can contribute to biostabilization and bioturbation.

Table 2.2: Examples of how biological matter influences sediment dynamics (Thompson et al. 2017).

Biological Presence	Impact	Effect
Biofilms	Impact bed cohesiveness and bed roughness	Stabilize
Diatoms & Bacteria	Excrete EPS, increasing sediment cohesion	Stabilize
Mollusks & Cockles	Armor bed and protect it from flow; deposit fecal pellets and aggregates, altering bed roughness	Stabilize/ Destabilize
Anthropods/Benthic Invertebrates	Small animals that burrow and tunnel in sediment; densities can exceed 100,000m^{-2}; birds feed on them and stir up sediment	Destabilize
Sea Grasses	Roots stabilize sediment; leaves alter boundary layer structure	Stabilize
Lugworms	Leave casts on the bed surface, altering bed roughness and boundary layer structure	Stabilize/ Destabilize

Biological matter present on the surface of the bed increases the bed roughness (e.g. lugworm casts). Changes to bed roughness can reduce or enhance transport rates depending on the nature of the interaction between the flow and the bed. In one sense, a higher bed roughness (larger bed forms) lowers transport rates due to the higher friction and drag, which impede flow. However, bed aberrations can also induce turbulent eddies, which stir up sediment resulting in higher transport rates. Biological effects are subject to seasonal variation and vary spatially as well, which makes it difficult to generalize about net impacts on a large scale (Thompson et al. 2017). Investigating the biological factors influencing sediment dynamics in SFB is beyond the scope of this study, but an understanding of the potential effects is necessary to properly interpret in-situ data and fully consider the processes at work in the system.

2.2.2. Net Transport

The transport of mud depends on hydrodynamics, the availability of sediment, and the age of the sediments deposited on the bed (degree of consolidation) (van Maren 2013). The energy required to mobilize cohesive sediments is much larger than that required to keep it in suspension, which means that particles can be transported under calmer conditions than those required to entrain them. Therefore, the concept of a deposition threshold does not hold for fine sediment (Winterwerp & van Prooijen 2016). As a result, in tidally influenced environments, sediment fluxes are often quite large compared to the net excursion observed. The suspended transport of fine sediments can be categorized into that caused by baroclinic and barotropic mechanisms.

Baroclinic Mechanisms

Baroclinic processes are generated by horizontal gradients in water density. The main baroclinic mechanisms causing net suspended transport are gravitational (estuarine) circulation and tidal straining. Varying temperature and salinity fields can cause horizontal density gradients in a basin, thus inducing gravitational circulation patterns. Refer to Section 2.1.4 and Pubben (2017) for a description of density-driven circulation patterns in SFSB.

Gravitional circulation is influenced by a phenomenon known as tidal straining, whereby tidal flows periodically reinforce or destabilize vertical stratification. Considering an estuary with a freshwater source at its landward boundary, stable stratification is the case where freshwater flows seawards over denser saline water flowing landwards, resulting in a classic estuarine circulation pattern. During ebb, this pattern is reinforced by the flow of less saline water seawards towards the mouth. During flood, unstable stratification occurs, whereby saline water flows landwards near the surface. Unstable stratification results in a more mixed, less stratified basin. If stratification during ebb is sufficiently developed, it can dominate the vertical transport of momentum caused by tidal straining, and persistent stratification is observed (Winterwerp & van Prooijen 2016). Mathematically, this pheonomena is described as the covariance of the eddy viscosity and the vertical shear of the longitudinal velocity component of the tide (Burchard & Schuttelaars 2012).

The direction of density-induced currents in estuaries is typically not uniform throughout the water column, thus the vertical sediment distribution is needed to infer net transport fluxes.

Barotropic Mechanisms

In tidally influenced embayments, residual transport is a result of the imbalance between ebb and flood (Gatto et al. 2017). Lag effects, tidal asymmetry, and basin geometry control the magnitude and direction of the net transport of fine sediments. Various barotropic mechanisms that can contribute to the net transport of cohesive material are outlined here.

Velocity Asymmetry

Velocity asymmetry refers to differences between the maximum flood and ebb velocities over the tidal cycle (a skewed tidal velocity signal). Flood dominance and ebb dominance refer to tidal systems with stronger flood and ebb currents, respectively. In general, basins with extensive intertidal flats and deep channels tend to be ebb dominant ($h_{LW} > h_{HW}$), whereas basins with less intertidal area and shallow channels tend to be flood dominant ($h_{HW} > h_{HL}$). In addition to basin geometry, a residual seaward return current can be generated by a progressive tidal wave in the same way that undertow

currents are generated in coastal environments due to Stoke's drift. Such a residual current yields a vertical shift of the horizontal velocity curve, implying that the maximum flood current and maximum ebb current are of different magnitudes (Bosboom & Stive 2013, Gatto et al. 2017). The effect of peak velocity asymmetry is generally associated with non-cohesive sediments that react more instantaneously to changes in flow. Nonetheless, the instantaneous suspended sediment transport rate is related to the velocity cubed, and thus velocity asymmetry does impact the net transport of fine sediments, as shown below:

$$S(t) = Q \cdot C \tag{2.5}$$

$$Q \propto U \tag{2.6}$$

$$C \propto E \propto \tau \propto U^2 \tag{2.7}$$

$$\therefore S(t) \propto U^3 \tag{2.8}$$

with S = sediment transport, Q = volumetric flow velocity, C = sediment concentration, U = flow velocity, E = erosion flux, and τ = bed shear stress (Gatto et al. 2017).

Slack Asymmetry
Slack asymmetry refers to the sawtooth asymmetry of the horizontal tidal signal, which means that high water slack and low water slack are not of the same duration (Bosboom & Stive 2013). Slack asymmetry means that particles have more time to settle at high water than at low water or vice versa, potentially yielding net transport.

Settling Lag
Fine sediments entrained in flow continue to move horizontally once the current velocity drops below a theoretical threshold value for deposition. Settling lag is the residual effect of this horizontal displacement under unbalanced, reversing flows. Once the flow drops below a certain threshold velocity the particle will start to settle down towards the bed. Consider a particle transported from the mouth towards the landwards end of a basin by the tide. Before flow reversal, the velocity drops below the threshold, and the particle begins to settle. As it moves downwards in the water column, it continues to move horizontally such that it hits the bed in a position further landwards than when it started to settle. As a result, the re-entrainment of the particle is delayed; the time between flow reversal and the point at which the flow is strong enough to re-mobilize particles is shorter at the mouth than at the landward boundary, thus flood will induce more transport than ebb. Longitudinal changes in bathymetry and the difference in water depth between flood and ebb tides also impact the horizontal trajectories of particles, thus contributing to settling lag (Bosboom & Stive 2013, Gatto et al. 2017, Pritchard & Hogg 2003, van Maren 2013, van Straaten & van Kuenen 1958).

Threshold lag
If we consider the case where flow velocities are damped longitudinally landwards along a basin, landwards net transport is expected as a result of settling lag. Threshold lag is a mechanism that can enhance this residual transport. With each tidal cycle, settling lag will cause a particle to deposit on the bed further towards the end of the basin. As a result, it will take increasingly longer for the ebb current to mobilize the particle again, thus contributing to further residual landwards transport. If this feedback of settling lag and threshold lag continues, the local velocities may never again exceed the critical velocity to resuspend the particle. van Straaten & van Kuenen (1957) identified this case as final settling lag (Gatto et al. 2017).

Scour lag
Scour lag occurs when the flow velocity needed to mobilize a particle is faster than that below which deposition will occur ($U_{E,crit} > U_{D,crit}$). Under this condition, the entrainment of sediment after flow reversal will be further delayed, contributing to net landwards transport (Pritchard & Hogg 2003, van Straaten & van Kuenen 1958).

Though the specific barotropic mechanisms contributing to net transport were not individually quantified in this study, understanding the potential drivers of tidally-driven transport is important to be able to interpret and explain model results.

2.2.3. Modelling Fine Sediments

In systems dominated by fine sediments, sediment transport depends on (1) fluid dynamics, (2) sediment availability in the water column, and (3) the age of the sediments deposited (van Maren 2013). This chapter explained the main processes controlling vertical sediment exchange and horizontal net transport of mud, but the degree to which these are described in a numerical model depends on model capabilities and the level of complexity needed to produce the intended results.

With respect to fluid dynamics, both the bed shear stresses and the vertical velocity profile need to be described well to model fine sediments (van Maren 2013). In this study, wave and current-induced bed shear stresses and flow velocities are computed in the the hydrodynamics model and 10 vertical layers are resolved. However, due to the offline coupling between the sediments model and the hydrodynamics model, feedback between sediment concentration and fluid behavior cannot be accounted for (see Section 5.1.3, which discusses sediment-density coupling).

Sediment availability in the water column is dependent on the amount of sediments delivered by rivers, bed composition, and the way that deposition and resuspension are defined. Measured sediment loads entering through gauged river boundaries were used to force model boundaries, and a spatially-varying bed composition was initialized in the model, as explained in Section 3.2.6. In reality, varying rates of flocculation and biological matter in the bed influence sediment settling and erosion; however, in this study, these effects are not simulated in the DELWAQ model.

The age of deposited sediments impacts the level of consolidation and cohesive strength of bed material. To model bed consolidation, a very small time step and high vertical resolution is needed (van Maren 2013), so simulating compaction on large spatial and temporal scales is not currently feasible.

Though not all processes at work in reality are implemented in the DELWAQ model, it is important to understand how these effects can influence sediment dynamics to properly interpret comparisons between measured and modelled sediment behavior. If the model is able to describe SPM dynamics and sediment fluxes well enough to answer the given research questions, then resolving additional processes only introduces unnecessary complexity.

The limitations inherent in the DELWAQ model in this study and the potential to simulate additional processes are discussed in Section 5.1.3. The next chapter explains how the dominant forcings shaping the SFB estuary and processes controlling fine sediment dynamics were incorporated into the DELWAQ model setup.

3

Methods

The previous chapter gave an overview of the processes controlling the exchange of sediment between the bed and the water column and the primary mechanisms driving fine sediment transport in an estuarine environment. Investigating these processes on a scale beyond that which is captured by in-situ data is difficult, and numerical models provide a useful tool to achieve a system-wide understanding of sediment dynamics. This chapter explains the advantages of a modelling approach, the set-up of the DELWAQ sediment transport model, and the calibration process.

3.1. Modelling Framework

To efficiently investigate sediment pathways under different hydrodynamic conditions, a sediment transport model was developed to identify patterns and trends on a system-wide scale. Simulating the complex hydrodynamic forcings controlling sediment transport in SFB is computationally expensive, so an offline coupling between a hydrodynamic model (in D-FLOW) and a sediment tracer model (in DELWAQ) was applied, eliminating the need to re-calculate the hydrodynamics for each model run. This section outlines the justification and set-up of the fine sediments model.

3.1.1. Modelling Approach

To understand the sediment dynamics of the SFB system, the complex processes governing the cycle of erosion and deposition (mixing, flocculation, settling, consolidation, compaction) must be considered. Collecting the data necessary to describe these processes is difficult. In-situ data collection requires advanced instrumentation and many measurements are needed to capture spatial and temporal heterogeneity, making such campaigns expensive and labor-intensive. Laboratory experiments offer opportunities to study small-scale processes in a more controlled environment, but often the extraction of sediment from its natural environment changes its properties (Brand et al. 2015). Numerical models, however, serve as a valuable tool to study sediment dynamics on a system-wide scale and can resolve patterns that are indiscernible with in-situ data alone. As a result of past and ongoing initiatives to better understand the SFB system, a wealth of data has been collected, which can be used to calibrate and validate numerical simulations. The application of a validated model to explore scenarios that have not been observed in reality provides a heightened level of system understanding and an ability to predict system response to a wide range of conditions.

3.1.2. Choice of Model: DELWAQ

This study investigates sediment pathways for a given bathymetry, thus obviating the need to simulate morphodynamics and making DELWAQ a suitable choice. Pubben (2017) calibrated and validated a Delft3D FM hydrodynamic model of SFB that captures the complex 3D density-driven circulation patterns observed in South Bay. The output from the D-FLOW model can be used for an offline coupling with a DELWAQ simulation, so the complex 3D hydrodynamics do not need to be re-calculated for each simulation. This reduces the computational run time significantly. To simulate a 14-month period (one year of interest precluded by two months of hydrodynamic spin-up), the D-FLOW simulation takes approximately 10 days to run, while the DELWAQ sediments model developed in this study only takes

11 hours. As described in Section 1.1.2, fine sediments have major implications on water quality, and the use of DELWAQ to simulate suspended sediment dynamics provides opportunities to link calculated SPM fields and transport pathways to other water quality modelling initiatives in the SFB region.

3.1.3. D-FLOW/DELWAQ Coupling

In DELWAQ, the transport of mud is numerically described by solving the advection-diffusion equation with erosion and deposition as bed boundary conditions (Deltares 2017, van Maren 2013). For each computational volume, the D-FLOW model computes time-dependent hydrodynamics (including water levels, flow velocities, and vertical dispersion), salinity, and temperature. The bed shear stresses are also calculated based on hydrodynamic forcings during the D-FLOW simulation. In the case of a D-FLOW/DELWAQ coupling, the output from Pubben (2017)'s hydrodynamic model is used to solve the 3D advection-diffucion equation for fine sediments in DELWAQ, and the bed shear stresses are used to calculate erosion and deposition fluxes (Achete et al. 2015, Deltares 2016*b*, 2017). The erosion rate and suspended sediment concentration scales directly with the bed shear stress, so it is important that the shear stresses are accurately described in the model. Validation of the calculation of bed shear stresses by the D-FLOW model was performed by van Kempen (2017), and the methods by which the magnitude of the stresses were calculated are described in Appendix A.

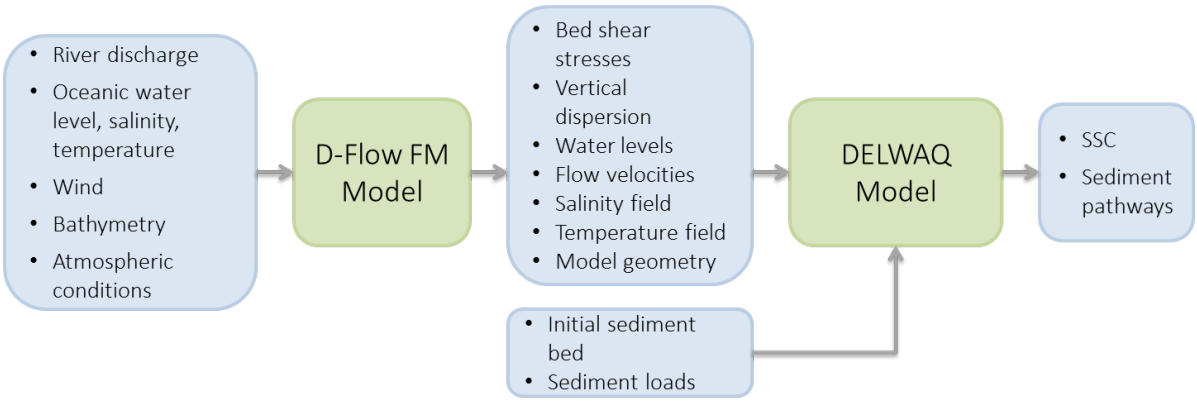

Figure 3.1: Diagram showing flow of information between coupled D-FLOW and DELWAQ models.

3.2. DELWAQ Model Set-Up

The remainder of this chapter describes the set-up and calibration of the DELWAQ sediment transport model.

3.2.1. Simulation Time

The hydrodynamics forcing the sediment tracer model come from a D-FLOW model that was calibrated and validated for WY 2013 by Pubben (2017) and adjusted to model WY 2015 (October 1, 2014 - September 30, 2015) by van Kempen (2017). Output from the D-FLOW model simulates one year following a 2 month spin-up period, for a total of 14 months (August 2014-October 2015). All DELWAQ simulations began two months after the start date of the D-FLOW simulation to ensure that results were not skewed by the hydrodynamic spin-up period. Based on data availability and observed hydrodynamic conditions, WY 2015 was chosen as a baseline year to develop and calibrate the DELWAQ model. Sacramento and San-Joaquin River discharge and SSCs from WY 2017 were implemented to observe how the system responds to high Delta discharge (van Kempen 2017). The hydrographs showing the differences in Delta discharge between WY 2015 and WY 2017 are shown in Figure 3.2. In northern California, the winter of 2017 remains the wettest in recorded history (Downing-Kunz et al. 2017). Further descriptions of the different hydrodynamic scenarios to which the model was applied are given in Section 4.1.2.

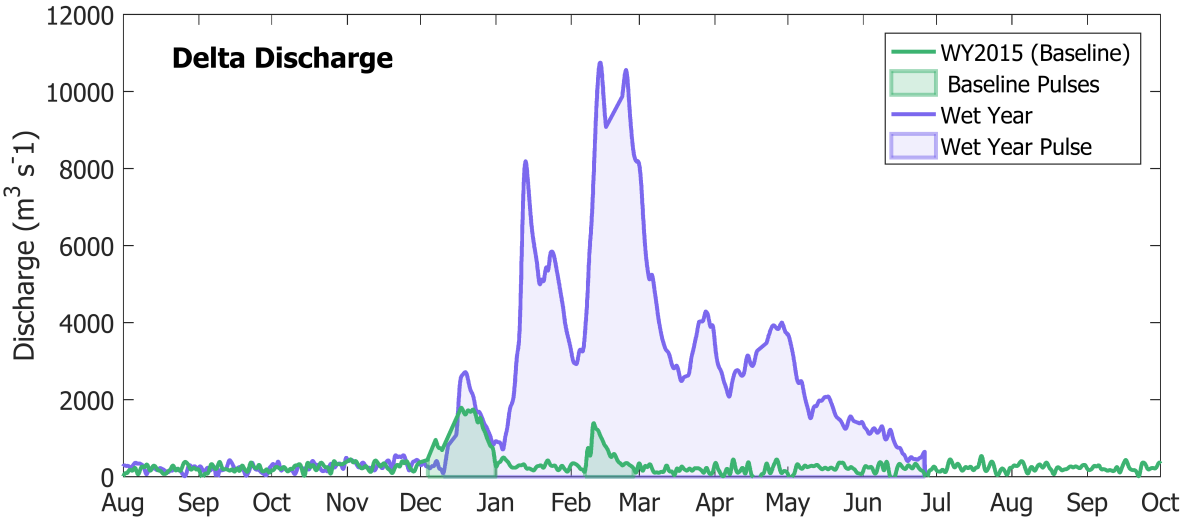

Figure 3.2: Rate of combined discharge from the San-Joaquin and Sacramento rivers entering the SFB estuary through its northern boundary. During the baseline year two periods of high Delta discharge deliver pulses of freshwater to the system in December and February. During the wet year, the period of high delta discharge lasts from December through June, with pulses of extreme discharge rates observed in February and March.

3.2.2. Hydrodynamics

The water levels, flow velocities, vertical dispersion, temperature, salinity, and bed shear stresses calculated for each computational volume and each timestep are fed into DELWAQ as output from the D-FLOW model. The hydrodynamic model accounts for the seasonally varying 3D density-induced circulation that is described in Section 2.1.4. At river boundaries, it is forced with measured discharge rates superimposed on the corresponding tidal signal. Waves are calculated in the D-FLOW model based on wind speed and fetch and water depth. The bottom roughness in the hydrodynamic model was represented by a constant Manning Coefficient. The wind field is determined based on hourly data from wind stations throughout the study area and interpolated onto a regular grid using a Wind on Critical Surface Streamlines (WOCCS) model (Pubben 2017). For further information about the set-up of the hydrodynamic model, the reader is directed to Pubben (2017) and van Kempen (2017).

3.2.3. Geometry

The unstructured, 3D model grid consists of 10 σ-layers and 51,640 segments per layer, making for a total of 516,400 computational volumes. Each σ-layer represents 10% of the water depth, rather than a fixed distance above the bed; this is important to bear in mind while interpreting modelled SSCs linked to a specific vertical layer. The spatial resolution varies over the domain, with coarser rectangular cells covering the ocean area and most of the primary channel, and finer less regular cells covering the flats and tributaries. The bathymetry is courtesy of SFEI and UNESCO-IHE (van Kempen 2017). The domain contains North Bay (Suisun Bay, Carquinez Strait, San Pablo Bay, and San Rafael Bay), Central Bay, and South Bay.

3.2.4. Boundary Conditions

Freshwater enters the model through five river boundaries. At the northeastern boundary, the San Joaquin and Sacramento rivers discharge freshwater into North Bay via the Delta. In the model, three main tributaries deliver freshwater directly to South Bay: Coyote Creek, Guadalupe River, and Alameda River. The five river boundaries are forced with high-frequency (15-minute interval) SSC data courtesy of USGS (US Geological Survey 2017). Two mud fractions (characterized by different fall velocities) are simulated, and it is assumed that the sediments delivered by rivers consisted of 50% of the lighter fraction and 50% of the heavier fraction. Additionally, ten wastewater treatment plants are accounted for in the model and discharge water, but no sediments, into Central and South Bay (San Francisco Estuary Institute 2017).

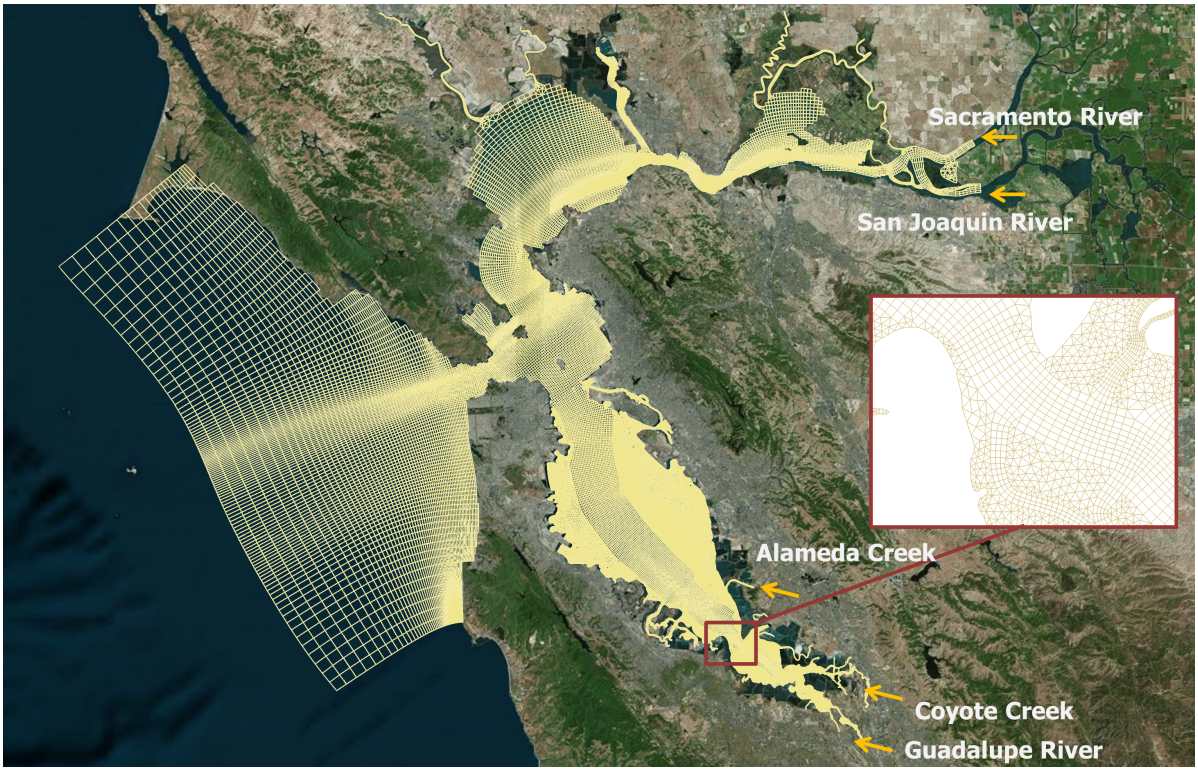

Figure 3.3: Unstructured model grid and river boundaries for D-FLOW and DELWAQ simulations. The five river boundaries shown are forced with high frequency measured discharge and sediment concentration data.

3.2.5. Bed Model

A number of sediment bed models have been developed to describe the erosion rate of cohesive sediments. Determining the most appropriate model to apply depends on site specific conditions and the degree of complexity needed to produce the desired results. Brand et al. (2015) compared four different bed models with respect to their ability to interpret SPM and vertical sediment flux measurements in SFSB. The study concluded that the linear erosion model led the nonlinear erosion model, flux amplitude model, and depth-dependent model in terms of model performance and sensitivity. This suggests that a formulation where the erosion flux is proportional to excess bed shear stress can be applied to simulate vertical sediment exchange in South Bay.

Partheniades-Krone Zeroth Order Model

By default, the Partheniades-Krone concept is applied in DELWAQ to calculate the erosion and sedimentation of cohesive sediments (Deltares 2017). Partheniades (1962) proposed an expression that is widely used to describe the erosion of well-consolidated, homogeneous beds. In his linear model, the erosion of material is proportional to the excess bed shear stress. The erosion parameter (M) and critical shear stress ($\tau_{E,crit}$) are both dependent on local sediment properties and environmental conditions. Eroded material enters the water column and increases the local suspended sediment concentration.

$$E = M\left(\frac{\tau_b}{\tau_{E,crit}} - 1\right) \tag{3.1}$$

with:

E = erosion rate $[gm^{-2}d^{-1}]$
M = first order erosion rate $[gm^{-2}d^{-1}]$
τ_b = bed shear stress $[Pa]$
$\tau_{E,crit}$ = critical shear stress for erosion $[Pa]$

Krone (1962) described sediment deposition with the following formulation:

$$D = \omega_s \cdot C \cdot \left(1 - \frac{\tau_b}{\tau_{D,crit}}\right) \tag{3.2}$$

with:

D = deposition rate $[gm^{-2}d^{-1}]$

C = concentration of suspended matter near the bed $[gm^{-3}]$

ω_s = fall velocity $[m/d]$

τ_b = bed shear stress $[Pa]$

$\tau_{D,crit}$ = critical shear stress for deposition $[Pa]$

In environments characterized by fine sediments, it is common for gross deposition to always occur, with net deposition observed when the deposition flux exceeds the erosion flux (personal communication, Thijs van Kessel, April 5, 2018). To represent this, $\tau_{D,crit}$ can be set to a large value, such that Equation 3.2 is reduced to

$$D = \omega_s \cdot C \tag{3.3}$$

Limitations of Classical Approach

The "classical" Partheniades-Krone approach has been widely applied to describe surface erosion and deposition of cohesive sediments. However, the simplicity of this approach lends itself to various limitations. As the zeroth order calculation of resuspension flux is independent of the amount of sediment available, model behavior is very sensitive to variations in the erosion parameter (M), leading to a less robust calibration. Further, no equilibrium sediment mass per unit area exists in the the classical approach - sediment mass approaches zero for areas with high shear stresses or low sediment supply and infinity for areas with low shear stresses or high sediment supply (van Kessel et al. 2011). The degree of complexity to which the exchange of sediment between the bed and the water column is resolved in the classical Partheniades-Krone approach is severely limited as well. To better resolve processes occurring in the near-bed region and to achieve a more stable model response, the buffer layer sediment model applied by van Kessel et al. (2011) was implemented in this study.

Buffer Layer Model

The Partheniades-Krone formulations form the basis of the buffer layer approach, with modifications to the model made by van Kessel et al. (2011). In this framework, the bed consists of two layers: the upper layer (the fluff layer), and a layer underneath (the buffer layer). As shown in Figure 3.4, the fluff layer and buffer layer are abbreviated as S1 (sediment layer 1) and S2 (sediment layer 2), respectively. The thin fluff layer erodes and accumulates sediment over the course of a tidal cycle, whereas the buffer layer is only eroded during more energetic conditions, such as spring tides or storms. Conceptually, the fluff layer is the easily erodible, unconsolidated mud film that forms on top of a solid bed during slack tide. The buffer layer can be thought of as a sandy matrix with a varying fraction of fines (van Kessel et al. 2009). It provides temporary storage for cohesive sediments, and resuspension from this layer is buffered by sand. As this study is focused on the pathways of cohesive sediments, only mud is exchanged between the bed and the water column. The sandy matrix in S2 buffers the resuspension of mud stored in this layer, but the sand itself is not mobilized.

The storage capacity of the buffer layer is dependent on the sediment density, porosity, and thickness of the lower layer, and the residence time of mud in this layer is dependent on the rate of exchange of mud with the water column relative to the amount of mud storage. The storage capacity and residence time in the buffer layer are important calibration parameters, which can be adjusted by altering the parameters describing bed exchange (M, τ_{crit}, ω_s) or by changing the thickness of the buffer layer (d_2) (van Kessel et al. 2011).

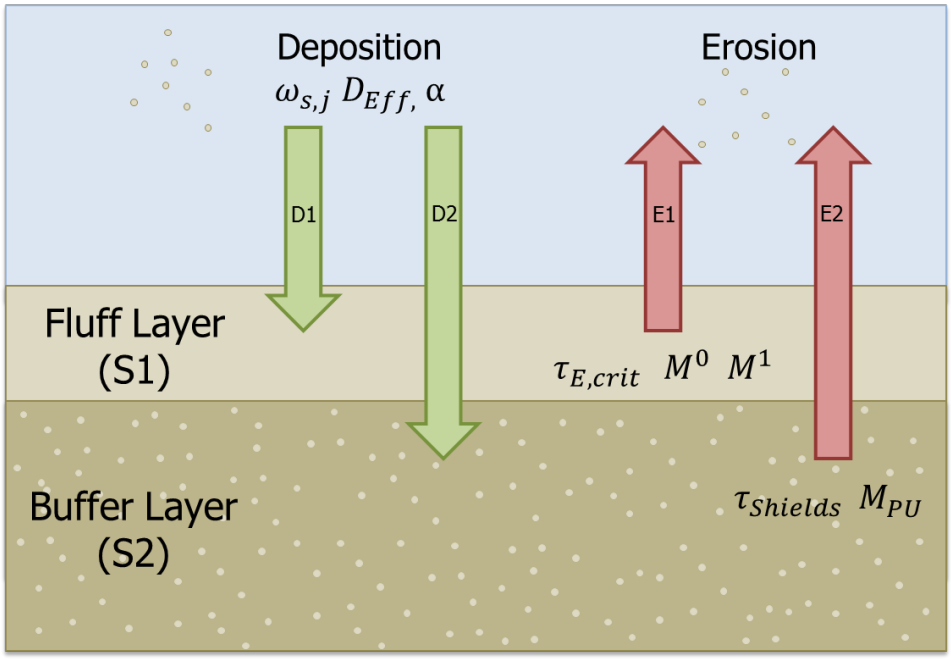

Figure 3.4: Schematic representation of buffer layer model, wherein deposition to S1 and S2 and erosion from S1 and S2 occur simultaneously. Index j represents cohesive sediment fraction. Mud in the fluff layer has a short residence time, while sediment can be stored in the buffer layer for longer periods of time between high energy events. S1 is composed of entirely mud, whereas the buffer layer consists of a sand matrix with a variable mud fraction (van Kessel et al. 2009). In this way, the effect of sand in the bed is included in the model, but the transport of sand is not.

Deposition
The sedimentation fluxes into layers S1 and S2 are calculated as

$$D1 = (1 - \alpha)\, \omega_s C \cdot D_{eff} \tag{3.4}$$

$$D2 = \alpha \cdot \omega_s C \cdot D_{eff} \tag{3.5}$$

where α is the fraction of sedimentation entering the buffer layer. The coefficient α can represent infiltration of fines into the lower layer by wave and tidal motion or bioturbation. The parameter D_{eff} represents deposition efficiency and is introduced to control the intensity of the vertical sediment exchange between the bed and the water column independently from fall velocity. If $0 < D_{eff} < 1$, the gross deposition flux is reduced compared to the calculated settling flux. Conceptually, this simulates the formation of a mobile fluff layer, thus enhancing near-bed transport (van Kessel et al. 2011). The deposition efficiency can be used to control the intensity of the water-bed exchange independently from the settling velocity (personal communication, Thijs van Kessel, April 5, 2018).

Erosion
One of the limitations of the classical zeroth order Partheniades-Krone approach is that the erosion rate is independent of the amount of sediment available, which is only valid for a bed composed entirely of mud. In cases where the fluff layer doesn't completely cover the solid bed underneath, a zeroth order erosion flux cannot be assumed. Introducing a first-order erosion rate, which scales with the mass of sediment in the bed, better represents the case where the roughness height of the solid bed exceeds the thickness of the fluff layer (see Figure 3.5). Further, the first order calculation of resuspension implies the existence of an equilibrium sediment mass for any combination of bed shear stresses and sediment supply. Deviations from the equilibrium mud content in the buffer layer can serve as a proxy for morphological evolution. The resuspension flux from the fluff layer, S1, is calculated as:

$$E1 = min\left(m_1 \cdot M^1,\, M^0\right) \cdot \left(\frac{\tau_b}{\tau_{E,crit}} - 1\right) \tag{3.6}$$

with:

m_1 = mass of sediment in S1 $[kg]$

M^0 = zeroth order resuspension flux $[kg\,m^{-2}s^{-1}]$

M^1 = first order resuspension flux $[s^{-1}]$

The resuspension flux ($E1$) is proportional to the excess shear stress times a first order resuspesion rate until a certain sediment mass per area is reached, beyond which a zeroth order resuspension rate is applied. The transition from first order to zeroth order erosion occurs for an absolute sediment mass of $m_1 = M_0/M_1\ kg\,m^{-2}$ (van Kessel et al. 2011).

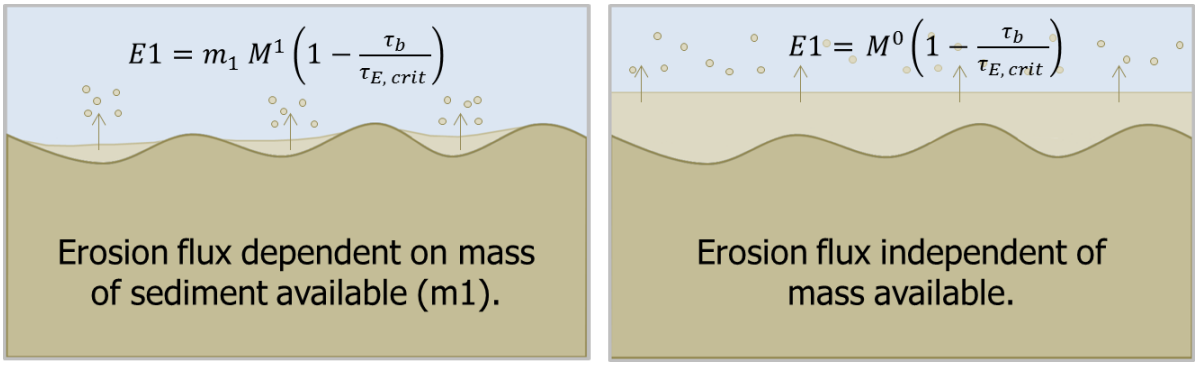

Figure 3.5: Schematic showing switch between first order (left) and zeroth order (right) calculation of resuspension flux. The upper light brown layer represents the fluff layer, and the lower dark brown layer represents the buffer layer.

A van Rijn (1993) pickup formulation is applied to calculate the re-suspension flux from the buffer layer. The erosion flux from S2 is proportional to the fraction of mud in S2, not the absolute mass. This is an important distinction, because in this way the thickness of the buffer layer can be used to tune the timescales of system response. For the same mass of mud, a thicker buffer layer will have a smaller fraction of fines, so suspension fluxes will be less. Conversely, vertical sediment fluxes will be higher for a thinner S2 layer. The excess shear stress is raised to the power of 1.5, an empirically determined value for the mobilization of sand (van Rijn 1993).

$$E2 = p_2 M_{PU}\left(\frac{\tau_b}{\tau_{Shields}} - 1\right)^{1.5} \tag{3.7}$$

$$p_2 = \frac{m_2}{d_2\,(1 - n_{S2})\,\rho_{sand}} \tag{3.8}$$

$$M_{PU} = F_{ResPU} * \rho_s\,((s-1)\,gD_{50})^{0.5}\,D_*^{0.3} \tag{3.9}$$

p_2 = fines fraction in S2 $[-]$

d_2 = thickness of layer S2 $[m]$

n_{S2} = porosity of layer S2 $[-]$

F_{ResPU} = van Rijn (1993) pickup factor $[-]$

$s = \rho_s/\rho_w$ $[-]$

g = gravitational acceleration (9.81 $m\,s^{-1}$)

$D_* = D_{50}\left((s-1)\,g/\nu^2\right)^{1/3}$ = dimensionless particle size $[-]$; ν = kinematic viscosity $[m^2\,s^{-1}]$

D_{50} = grain size of sand buffer $[m]$

$\tau_{Shields}$ = critical shear stress for sand mobilization in buffer layer $[m]$

3.2.6. Initial Bed Composition

The bed composition at the start of the model defines the amount of each sediment fraction initially present in the bed. Once the simulation starts, sediments will be redistributed throughout the model domain until the hydrodynamics are in dynamic equilibrium with the bed - finer sediment will settle in calmer areas and will be swept away from areas with higher shear stresses. The time before this dynamic equilibrium is achieved is called a model spin-up period, and the closer the initial bed composition is to equilibrium conditions, the less time is required for the model to adjust. During spin-up, the model does not not necessarily simulate realistic behavior, as the bed composition is still adjusting to hydrodynamic conditions. As explained in Section 3.2.5, for a given shear stress environment and sediment supply, an equilibrium mass of mud in the buffer layer framework exists. A Bed Composition Generation (BCG) simulation was done to determine an appropriate initial sediment bed composition.

Bed Composition Generation Simulation

A BCG run is a numerical simulation that allows for the redistribution of sediments to create a bed composition condition that is closer to dynamic equilibrium than a uniform sediment distribution. The goal is to reduce the magnitude of unrealistic behavior observed during the model spin-up period. An initial guess for the bed composition distribution was created. In layer S1, mud was initialized on the flats (defined as shallower than 5m depth), as shown in Figure 3.7. The initial mass of mud in the fluffy layer (S1) was estimated based on observed fluctuations of SSC over the tidal cycle and the local water depth. The mass in the fluffy layer can be estimated by $\Delta C \cdot h$ (van Kessel et al. 2011). Layer S2 was initialized as being spatially uniform with an initial mud fraction (p_2) of 0.3. The model was forced with hydrodynamics simulating WY 2015. The resulting sediment map was used as input for another simulation forced with the same hydrodynamics. This process was repeated 11 times as the amount of mud per area in the bed converged towards an equilibrium mass. The following map shows the results of the BCG "spin-up" and was used as the initial bed composition in the model. After the BCG process, the sandy sediments had mostly settled in the channels and the fine sediments had settled on the flats, which is consistent with observations and expectations based on the distribution of bed shear stresses (Achete et al. 2015, van der Wegen et al. 2010, 2011).

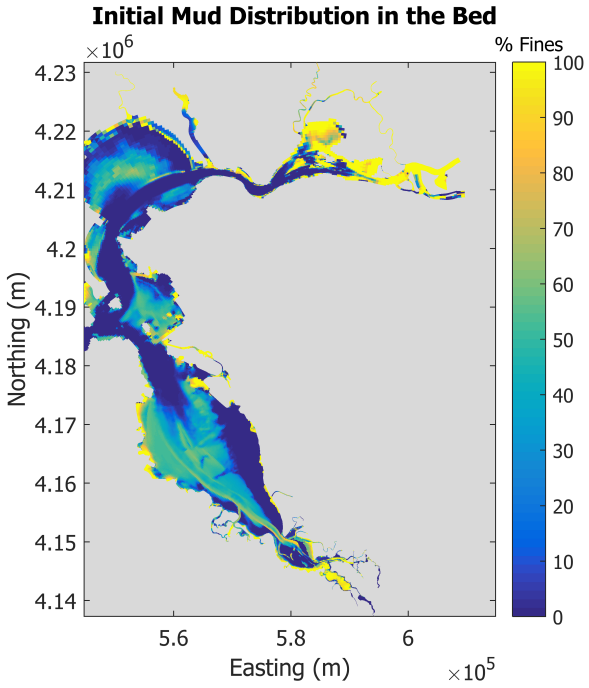

Figure 3.6: Initial bed composition for DELWAQ simulations as determined by BCG runs. The thin (on the order of 1 mm) fluffy layer is composed of pure mud. The buffer layer has a fixed thickness of 0.1 m, and the fines fraction (3.8) in this layer varies.

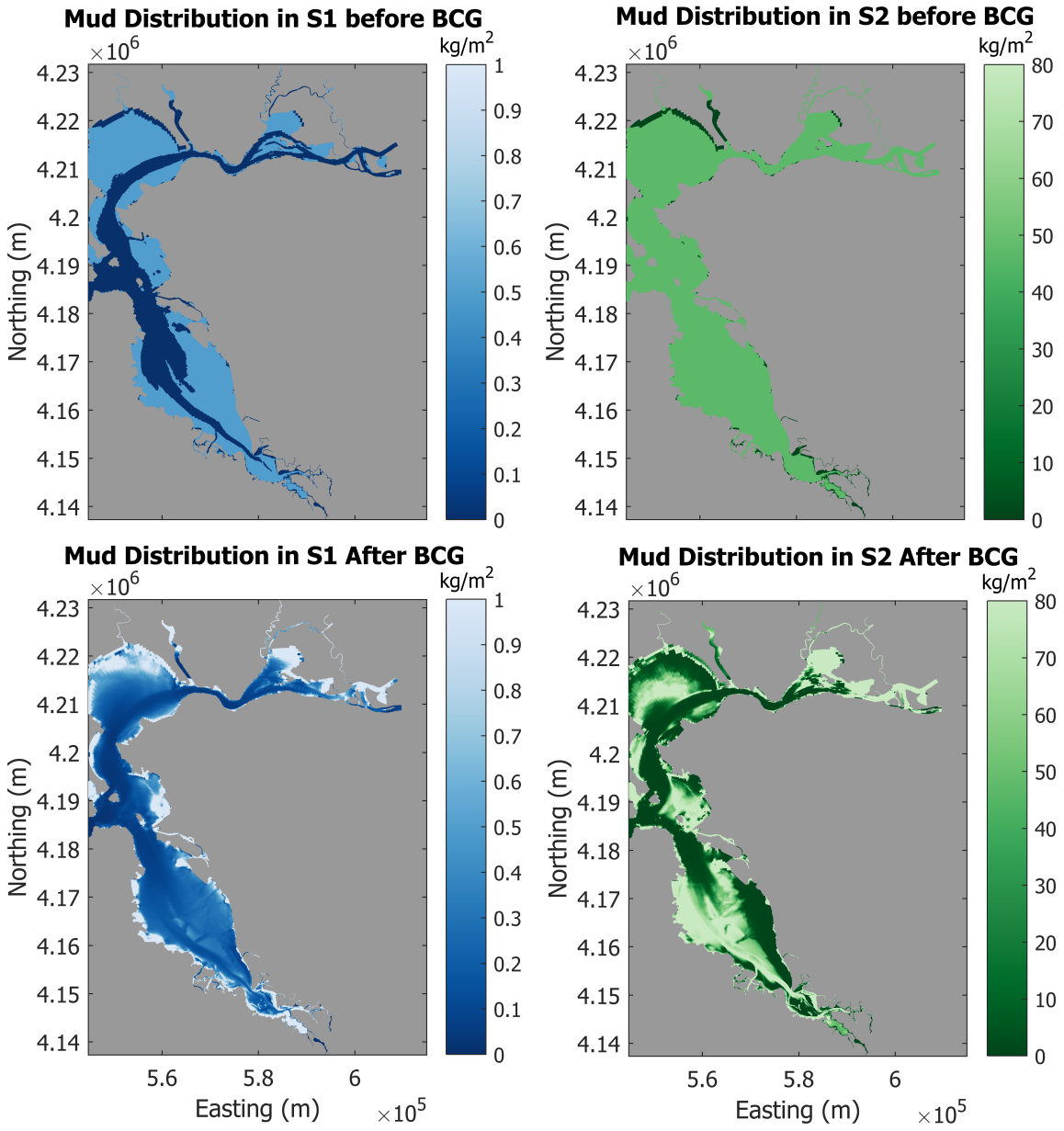

Figure 3.7: Distribution of mud in the fluffy layer (S1) and buffer layer (S2) before and after the BCG procedure. The result of the BCG simulation is imposed as an inital condition for the DELWAQ model.

3.2.7. Mud Parameters

Mud transport can be modelled by defining the settling velocity of sediment (ω_s), the critical shear stress for erosion of the bed ($\tau_{E,crit}$), and the erosion parameter (M). Due to flocculation, the fall velocities of muddy fractions are representative of floc settling rates, not those of individual mud particles. Previous studies were used to determine initial best guesses for the parameters controlling mud transport in South Bay, and a model calibration was done to tune these values.

Previous Studies

Motivated by the broad implications of fine sediments on water quality, habitat restoration, and navigation, various studies have identified mud transport characteristics throughout SFB. The relevant findings of these studies are explained here and used to identify initial values for the parameters applied in the DELWAQ model prior to calibration.

Table 3.1: SFB fine sediment transport parameters from literature. The range of values applied or determined in each study is shown.

ω_s $[mms^{-1}]$	$M[gm^{-2}\ s^{-1}]$	$\tau_{E,crit}$ $[Pa]$	**Location**
0.1-0.25	0.02	0.15-1.05	Suisun Bay[1]
0.1-0.275	0.018	0.1-1.1	Suisun Bay[2]
0.15-0.38	0.025-10	0.125-0.5	San Pablo Bay[3]
0.024-0.4	0.1	0.05-0.8	San Pablo Bay[4]
-	0.013-0.047	0.1-0.4	Alcatraz[5]
2.8	-	0.049	Richmond[6]
1.0 - 10.0	-	-	ATF[7]
-	-	0.12-2.56	ATF[8]
0.4-1.0	0.01-0.05	0.3-0.4	North Bay[9]
7.0e-4 - 0.9	0.068-0.274	0.068-0.11	South Bay[10]
0.011-1.62	-	0.25	South Bay[11]

1 - Ganju & Schoellhamer (2009); 2 - Ganju et al. (2007); 3 - Achete et al. (2015); 4 - van der Wegen et al. (2011); 5 - Teeter (1987); 6 - Sternberg et al. (1986); 7 - Kranck & Milligan (1992); 8 - Jones (2008); 9 - McDonald & Cheng (1997); 10 - Brand et al. (2015); 11 - van Kempen (2017)

As summarized in Table 3.1, various studies determined mud transport parameters via in-situ measurements (Kranck & Milligan 1992, Sternberg et al. 1986), and laboratory experiments (Jones 2008, Teeter 1987). Appropriate values were also chosen and applied in numerical modelling studies (Achete et al. 2015, Brand et al. 2015, Ganju & Schoellhamer 2009, Ganju et al. 2007, McDonald & Cheng 1997, van der Wegen et al. 2011, van Kempen 2017). Previous investigations of sediment dynamics in SFB provide a range of reasonable values to apply in the calibration of the DELWAQ model in this study. To determine the most appropriate values to describe sediment dynamics in South Bay using the Buffer Layer Model, the model was calibrated using measured SSC data. This procedure is discussed in the next section.

3.2.8. Model Calibration

The model was calibrated based on measured suspended sediment concentrations collected by USGS and provided by SFEI. High-frequency (15-minute interval) SSCs were collected during WY 2015 at Dumbarton Bridge at two elevations, approximately 1.2 m and 7.6 m above the bed. Suspended sediment data is also available at other locations throughout the Bay, but not for the time period of calibration (WY 2015). These data were used to compare model results to the measured values at the corresponding location and elevations. Table 3.2 shows the range of parameters that were used to calibrate the model.

The measured time series at the Dumbarton measurement station were recorded at two fixed elevations above the bed, and the corresponding modelled SSC time series were extracted from model observation points associated with the tenth (bottom) and sixth vertical layers. The sum of the RMSEs between the measured and modeled SSC values closer to the bed (1.2 m) and higher in the water column (7.6 m) at Dumbarton Bridge were used to evaluate model performance. One parameter was altered at a time, and three-to-four values were tested for each parameter. The value that yielded the lowest combined RMSE value was applied as the next parameter was tuned.

The fall velocity of both mud fractions (ω_{s1}, ω_{s2}), the first and zeroth erosion rate from the fluffy layer ($M_{0,S1}$, $M_{1,S1}$), the erosion rate from the buffer layer (M_{S2}), and the critical erosion thresholds for both bed layers ($\tau_{S1,crit}$, $\tau_{S2,crit}$) were prioritized as calibration parameters. The parameter settings that yielded the best model performance, as determined by the lowest combined RMSE, are given in Table

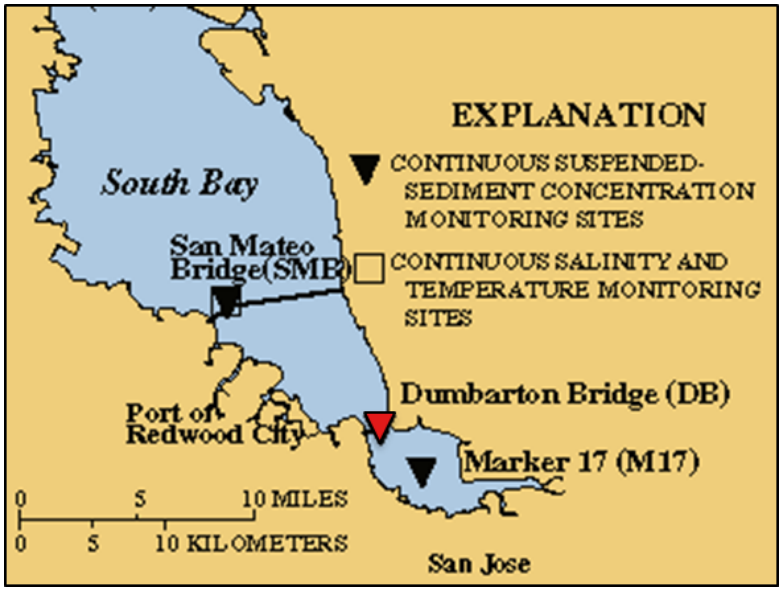

Figure 3.8: USGS measurement station at Dumbarton Bridge (Station 373015122071000) is indicated with red marker. High-frequency suspended sediment concentration data from two elevations in the water column was used to calibrate the DELWAQ sediments model.

3.2. The calibration revealed that resuspension from the fluffy layer is more sensitive to the zeroth order erosion parameter than the first order erosion parameter. When tuning the fall velocities, the SSC time series was only significantly impacted when the fall velocity of the heavier sediment fraction was less than 0.5 mms^{-1}. See Appendix C for plots showing the sensitivity of SSCs to each parameter.

The RMSE of the final parameter settings is 133 mg/L at the point closer to the bed and 84 mg/L at the point near the surface. The model captures SSC fluctuations corresponding to the spring/neap tidal signal better than fluctuations over the ebb-flood timescale, as shown by the daily averaged time series shown in Figure 3.9. The RMSE between daily averaged modelled and measured SSCs is 64 mg/L near the bed and 56 mg/L at the point higher in the water column. The modelled SSC at Dumbarton Narrows is underestimated for the period between March and August, a time during which strong diurnal winds are observed in the Bay Area (see Figure 3.9). This discrepancy could be caused by a number of factors discussed in Section 5.1.1.

Table 3.2: Range of values used to tune mud transport parameters during model calibration.

Parameter	**Range of Values Tested**		**Value Applied**
	Low	High	
ω_{s1} $[mm\,s^{-1}]$	0.25	0.75	0.50
ω_{s2} $[mm\,s^{-1}]$	0.05	0.15	0.10
$M_{0,s1}$ $[kg\,m^{-2}\,s^{-1}]$	0.0001	0.0120	0.0006
$M_{1,s1}$ $[d^{-2}\,s^{-1}]$	0.5	20	1
$\tau_{s1,crit}$ $[Pa]$	0.1	0.3	0.15
$\tau_{s2,crit}$ $[Pa]$	0.85	0.95	0.90
M_{s2} $[-]$	3.0E-07	3.0E-05	3.0E-06

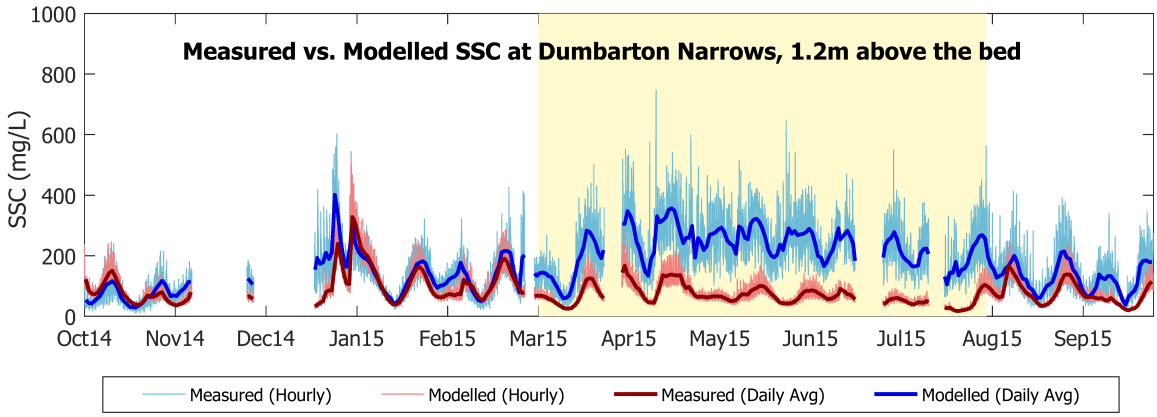

Figure 3.9: Modelled versus measured suspended sediment concentrations at Dumbarton Bridge measurement station. Measured values shown were taken 1.2m above the bed, and the modelled values shown were extracted from the x and y coordinates corresponding to the measurement station at 10% of the water depth. The yellow box shows a time period during which measured SSC behavior is not well captured by the model. The correlation between measured and modelled values is over twice as strong when this period is excluded from consideration, as discussed in Chapter 5.

3.2.9. Model Output

Observation areas - areas in the model domain at which information is stored - were established in the form of observation points and transects (cross-sections). Observation points consist of individual computational volumes at which specified variables are monitored. They can be defined for a specific vertical layer or depth averaged. Transects are continuous vertical surfaces extending through the depth of the water column across which fluxes are measured during simulations. Twenty eight transects and 32 observation points were created, as seen in Figure 3.10. For an explanation of how the cross-sections are defined in the DELWAQ model, see Appendix D.

3.2.10. Sediment Tracers

The processes governing sediment dynamics vary spatially throughout SFB. North Bay receives large inputs of freshwater from the Sacramento-San Joaquin River Delta, whereas South Bay water properties are dependent on density-driven exchanges between Central Bay and South Bay. The different geometries of North and South Bay mean that tidal and wind forcing impact fluid dynamics differently in the northern and southern reach. Within South Bay, wind wave resuspension plays a larger role on the shallow flats, while vertical and horizontal density gradients are more present in the deep channel. To study the behavior of sediments in different parts of the Bay, sediments originating in different areas of the model domain and sediments entering through each of the five river boundaries were labeled and their pathways traced over various simulations. Figure 4.1 shows a map of the sediments labeled in the bed.

The DELWAQ model that was developed and calibrated in this study serves as a powerful tool to study the complex mechanisms that influence sediment dynamics in SFB. The following chapter presents the results of the application of the sediment transport model to various hydrodynamic scenarios.

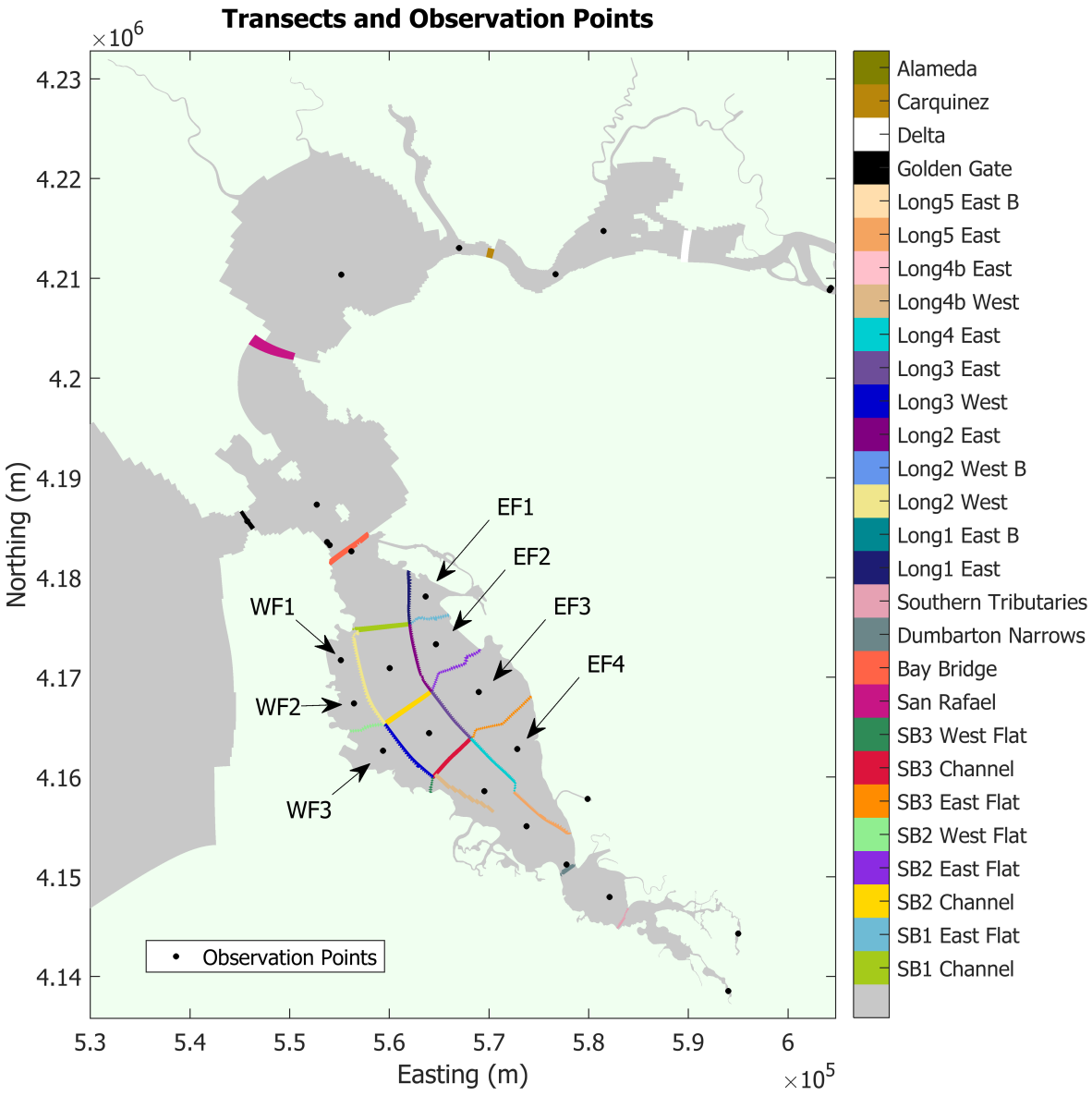

Figure 3.10: Monitoring cross-sections (transects) established throughout model domain. Sediment fluxes are measured across each transect over the course of a simulation, allowing for gross and cumulative sediment fluxes to be calculated.

4

Results

During the first phase of this study, a DELWAQ sediments tracer model was developed and calibrated to simulate sediment transport in San Francisco Bay. During the second phase, the calibrated model was applied to D-FLOW hydrodynamics to achieve a better understanding of sediment pathways in South Bay and to address the research questions motivating this study. Three simulations were executed tracing the pathways of specific sediments, and the model was applied to four different hydrodynamic scenarios to isolate the effects of wind, density-driven circulation, and extreme rates of Delta discharge. The results of these applications are presented here.

4.1. Model Application

One of the major advantages of numerical models over measured data is that they can be easily applied to study a range of time periods representing various conditions. To address the research questions posed in Section 1.3, the DELWAQ model set-up was adjusted to study specific sediment pathways under various hydrodynamic scenarios, which are described here.

4.1.1. Sediment Tracers

Tracing sediments initialized in different areas of the bed or entering the system through river boundaries reveals information about the relative contribution of sediments from different origins to sediment transport. Due to the large amount of data produced by the tracer simulations, deciding which sediments to trace for different scenarios was a tradeoff between the number of sediment labels applied and the length of the simulations. Three tracer simulations were run to study the pathways of specific sediments.

1. **Baseline Tracer Simulation (WY 2015):** The bed was categorized into ten different areas: Suisun Bay, Carquinez Strait, San Pablo Bay, San Rafael, Central Bay, Channel (SB), West Flat (SB), East Flat (SB), South of Dumbarton, and ”other” (see Figure 4.1). Sediments entering through the San Joaquin and Sacramento Rivers were collectively labeled as ”Delta” sediments. Sediments entering through the Guadalupe, Alameda, and Coyote tributary boundaries were each given a unique label. Simulating fourteen sediment tracers, each consisting of two mud fractions, is computationally expensive and generates enormous output files. For this reason, the labeled sediments were only simulated for one year representative of baseline conditions, WY 2015.

2. **North Bay Simulation (5 years):** To better understand how sediments enter and are redistributed within South Bay, a series of simulations was run with a ”North + Central Bay” tracer, in which sediments starting north of Bay Bridge (Central Bay, San Rafael, San Pablo Bay, Carquinez Strait, Suisun Bay, and Delta sediments) were collectively labeled and traced over the course of five years (each year with the same WY 2015 hydrodynamics). Only Delta sediments entering the system during the first year were labeled and traced.

3. **Delta Sediments Simulation (4 years):** A tracer simulation of four years was executed to study the pathways taken by sediments entering through the San Joaquin and Sacramento River

Delta. In this simulation, only sediments entering the system through the Delta during the first year were labeled and traced.

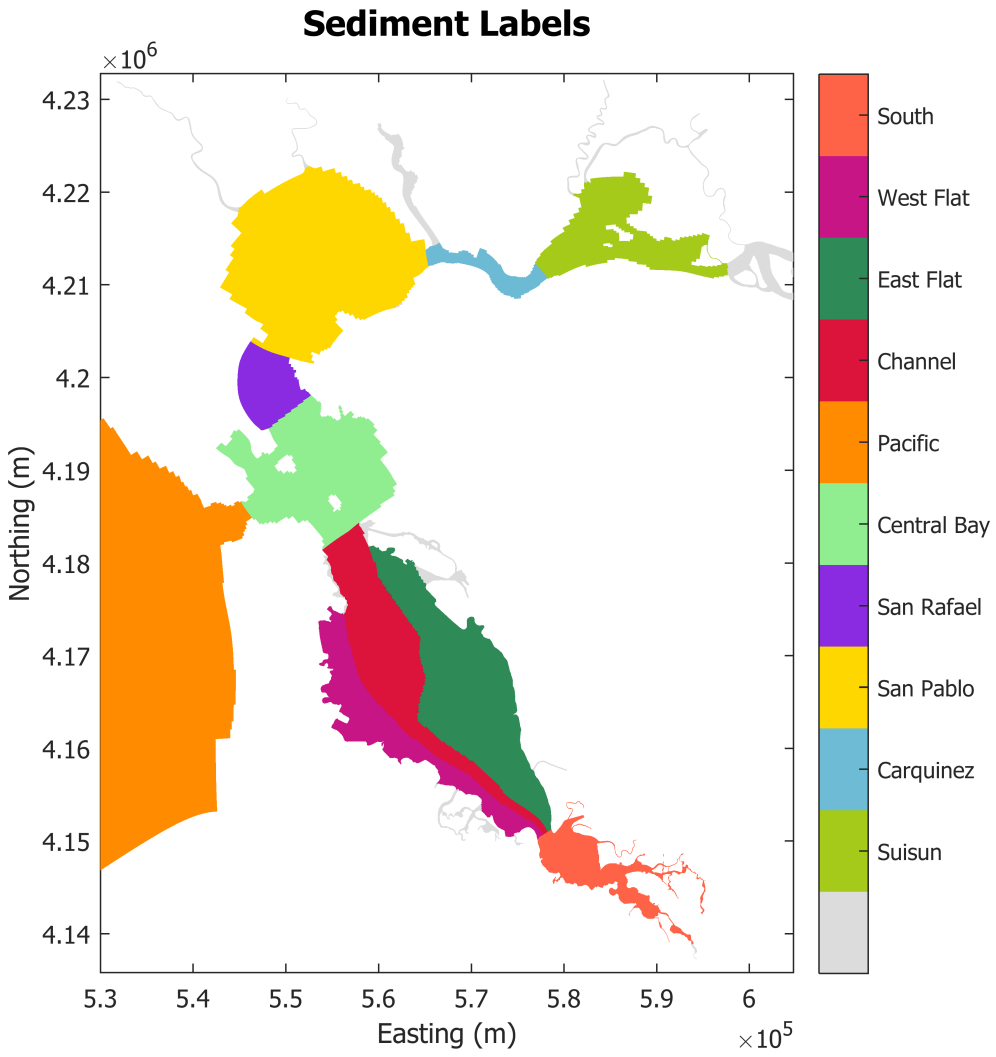

Figure 4.1: Map of the model domain showing how the sediments in the initial bed were labeled during the first tracer simulation. In addition to the 11 areas of the bed that were labeled at the start of each simulation, sediments entering through the five river boundaries represented in the model (Sacramento River, San-Joaquin River, Alameda Creek, Guadalupe River, and Coyote Creek) were labeled as well.

4.1.2. Hydrodynamic Scenarios

Hydrydynamics from WY 2015, representing baseline conditions, were used to calibrate the DELWAQ model; following calibration, the model was applied to different hydrodynamic scenarios to better understand the driving mechanisms of sediment transport in SFB. The four hydrodynamic simulations were run in Delft3D FM by van Kempen (2017). Complete data (discharge and sediment concentrations) was not available for all of WY 2017, representative of a particularly wet year. The wet year and barotropic simulations were therefore run with hydrodynamics from WY 2017 up until July 19th, 2017 after which the hydrodynamics from July 20th-October 1st, 2015 were applied. The period of missing data is during the dry season, so freshwater and sediment inputs during this period are not likely to vary significantly between WY 2015 and WY 2017. Hydrographs showing Delta discharge for WY 2015 and WY 2017 are shown in Figure 3.2. Water temperature and salinity for each of the 516,400 grid cells was provided hourly by the D-FLOW model.

Table 4.1: Hydrodynamic scenarios to which DELWAQ model was applied.

Name of Simulation	Time Period	Temp. & Sal.	Wind
Baseline	WY 2015	Hourly	Hourly
Wet Year	WY 2017*	Hourly	Hourly
No Wind	WY 2015	Hourly	None
Barotropic	WY 2017*	None	Hourly

*Complete data for WY 2017 was not available at the time these simulations (Wet Year and Barotropic) were run. Therefore the time period modelled is 01/08/2016-19/09/2017 & 20/09/2015-01/10/2015.

The salinity and temperature fields impact sediment transport in two ways. First, gradients in water density induce 3D circulation patterns, which advect suspended sediments and can significantly influence sediment pathways. This effect is accounted for in the hydrodynamics computed by the D-FLOW model. To study the impact of temperature and salinity-induced density-driven currents on sediment transport, the barotropic simulation excluded the temperature and salinity fields. Salinity and temperature (in addition to other water properties) also impact the flocculation and settling rates of suspended particles. The impacts of temperature and salinity on flocculation rates and settling can be simulated in DELWAQ, as explained in Appendix B, but were not implemented in this study.

Sustained wind shear on the water surface can generate currents, and wind can also generate waves. The combined, non-linear effect of wind-induced currents and waves on sediment transport is accounted for in the bed shear stresses computed by the D-FLOW model, as wind is not simulated in DELWAQ. See Appendix A for details about the calculation of the bed shear stresses. The same wind forcing from WY 2015 was applied to the three scenarios with wind (baseline, wet year, and barotropic).

4.2. Tracer Analysis

The remainder of this chapter presents the results of the model applications. This section discusses the results of the three DELWAQ simulations with varying sediment tracer configurations.

4.2.1. Tracer Simulation I: One Year, 14 Tracers

The baseline tracer simulation traced the pathways of fourteen groups of sediments over the course of one year (WY 2015). These results resolve the differences in sediment behavior in different areas of the Bay-Delta system; however, they are only representative of the conditions observed during WY 2015. The labels referred to ten different areas of the bed, sediments entering from the Delta, and sediments entering from each of the three local tributaries (Figure 4.1). The output from the tracer simulation contains a wealth of information about where sediments of different origins go, when this transport occurs, and the mechanisms controlling residual sediment fluxes. To get an idea as to what controls South Bay's sediment budget, the contributions of different sediments to flux across Bay Bridge (at the mouth of South Bay) and across Dumbarton Narrows (landwards boundary of area considered in this study) were evaluated.

Figure 4.2 shows the cumulative sediment flux across Bay Bridge and Dumbarton Narrows of sediments starting in different areas of the bed or entering through river boundaries. The largest contributors to South Bay sediment import across Bay Bridge (residual landwards transport) for the simulated WY 2015 are San Pablo Bay (332 kT), Central Bay (193 kT), and Suisun Bay (78 kT). Only 25kT of Delta sediments enter and remain in South Bay, which is less than 10% of the amount of San Pablo Bay sediments entering over a one-year period.

The transport of east flat and west flat sediments across the Bay Bridge and Dumbarton transects is enhanced during wind events, as shown by a steepening of the cumulative transport curves in Decem-

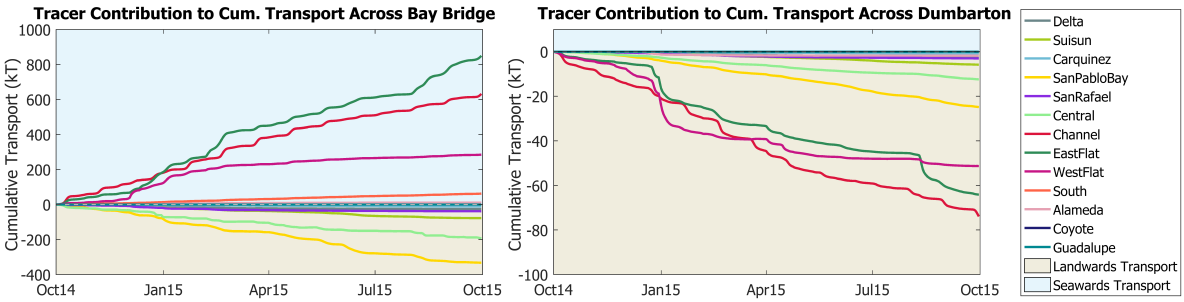

Figure 4.2: Contribution of different sediment tracers to cumulative transport across Bay Bridge and Dumbarton Narrows. The seawards flux of sediments originating south of Dumbarton Narrows is not shown. See Figure 4.1 for a map of the sediment labels.

ber, the beginning of January, and August (Figure 4.2). The impact of wind wave resuspension on sediment transport in South Bay is further discussed in Section 4.2.1.

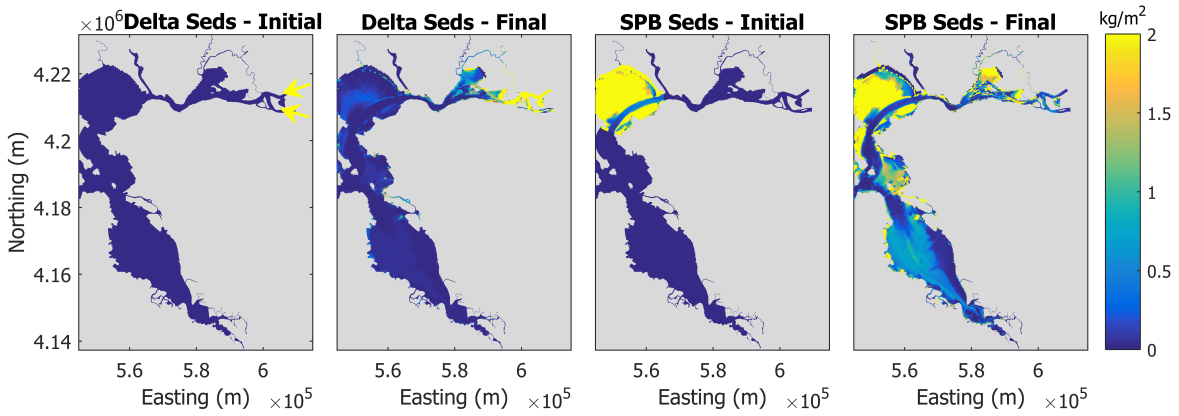

Figure 4.3: Initial and final distribution of Delta sediments and San Pablo Bay sediments in the bed after 1 year (WY 2015). Approximately 332 kT of sediment originating in the bed of San Pablo Bay enter and remain in South Bay; only 25 kT of Delta sediments enter and remain in South Bay during the WY 2015 simulation.

The dispersal of sediments originating in the bed in San Pablo Bay was compared to the dispersal of sediments entering through the Sacramento and San Joaquin Rivers during WY 2015 (Figure 4.3). Most Delta sediments entering the model settle landwards of Carquinez Strait for the WY 2015 simulation, during which the maximum observed Delta discharge rate was approximately 2,000 m^3/s.

South Bay Sediments

Sediments originating in the bed in South Bay contributed more to landwards flux into southern SFSB (south of Dumbarton Narrows) than those entering South Bay across Bay Bridge. Sediment fluxes of mud initialized on the east flat, west flat, and in the channel between Bay Bridge and Dumbarton Narrows were compared to investigate differences in behavior between sediments originating in different areas.

The sum of each type of sediment exiting the system (landwards across Dumbarton Narrows and seawards across Bay Bridge) was calculated. Of the total amount of sediment exiting South Bay, approximately 13% of exported west flat sediments, 8% of exported east flat sediments, and 22% of exported channel sediments were transported landwards into southern South Bay, indicating that the primary pathway for sediment removal from the system is seawards across Bay Bridge.

Comparing the net flux and the gross flux of sediments originating in South Bay (Figure 4.4) shows that residual sediment transport is the net result of unbalanced oscillatory fluxes driven by the tide.

The transport of sediment originating on the flats across Bay Bridge and Dumbarton Narrows is more episodic than that of sediment originating in the channel, likely due to the resuspension of sediments on the flats during wind wave events. Section 4.2.1 discusses the correlation between wind events, suspension on the flats, and the resulting transport across Bay Bridge and Dumbarton Narrows.

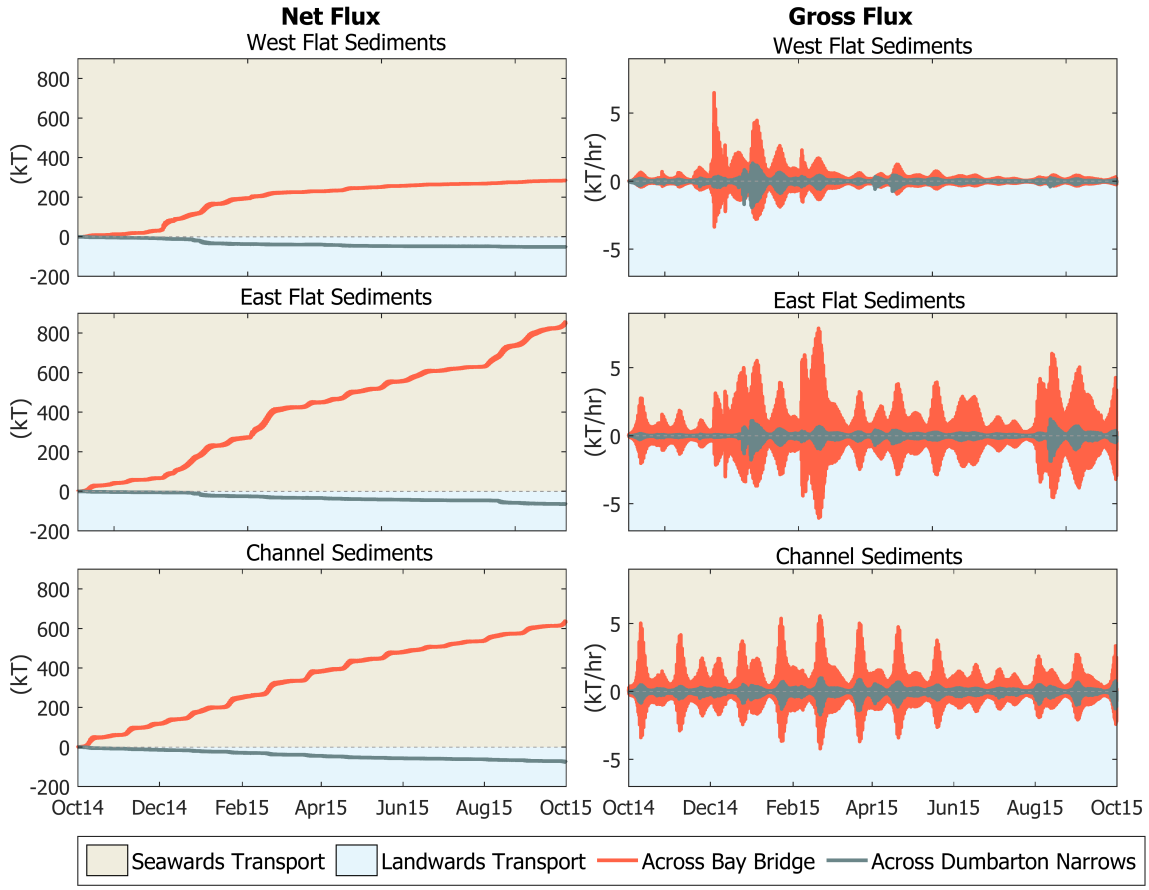

Figure 4.4: Behavior of sediments starting in the bed in South Bay. Sediments initialized in the bed in South Bay are categorized as east flat, west flat, or channel sediments (see Figure 4.1 for a map of the different sediment tracers). The net flux and gross flux of these three types of sediment are shown for two transects at the seawards and landwards boundaries of South Bay: Bay Bridge and Dumbarton Narrows.

Resuspension on the Flats

Resuspension of sediments on the shallow tidal flats occurs when currents and wave action induce shear stresses at the bed that exceed the critical erosion threshold. Figure 4.5 shows the relationship between the modelled gross sediment flux at the seawards and landwards boundaries of South Bay, SSC, and wind. The results show that the wind direction affects local SSCs on the eastern and western flats. Southerly winds are more likely to cause high SSCs further north on the flats (at points EF1 and WF1). Conversely, northerly winds are more likely to cause high SSCs further south on the flats (at points EF4 and WF3). Comparing the daily averaged sediment flux across Bay Bridge (orange line) and Dumbarton Narrows (gray line) to SSC concentrations on the flats suggests that high sediment concentrations further north could cause higher sediment fluxes across Bay Bridge and higher concentrations further south could cause higher sediment fluxes across Dumbarton Narrows. For both east flat and west flat sediments, spikes in SSC at the southern most observation point correspond to the largest magnitude of sediment flux landwards across Dumbarton Narrows, which implies that northerly winds could contribute to the trapping of sediment in southern SFSB. Westerly winds (which are dominant during the summer months) contribute to resuspension on the east flat, but have less of an effect west flat, likely due to differences in fetch.

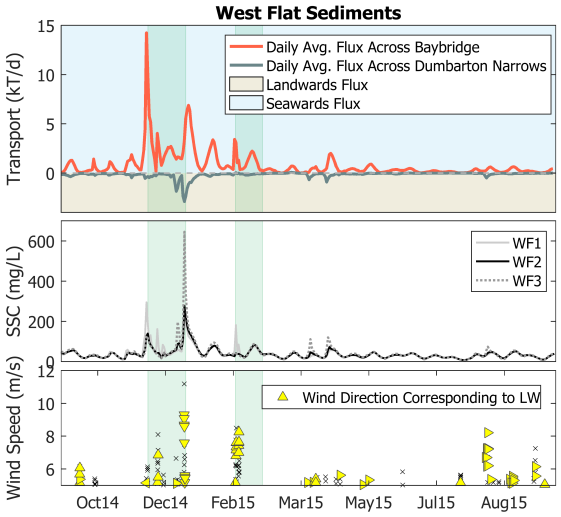

(a) **Top:** Daily averaged net flux of sediments originating in the bed on the west flat across Bay Bridge and Dumbarton Narrows. **Middle:** Daily-averaged SSC at mid-depth at three points: WF1, WF2, and WF3 located respectively on the northern, central, and southern west flat (3.10). **Bottom:** Hourly wind speed (above 5m/s threshold) and direction given by yellow triangles.

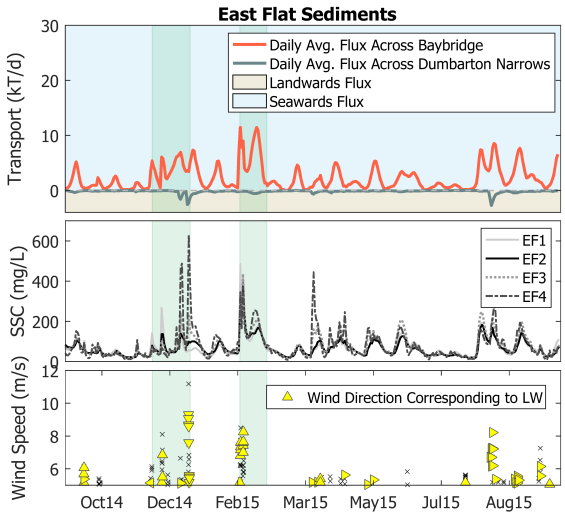

(b) **Top:** Daily averaged net flux of sediments originating in the bed on the east flat across Bay Bridge and Dumbarton Narrows. **Middle:** Daily-averaged SSC at mid-depth at four points (listed from north to south) EF1, EF2, EF3, and EF4 (3.10). **Bottom:** Hourly wind speed (above 5m/s threshold) and direction given by yellow triangles.

Figure 4.5: Relationship between daily averaged net flux of sediments originating on the eastern or western flat, SSC on the corresponding flat, and wind events. Yellow triangles represent times at which the hourly wind speed exceeds a 5 m/s threshold and corresponds to an ebb period (low water). Arrows pointing up represent winds from the south (225-180^{o}N), arrows pointing down represent winds from the north (<45^{o}N or >315^{o}N), arrows pointed to the right represent winds from the west (225-315^{o}N), and arrows pointed to the left represent wind from the east (45-135^{o}N). The vertical green bands show the time periods corresponding to large pulses of Delta discharge.

Figure 4.6 shows the relationship between modelled water depth and SSC near the bed at a point on the west flat during a wind event. The hourly values show that peak SSC concentrations in the DELWAQ model correspond to low water; the same trend is observed on the east flat. This suggests that the timing of strong winds and wave generation relative to the semi-diurnal tidal cycle is an important factor in determining SSC values and sediment fluxes. It should be noted that the modelled SSC values were extracted from observation points associated with a specific vertical σ-layer. As a fixed fraction of the water depth, the height of a σ-layer above the bed varies with water depth, so the relationship between SSC and water depth is affected by the fact that at low water, the observation point is closer to the bed than at high water. This matter is further discussed in Section 5.1.1.

Local Tributaries

Three of the local tributaries that deliver sediments directly to South Bay are accounted for in the DELWAQ model: Alameda Creek, Guadalupe River, and Coyote Creek. The Guadalupe River and Coyote Creek deliver freshwater and sediments through South Bay's landwards boundary near San Jose. The flux of sediments from these two tributaries seawards across Dumbarton Narrows is insignificant (orders of magnitude less) compared to the magnitude of sediments entering the main body of South Bay from Alameda, therefore the pathways of sediments from Guadalupe and Coyote Creek were not considered in this analysis.

Figure 4.7 shows the behavior of sediments entering South Bay from Alameda Creek. The sediment budget shows that sediments are delivered episodically, presumably after a local precipitation event, as the Alameda river drains from a local watershed. The sediment budget suggests that after pulses of Alameda sediments enter the system, some slowly exit South Bay seawards via Bay Bridge and some are removed from the system landwards, south of Dumbarton Narrows. Of the 22.3 kT of Alameda sediments that enter over the course of the year simulated, approximately 50% are exported across Bay Bridge and less than 1% travel and remain south of Dumbarton Bridge. The remaining Alameda

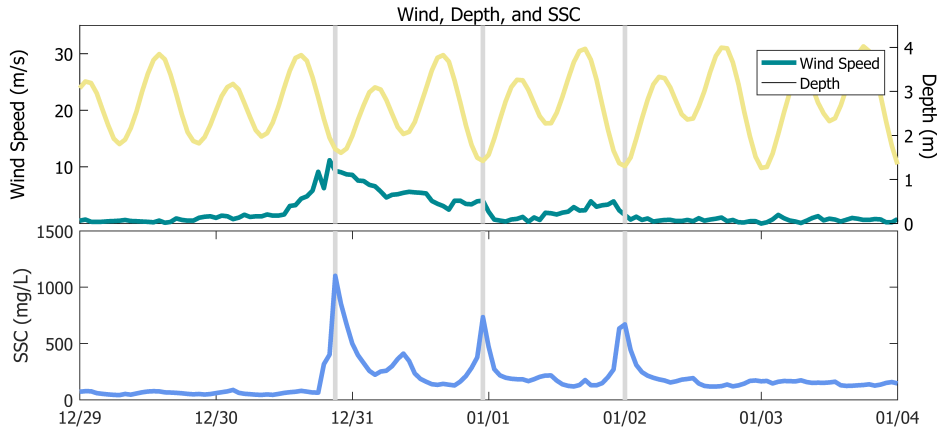

Figure 4.6: Relationship between wind, water depth, and SSC near the bed at WF1 (northern west flat) observation point. The highest SSC concentrations during this wind event are observed at low water, as shown by the gray vertical lines corresponding to SSC peaks.

sediments have a retention time in South Bay of longer than 9 months. The first pulse of Alameda sediments in December corresponds to a period of high Delta discharge, which influences the nature of water exchange between South Bay and Central Bay at Bay Bridge. Tracing the pathways of Alameda sediments for years with different hydrodynamic conditions could determine how the timing of Alameda discharge events relative to periods of high Delta discharge impacts the retention time of local (from a local watershed) sediments in South Bay.

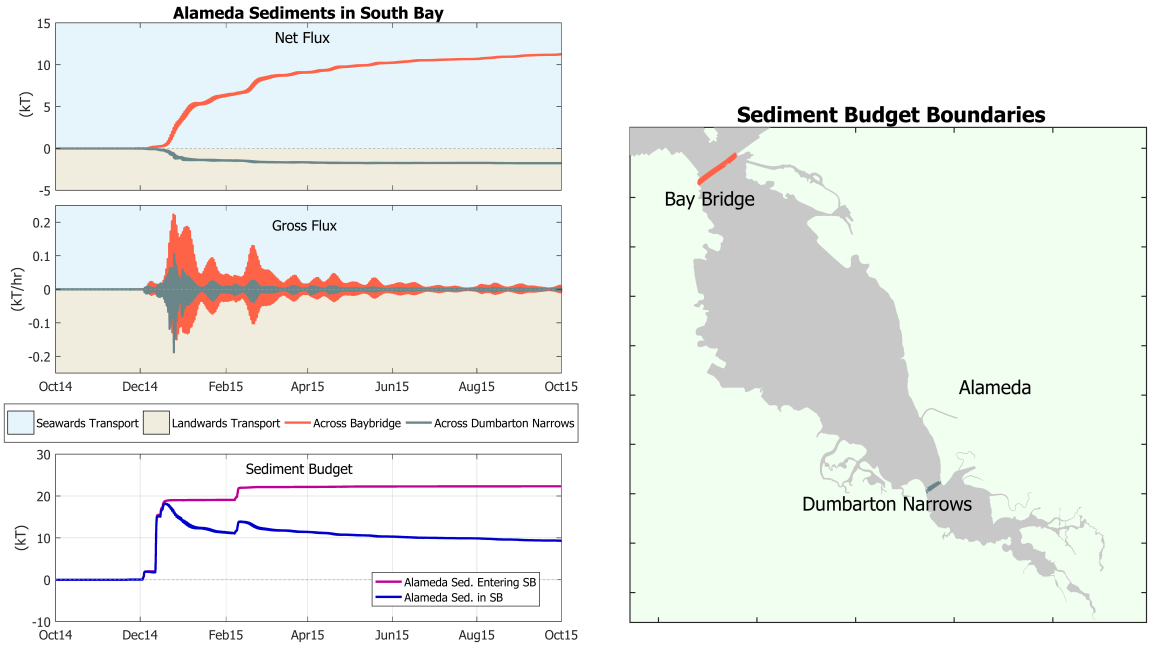

Figure 4.7: Behavior of sediments entering South Bay from Alameda Creek. The cumulative transport and net fluxes shown across the Bay Bridge transect and Dumbarton Narrows transect are only representative of sediments that enter the model domain via the Alameda River boundary. Of the 22.3 kT of sediment that enter from Alameda over the course of the year, approximately 50% are exported across Bay Bridge and less than 1% travel and remain south of Dumbarton.

4.2.2. Tracer Simulation II: Five years, North Bay Sediments

To investigate the fate of sediments entering South Bay via Bay Bridge, sediments starting north of Bay Bridge (including Central Bay, North Bay, and Delta Sediments) were traced over a five-year pe-

riod during which each year the hydrodynamics from WY 2015 were repeated. During the first year, sediments starting in the bed north of Bay Bridge and sediments delivered by the San Joaquin and Sacramento Rivers (Delta Sediments) were collectively labeled as "North Bay Sediments." Only sediments entering the model through the Delta during the first year were labeled and traced - sediments entering during subsequent years were not. The fate of these sediments is shown in Figure 4.8. The maps show that sediments entering South Bay tend to settle on the west flat and in the trench caused by dredging activities in the middle of South Bay. Further, sediments have a tendency to settle along the western bank of the primary channel that cuts through South Bay. This observation is consistent with findings by van der Wegen & Jaffe (2014)'s research into the controlling factors of accretion and narrowing of the major tidal channel observed further north in San Pablo Bay. Of the 1,600 kT of North Bay sediments that contribute to net landwards flux across Bay Bridge over the five year simulation period, approximately 10% are transported landwards across Dumbarton Narrows into far SFSB.

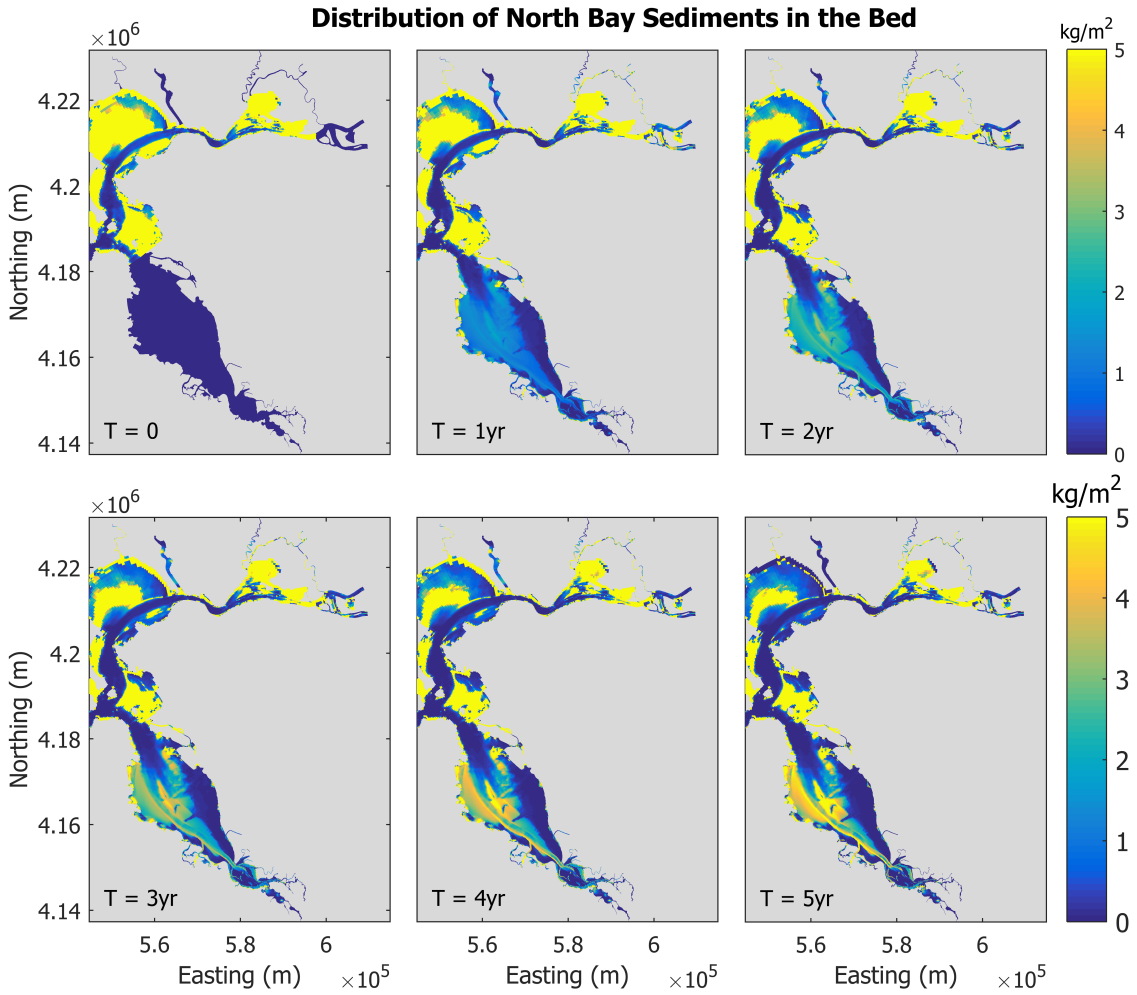

Figure 4.8: Distribution of North Bay sediments after a five-year simulation of the baseline year hydrodynamics. The initial sediment distribution is the result of the model spin-up procedure described in Section 3.2.6, which is why the sediment tracer is not uniformly distributed throughout Central and North Bay at T=0 years.

4.2.3. Tracer Simulation III: Four Years, Delta Sediments

Conventional wisdom is that sediment enters via the deep channel during periods of high Delta discharge and is redistributed on the shoals by wind waves in the summer (Brand et al. 2010, Conomos et al. 1985), but the origin of the sediments and the mechanisms that bring them into South Bay are uncertain. A tracer simulation was done to investigate the pathways of sediments entering the system

via the San Joaquin and Sacramento rivers during the first year of the simulation. These sediments were traced over the course of four years. The first three years simulate WY 2015 (maximum Delta discharge of approximately 2,000 m^3/s), and the fourth year simulates WY 2017, a wet year (maximum Delta discharge exceeding 10,000 m^3/s).

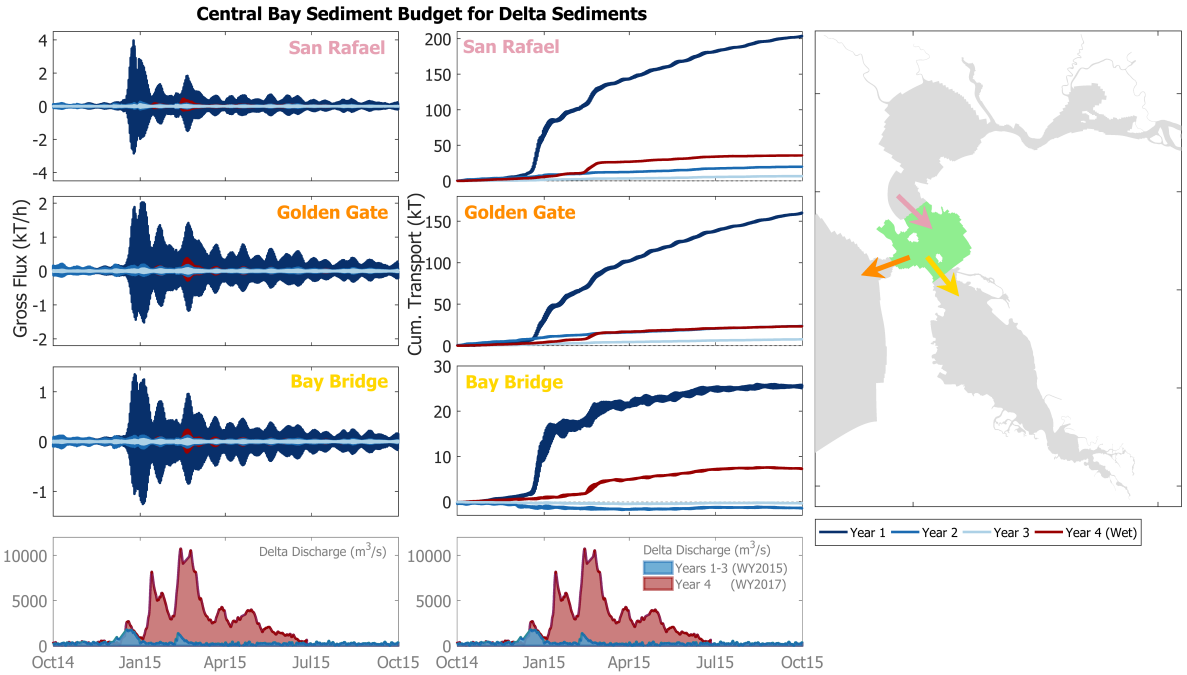

Figure 4.9: Sediment budget for Central Bay, only considering sediments originating from the San Joaquin and Sacramento Rivers during the first year of the four-year simulation. Positive transport is defined in the direction of the arrows (seawards across San Rafael, seawards across Golden Gate, and landwards across Bay Bridge).

Figure 4.9 shows the amount of Delta sediments entering and leaving Central Bay during each year of the simulation. During the first year, the labeled Delta sediments were delivered to the system; of the 203 kT of Delta sediments that passed landwards of the San Rafael transect during the first year, 160 kT (79%) of sediments exited the system via Golden Gate, and 26 kT (13%) entered South Bay. Most sediments delivered to the system settled landwards of Carquinez Strait during the first year (see Figure 4.3). During years two and three, which simulate the same hydrodynamics as the first year, the residual transport of the Delta sediments across Bay Bridge is seawards directed, meaning that more of the first year Delta sediments exit South Bay than enter. The fourth and final year simulated WY 2017 hydrodynamics, with extreme Delta discharge rates. The results show that the third and final Delta pulse (mid-February) with discharge rates exceeding 10,000 m^3/s contributed significantly to seawards transport of Delta sediments that had settled in North Bay during the first year. During the fourth year, 36 kT of first-year Delta sediments entered Central Bay across the San Rafael transect, 21% of which were imported into South Bay.

The first two pulses of Delta freshwater observed during WY 2017, with maximum discharge rates of approximately 2,700 and 8,000 m^3/s did not suspend and transport first-year Delta sediments as effectively as the third, extreme pulse. As shown in Figure 4.9, until the yearly maximum Delta discharge rates were observed in mid-February, the gross fluxes of first-year Delta sediments are smaller for the fourth year (red) than for the preceding three years (blue). In mid-February, the gross fluxes of traced sediments are bigger than those modelled during the second and third year.

The residual transport of traced sediments landwards across Bay Bridge during the fourth year was 28.5% the amount of residual transport modelled during the first year, when the sediments were delivered to the estuary. This suggests that extreme pulses of freshwater from the Sacramento and San Joaquin Rivers can effectively suspend and transport sediment that has previously accumulated in

North Bay from past Delta pulses.

4.3. Model Application to Different Hydrodynamic Scenarios

To better understand the mechanisms controlling sediment transport into and within South Bay, the DELWAQ model was applied to four hydrodynamic scenarios: the baseline case (WY 2015), a particularly wet year (WY 2017), WY 2015 with no wind, and WY 2017 without temperature and salinity.

4.3.1. Residual Flux

The cumulative flux across each transect was calculated based on gross fluxes observed over the course of each simulation. The final magnitude and direction of the cumulative transport across each transect represents the residual transport over the course of a year. The plots in Figure 4.10 show how the magnitude, and in a few cases direction, of the residual transport changes for the different hydrodynamic scenarios.

4.3.2. No Wind

Wind can influence transport patterns by generating wind-induced currents and by generating waves that entrain sediments in the water column. Compared to the baseline scenario, the direction of residual transport across all transects is the same with or without wind. The major difference between these two cases is that the magnitude of residual transport in the no wind case is much less than that for the baseline case. This is likely due to the fact that wind generates waves that suspend sediments on the flats, making them available for transport.

The comparison of residual transport across Bay Bridge during the simulation of WY 2015 and the case without wind (Figure 4.12a) shows that the magnitude of landwards residual flux across the mouth of South Bay is 44% less when wind is excluded from the model. This could be attributed to a lack of sediment suspension on the flats in North Bay during the no-wind scenario. As illustrated by Figure 4.11, the cumulative transport into San Pablo Bay across Carquinez Strait is only reduced by 18% by excluding wind, but the cumulative transport out of San Pablo Bay through San Rafael is reduced by 68%. This indicates that wind plays a role in suspending sediments in San Pablo Bay, making them available for transport seawards towards Central and South Bay.

4.3.3. Wet Year

The direction of residual flux across Bay Bridge (the mouth of South Bay) is in opposing directions for the baseline simulation and the wet year simulation; there is a net export of sediment during WY 2015 and a net import of sediment during the wet year simulated. Figure 4.12b provides insight into the direction of residual transport across Bay Bridge under different conditions. During the wet year, more sediment travels landwards across the Bay Bridge transect near the bed than in the WY 2015 case. The bulk of this landwards transport occurs between January and August. During this period following high and extreme Delta discharge rates an amplified classical estuarine circulation pattern can be observed; South Bay has recently been freshened and Central Bay returns to oceanic values. During this period, bottom currents at Bay Bridge are directed landwards, and the residual landwards flux near the bed is accelerated, as seen by the steepening of the cumulative transport curve.

Tide Error
An error in the tidal forcing for the WY 2017 simulations (Wet Year and Barotropic) was realized without ample time to re-run the D-FLOW model. The tidal signal superimposed on river discharge at the San Joaquin and Sacramento River boundaries is 180^o out of phase with the correct signal imposed at the sea boundary. The impact of this error on modelled sediment transport is unknown, however it may be responsible for differences in sediment fluxes near the bed across Bay Bridge between the baseline and wet year simulations prior to December. From October-December, the the Delta discharge magnitudes for WY 2015 and WY 2017 are comparable, so it is expected that sediment fluxes during this period are comparable as well.

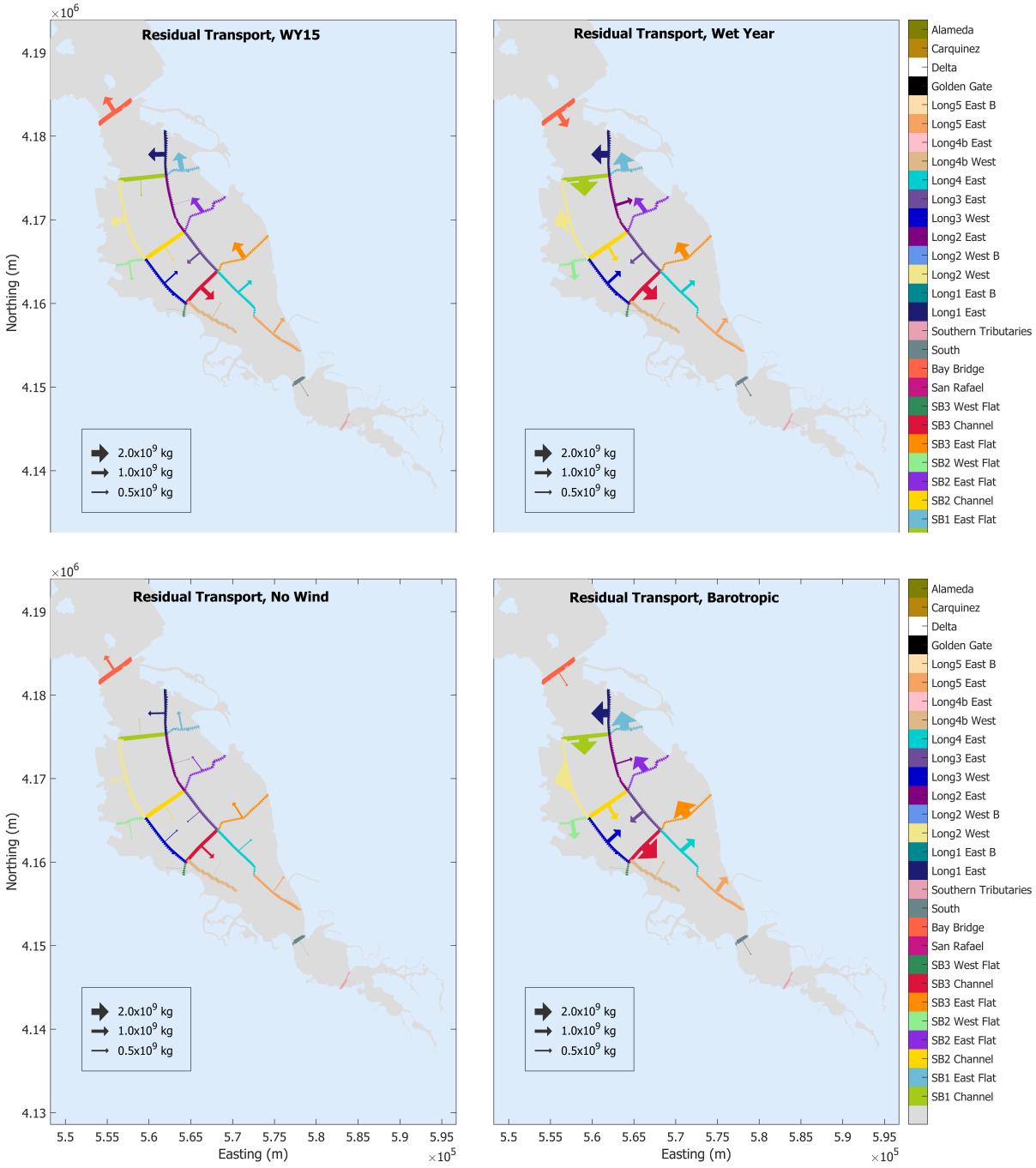

Figure 4.10: Residual sediment transport over the course of one year for four different hydrodynamic scenarios. The width of the arrows scales with the normalized magnitude of residual transport. The transport magnitudes for all scenarios were normalized by the same value, so the relative magnitude of transport can be compared for all simulations. The no wind simulation is is the same as the WY 2015 baseline simulation, but without wind. The barotropic simulation is the same as the wet year simulation, but without temperature and salinity.

4.3.4. Barotropic

Figure 4.12c shows the difference in sediment flux across Bay Bridge for the wet year and for the simulation excluding salinity and temperature. The residual transport including density-driven circulation is two orders of magnitude greater than that during the barotropic simulation. The impact of baroclinic circulation on sediment exchange at Bay Bridge is illustrated by comparing the behavior of sediment

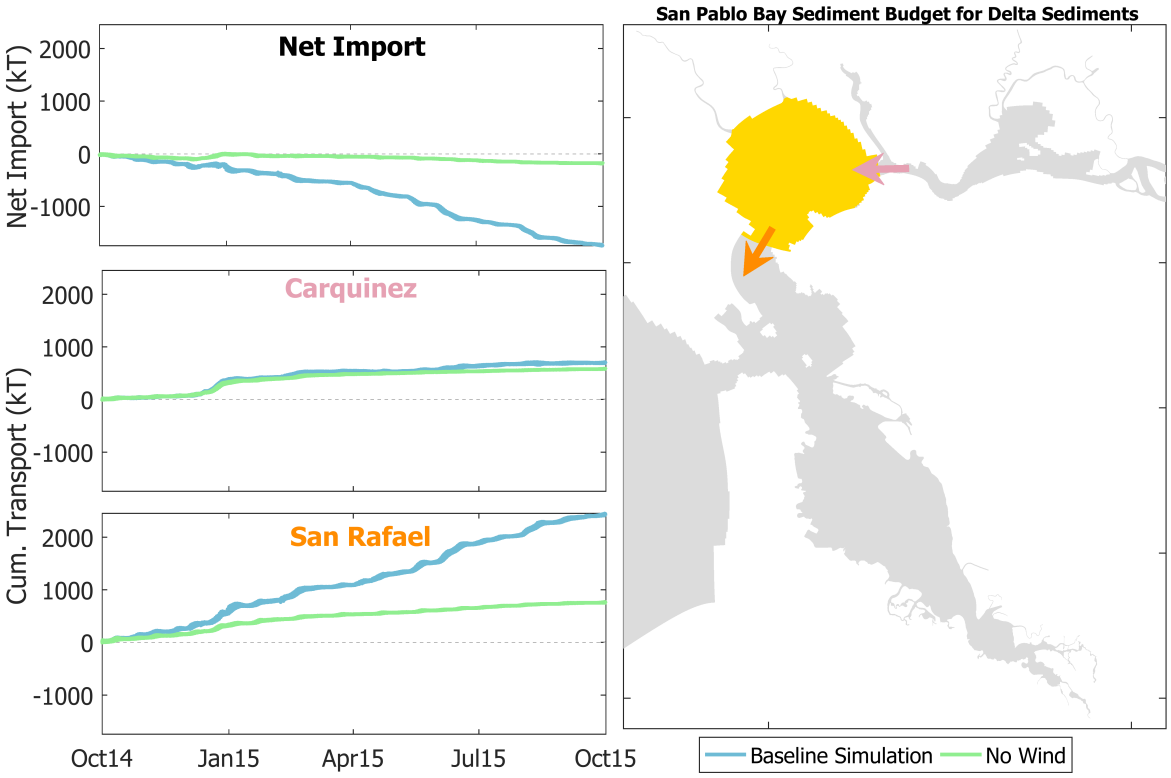

Figure 4.11: Comparison of sediment budgets for San Pablo Bay for the baseline simulation and the simulation without wind. The net import is calculated as the difference between residual transport into San Pablo Bay through Carquinez Strait and residual transport out of San Pablo Bay across the San Rafael transect.

fluxes near the surface and near the bed during the wet year and barotropic simulations. The plot on the right of Figure 4.12c shows that the direction of net near-bed and near-surface sediment transport responds to varying levels of Delta discharge during the wet year simulation, but during the barotropic simulation the direction of net surface fluxes is consistently seawards and the direction of net bottom fluxes is consistently landwards for the entire simulation.

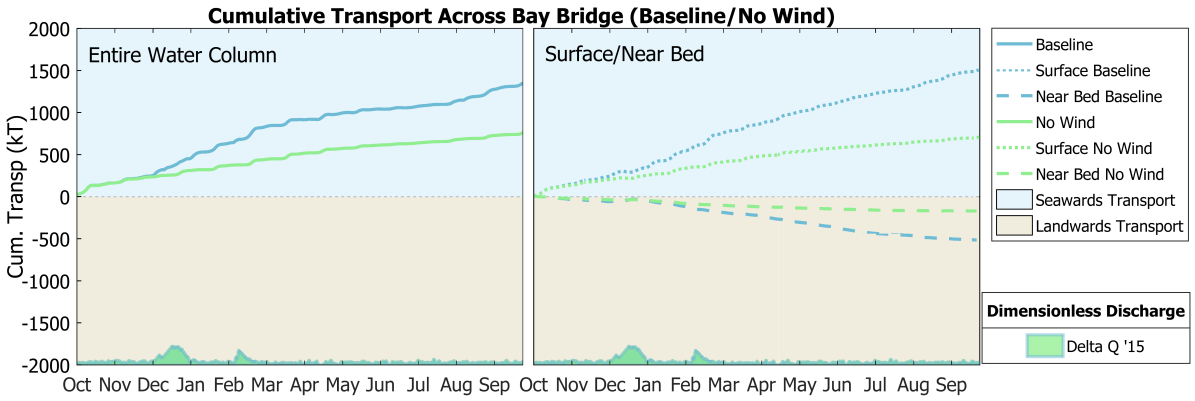

(a) Comparison of cumulative transport across Bay Bridge for the baseline simulation and the no wind simulation. The residual transport across Bay Bridge is approximately 44% less for the case without wind.

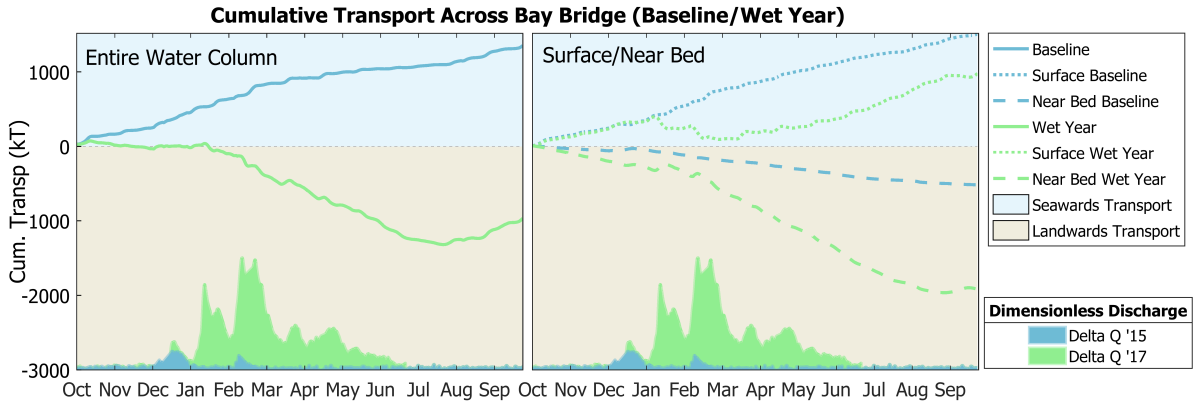

(b) Comparison of cumulative transport across Bay Bridge for the baseline (WY 2015) simulation and the wet year (WY 2017) simulation. The maximum Delta discharge during WY 2015 is approximately 2,000 m^3/s, and the maximum discharge rate for WY 2017 exceeds 10,000 m^3/s.

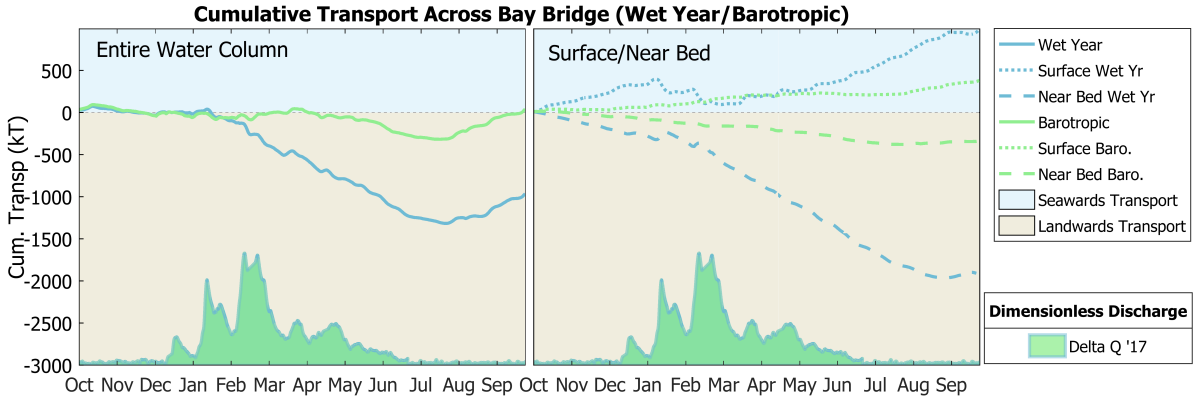

(c) Comparison of cumulative transport across Bay Bridge for the wet year simulation and the barotropic simulation, both forced with Delta discharge rates from WY 2017.

Figure 4.12: Comparisons of daily averaged cumulative transport across Bay Bridge transect between (a) the baseline and no wind simulations, (b) the baseline and wet year simulations and (c) the wet year and barotropic simulations. The plots on the right show the cumulative transport across Bay Bridge transect near the surface (upper three vertical layers of the water column) and near the bed (lower three vertical layers of the water column.

4.3.5. Exchange of Sediments between the Channels and the Shoals

Figures 4.13 and Figure 4.14 show sediment fluxes measured across transects separating the primary, deep channel from the western and eastern shallow flats in South Bay. By looking at the net fluxes and cumulative (residual) flux across each transect, Figure 4.13 suggests that residual transport is the result of asymmetrical net fluxes over diurnal and neap/spring tidal cycles. The magnitude of net sediment flux fluctuations is larger for the transects closer to the mouth of South Bay, likely due to the stronger influence of the tide in the north of South Bay. The pink horizontal line in the figures correspond to the strongest wind speeds observed during the time period modelled (>10m/s). Sediments suspended on the flats during this wind event were transported from the channel to the west flat across Transects #2 and #3 (see Figure 4.13). Wind-induced wave resuspension amplified transport from the channel to the east flat across Transects #6 and #7.

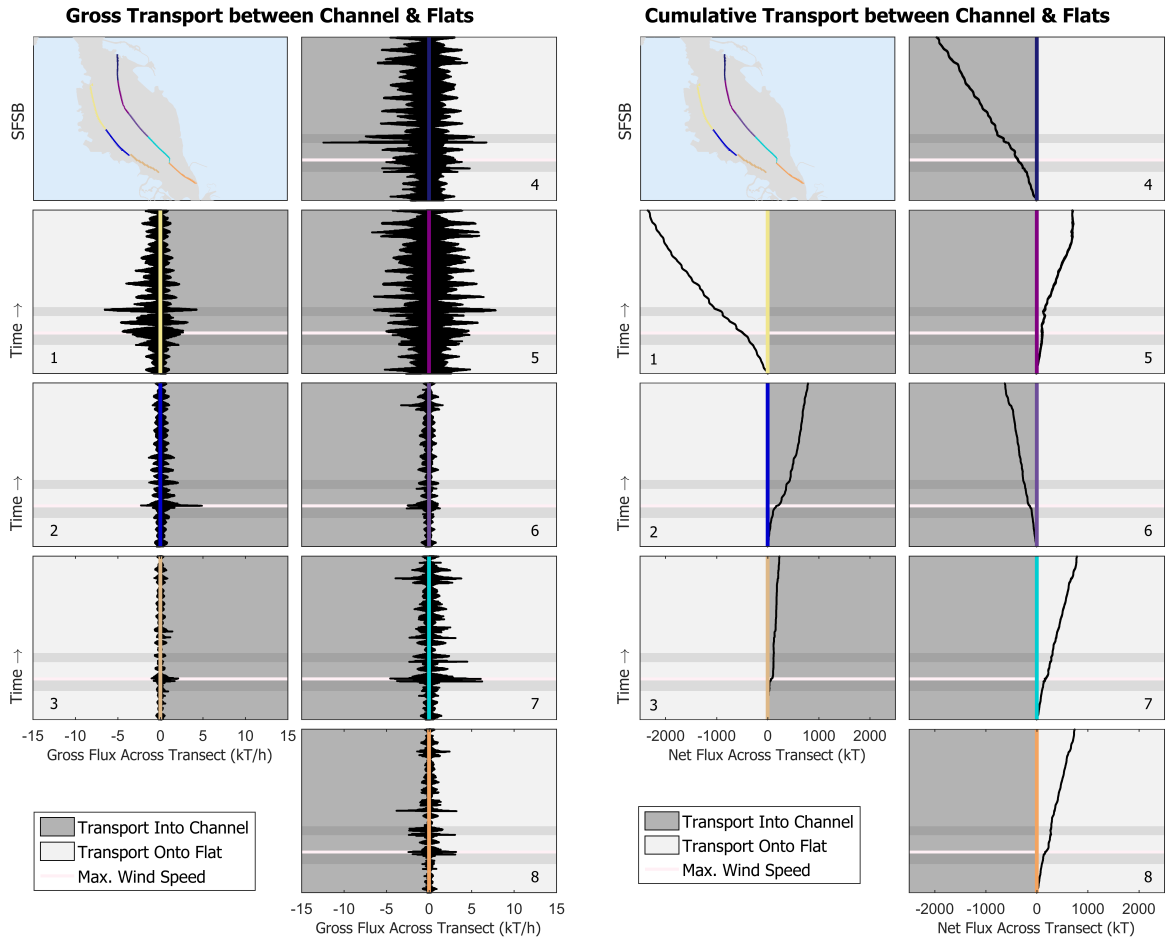

(a) Gross flux of sediment across transects parallel to the longitudinal axis of South Bay, separating the primary channel from the eastern and western flats.

(b) Cumulative transport of sediments across transects parallel to the longitudinal axis of South Bay, separating the primary channel from the eastern and western flats.

Figure 4.13: Sediment exchange between the channel and the eastern and western flats in South Bay for the baseline simulation. The dark gray areas represents the channel, flanked by the flats (lighter gray) on either side. The colors of the y-axes correspond to transects parallel to the channel, separating the channel from the flats. The location of the transects is shown in the maps in the upper left and in Figure 3.10. The horizontal gray bands represent the two time periods corresponding to pulses of freshwater from the Delta during WY 2015, and the horizontal pink line corresponds to the maximum wind speed event.

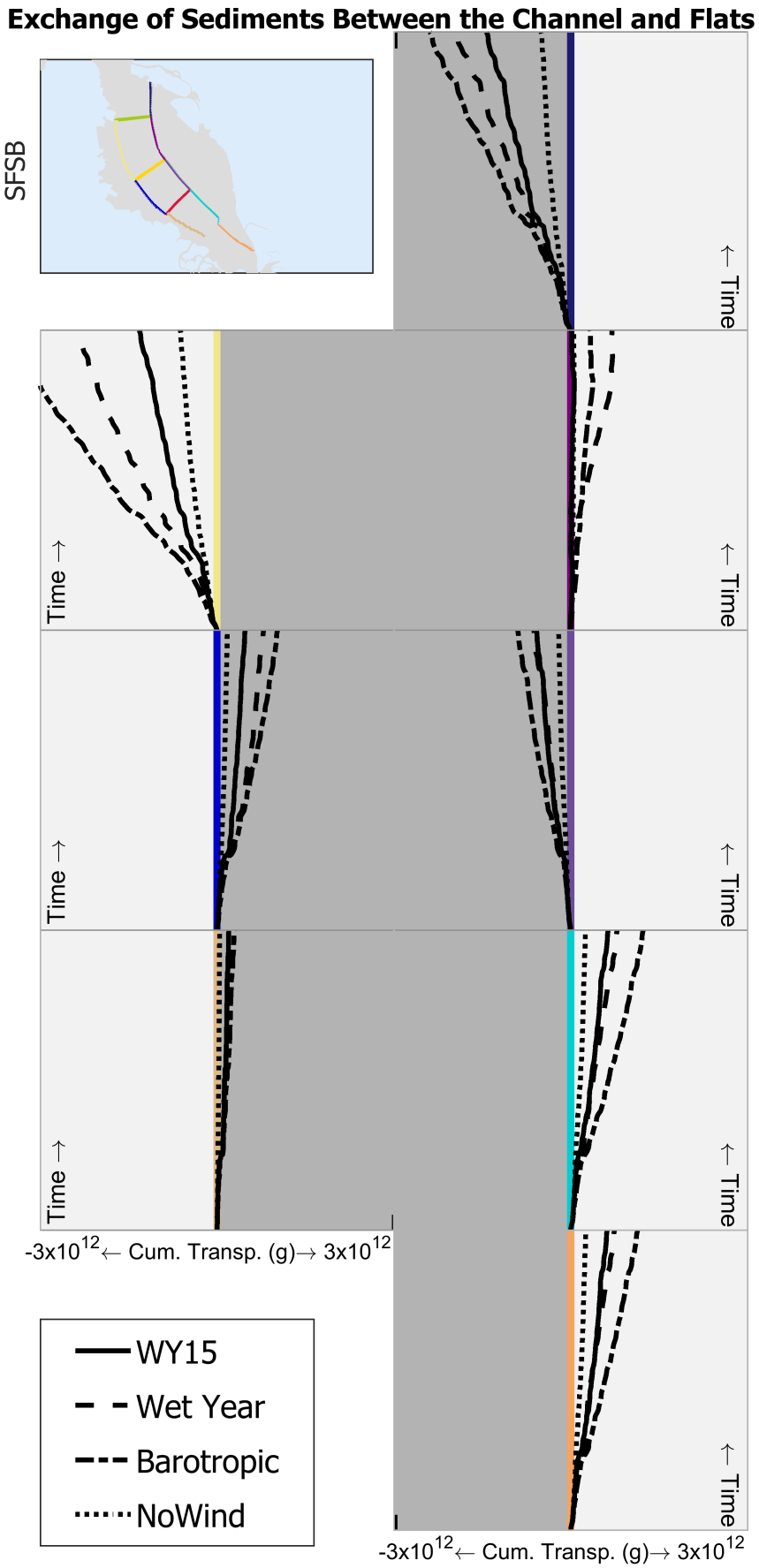

Figure 4.14: Exchange of sediments between the channel and the flats in South Bay for all scenarios. Each subplot contains the net transport of sediments across a transect parallel to South Bay's longitudinal axis. The color of the y-axis corresponds to the transect color in the map of South Bay (top left).

4.3.6. Correlation Analysis

To evaluate the impact of density-driven circulation on sediment transport in South Bay, salinity differences in South Bay were compared to sediment fluxes. The gross sediment fluxes across cross-sections in South Bay were monthly averaged to reduce the influence of the semi-diurnal and neap-spring tidal signals. These values were compared to the corresponding monthly averaged density differences in South Bay. Sediment fluxes were compared to vertical and horizontal "local" and "global" salinity differences. The vertical salinity difference refers to the difference in salinity between the surface and the bed at a given point, while the horizontal difference refers to the difference in depth-averaged salinity between two coordinates. Pubben (2017) found that salinity dominates over temperature in determining water density in SFB, so correlations between sediment fluxes and salinity differences indicate the influence of density-driven circulation on sediment transport.

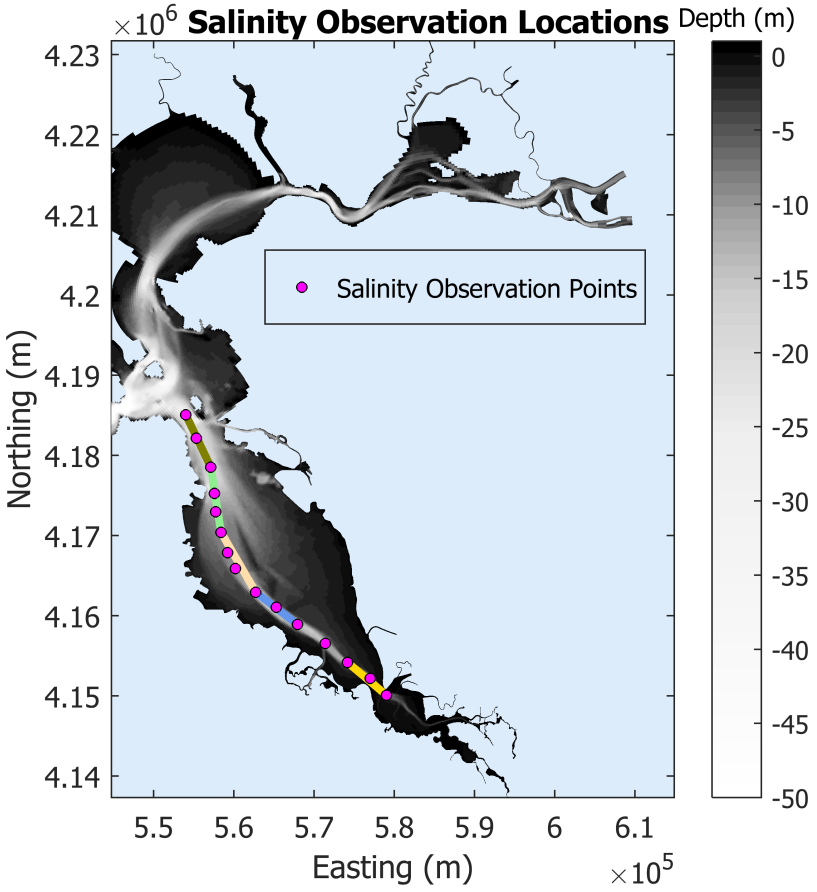

Figure 4.15: Location of points at which salinity information was used to calculate "global" and local salinity differences in South Bay. The colored lines show points that were used to calculate local salinity gradients.

Global vertical salinity differences were calculated by taking the difference between the average of the salinity values in the upper and lower vertical layers of the water column at each salinity station shown in Figure 4.15 for each timestep. The global horizontal salinity differences were calculated by taking the difference between the depth averaged salinity for each timestep at a station near the mouth (just south of Bay Bridge), and at a station just north of Dumbarton Narrows.

$$Global\,\Delta S_{Vert}\,(t) = \left(\frac{\sum_{p=1}^{npts} S\,(t,p)_{surface}}{npts}\right) - \left(\frac{\sum_{p=1}^{npts} S\,(t,p)_{bed}}{npts}\right) \tag{4.1}$$

$$Global\,\Delta S_{Horiz}\,(t) = \left(\frac{\sum_{l=1}^{nlayers} S\,(t,l)_{BayBridge}}{nlayers}\right) - \left(\frac{\sum_{l=1}^{nlayers} S\,(t,l)_{Dumbarton}}{nlayers}\right) \quad (4.2)$$

with:

ΔS = Salinity Difference $[ppt]$
t = timestep $[hr]$
$p\,/\,npts$ = salinity point / total number of salinity points (15); see pink dots in Figure 4.15
$l\,/\,nlayers$ = vertical layer of water column / total number of vertical layers (10)

The calculated global salinity station differences are shown in Figure 4.16 for both WY 2015 and WY 2017 hydrodynamics. The effect of the pulses of freshwater discharge from the Delta are noticeable, and the impact of the neap-spring tidal cycle is amplified during times when the salinity field is impacted by Delta Discharge, evidence of tidal straining. Notice in WY 2015 how the neap-spring signal present in the vertical salinity difference between January and March is dampened following the freshwater pulses. For both WY 2015 and WY 2017, the global, horizontal salinity difference between the mouth of South Bay and Dumbarton Narrows is around 1ppt during the dry period (low Delta discharge). A pulse of freshwater from the Delta freshens Central Bay with respect to South Bay, and the horizontal salinity difference temporarily becomes negative, generating reverse estuarine circulation. Following the initial pulse, Central Bay returns to oceanic salinity values, while South Bay maintains low salinity from the Delta Discharge flushing. This causes a horizontal salinity difference that is higher than the baseline difference at the beginning of the simulation (around 2-3ppt for WY 2015 and 8-9ppt for WY 2017). These patterns are consistent with the observations of salinity gradients in South Bay described by McCulloch et al. (1970) and Conomos et al. (1985).

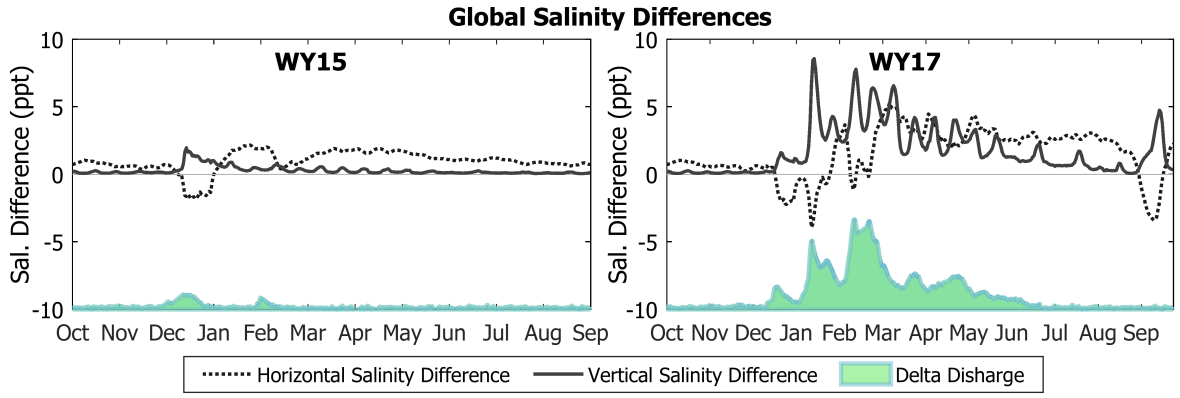

Figure 4.16: Global horizontal and vertical salinity differences across South Bay for the baseline simulation (WY 2015) and the wet yearr simulation. Values are daily averaged (over 24 time steps of one hour). The Delta discharge hydrograph is shown to compare the salinity gradients with Delta discharge. Evidence of tidal straining (periodic reinforcement of stratification due to the tide) is present, especially after the Delta freshwater pulses.

The local vertical salinity differences were calculated by taking the difference between the salinity near the bed and near the surface at the salinity point closest to each transect. The local horizontal salinity differences were calculated for each segment (seg in Equations 4.3 and 4.4), represented by a colored line in Figure 4.15. The depth averaged salinity difference between the most landwards and seawards stations of each segment was taken as the local horizontal salinity difference.

$$Local\,\Delta S_{Vert}\,(t,p) = S\,(t,p)_{bed} - S\,(t,p)_{surface} \quad (4.3)$$

$$Local\,\Delta S_{Horiz}\,(t,seg) = S\,(t,p_{seawards})_{seg} - S\,(t,p_{landwards})_{seg} \quad (4.4)$$

The outcome of the correlation analysis carried out to quantify the relationship between forcings and sediment behavior in South Bay is presented here.

Tidal Flats

The comparison between the baseline scenario and the baseline scenario without wind demonstrated the importance of wind and sediment suspension in determining sediment flux magnitudes. No significant correlation between SSC and wind speed were found on any of the 7 observation points distributed across the east and west flats. This is likely due to the fact that SSCs are not only dependent on wind speed. Rather, it is the timing of wind speed, wind direction, and water depth, that collectively influence SSCs. As these different forcings operate on varying timescales (diurnal wind patterns, gusty winds lasting hours, semi-diurnal tidal cycle, neap-spring tidal cycle), it is difficult to find direct correlations. Another possible explanation for the lack of strong correlations could be the location of the observation points at which the SSC time series were extracted. Behavior at observation points in shallower water (1-2m) might be more tightly linked to wind and wave events than on the middle of the flats (2-4m).

Figure 4.17 shows the correlation between north-south transport across two transects on the east flat and salinity differences in South Bay. The lack of a strong correlation indicates that density-driven circulation is not tightly linked to sediment transport on the flats.

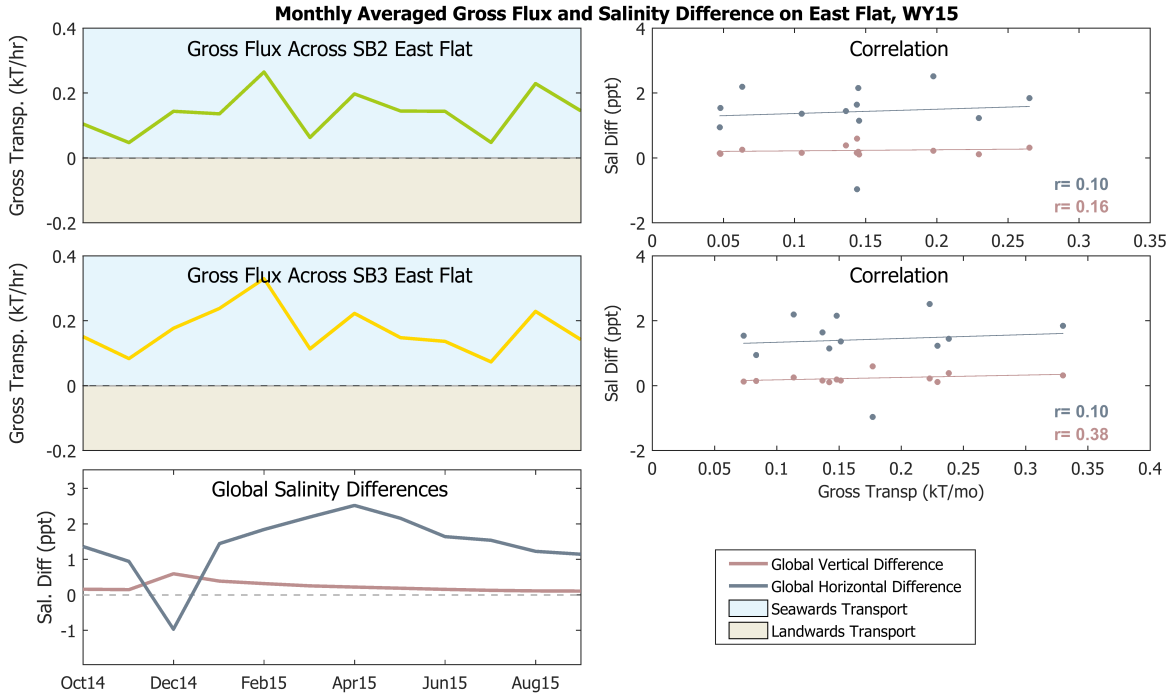

Figure 4.17: Correlations between monthly averaged gross transport across SB2 East Flat and SB3 East Flat transects and salinity differences. These transects are are perpendicular to the primary channel and located on the east flat in South Bay (see Figure 4.1 for transect map). There is not a strong correlation between transport across the east flat and salinity gradients in South Bay.

Channel

The cumulative transport curves (Figure 4.18) across several transects near the mouth of South Bay indicate that sediment transport in the northern channel is significantly impacted by freshwater discharge from the Delta for both the baseline scenario and the wet year scenario. This is evident by the change in slope of the cumulative transport curve that begins with the first freshwater pulse and lasts for months afterwards. To quantify the degree to which transport is related to Delta discharge, the monthly averaged gross transport across cross-sections in South Bay were compared to monthly averaged horizontal (Bay Bridge vs. Dumbarton) and vertical (surface vs. bed) salinity differences in South Bay. The results of the correlation analysis are shown in Table 4.2. The strongest correlation is between monthly averaged gross flux at the SB2 transect and the global horizontal salinity difference. See Figure 3.10 for a map of transect locations.

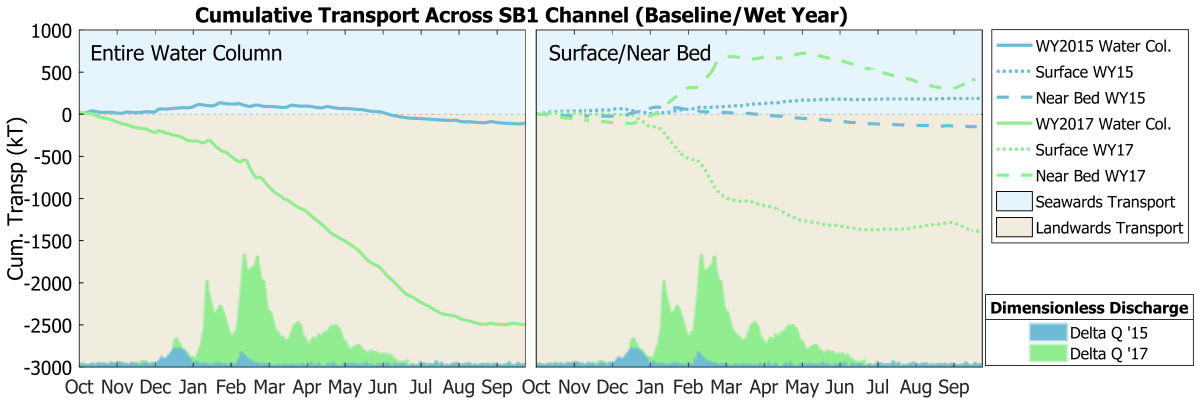

(a) Cumulative transport across transect SB1 Channel, which cuts across the main channel south of Bay Bridge.

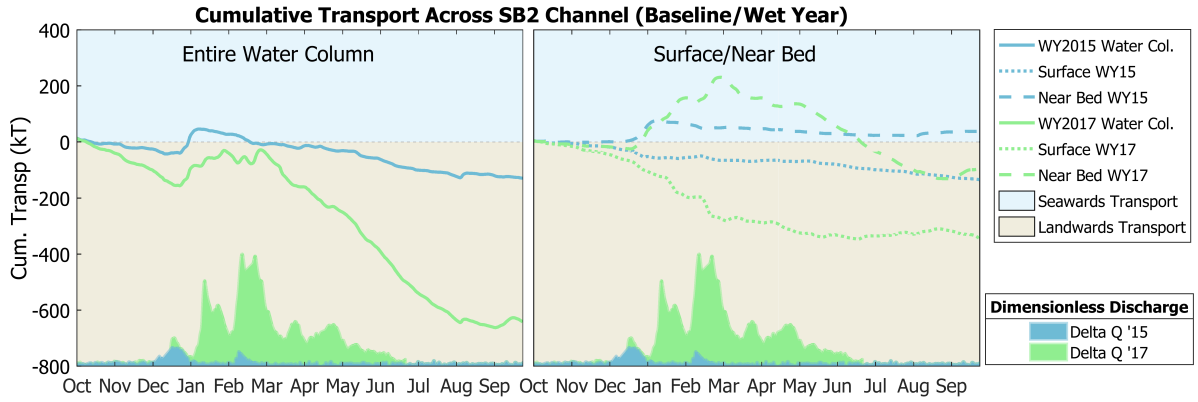

(b) Cumulative transport across transect SB2 Channel, which cuts across the main channel south of SB1 Channel. Gross flux across this cross-section showed the strongest correlation between salinity differences in South Bay.

Figure 4.18: Comparison of cumulative transport across channel cross-sections in northern South Bay for the baseline case (WY 2015) and a particularly wet year (WY 2017). See Figure 3.10 for a map showing transect locations. The surface transport and near-bed transport were calculated based on sediment fluxes across the top three and bottom three hydrodynamic layers.

Table 4.2: Pearson correlation coefficients between monthly averaged gross transport over certain transects and global and local vertical and horizontal salinity gradients in South Bay.

Transect	**Horizontal/ Vertical**	**Correlation Coefficients**			
		Baseline		**Wet Year**	
		Global Diff.	Local Diff.	Global Diff.	Local Diff.
Bay Bridge	Horiz.	0.62	-0.32	0.19	0.86
	Vert.	-0.68	-0.70	0.73	0.79
SB1 Channel	Horiz.	0.75	0.55	0.41	0.89
	Vert.	-0.63	-0.62	0.73	0.73
SB2 Channel	Horiz.	0.79	0.79	0.92	0.87
	Vert.	-0.60	-0.72	0.01	-0.25
SB3 Channel	Horiz.	0.24	0.02	0.64	0.41
	Vert.	0.29	0.02	0.42	0.15
Dumbarton Narrows/ South	Horiz.	-0.13	-0.63	0.19	0.08
	Vert.	0.47	-0.56	0.73	0.28

The model results suggest that the direction and magnitude of sediment flux in northern South Bay

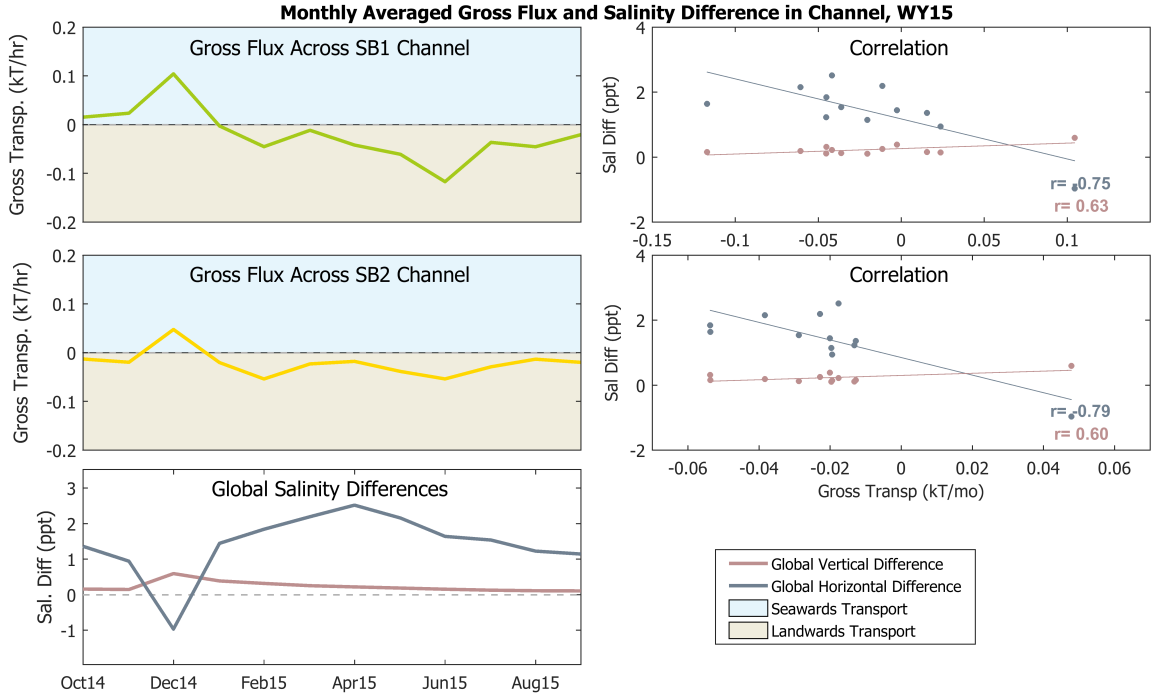

(a) Correlations between monthly averaged gross transport across transects SB1 Channel and SB2 Channel and global salinity differences for the baseline simulation.

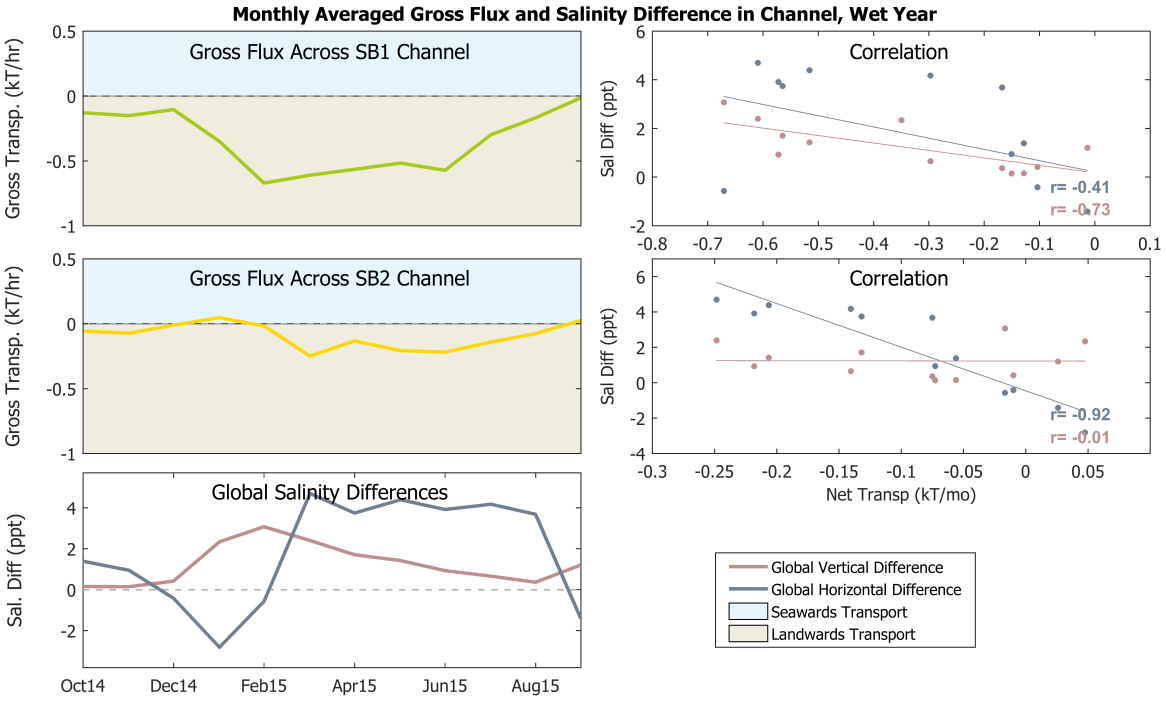

(b) Correlations between monthly averaged gross transport across transects SB1 Channel and SB2 Channel and global salinity differences for the wet year simulation.

Figure 4.19: Relationship between gross transport and salinity differences in South Bay channel for (a) the baseline simulation and (b) the wet year simulation.

varies significantly near the bed and near the surface, as illustrated by Figure 4.18. The correlation between monthly averaged gross fluxes and horizontal differences indicates that sediment transport near the mouth of South Bay is linked to currents induced by density gradients in South Bay. At the two cross-sections shown in Figure 4.18 (SB1 Channel and SB2 Channel, located landwards of Bay Bridge), the directions of residual sediment fluxes near the surface and near the bed are different during the period of high Delta discharge, characterized by higher salinity in South Bay than in Central Bay, and during the period of reducing delta Discharge, characterized by higher salinity in Central Bay than in South Bay.

In the beginning of the period of high Delta Discharge, before baroclinic flows have flushed South Bay with freshwater, the salinity in Central Bay becomes lower than that in South Bay (Figure 4.16). During this period, net sediment fluxes near the surface at SB1 Channel and SB2 Channel cross-sections are directed landwards and near-bed fluxes are directed seawards, evidence of reverse estaurine circulation.

In the period following high Delta Discharge (March-August), net flux across transects SB1 Channel and SB2 Channel is directed landwards both near the surface and near the bed, indicated by the negative/landwards slope of the cumulative transport curves in Figure 4.18. This suggests that during periods of reducing Delta discharge, transport across these transects is more tightly linked to the horizontal salinity gradient across South Bay's longitudinal axis.

During the wet year simulation, the direction of the residual flux across SB1 Channel transect near the surface is landwards directed and the residual flux near the bed is seawards directed; during the baseline simulation, residual flux near the surface is seawards directed, and residual flux near the bed is landwards directed. This indicates that the magnitude of Delta discharge influences the vertical distribution of net sediment flux in the northern channel of South Bay.

4.3.7. Delta Discharge & Sediment Exchange at Bay Bridge

The results of the tracer analyses and the application of the DELWAQ model to different hydrodynamic scenarios suggests that the nature of sediment exchange between South Bay and Central Bay is linked to horizontal salinity gradients along the longitudinal axis of South Bay, induced by varying degrees of freshwater discharge from the Sacramento and San Joaquin Rivers. The magnitude of Delta discharge influences whether South Bay will experience a net import or net export of sediments in a given year. Figure 4.20 shows the average gross sediment flux for each vertical layer of the water column across Bay Bridge for three different periods characteristic of low, high, and reducing Delta discharge. The average gross flux over these periods can be used as an indicator of residual flux. During periods of low Delta discharge (e.g. during the summer), residual flux near the surface dominates, and a net export of sediments from South Bay is observed. During periods of high Delta discharge, when the gravitational circulation reverses because Central Bay becomes less saline than South Bay, residual fluxes near the surface and the bed are landwards directed, and South Bay imports sediments. Once Central Bay returns to oceanic values, horizontal salinity gradients induce strong estuarine circulation, resulting in residual landwards near-bed transport that dominates over seawards-directed transport near the surface; as a result, South Bay imports sediments.

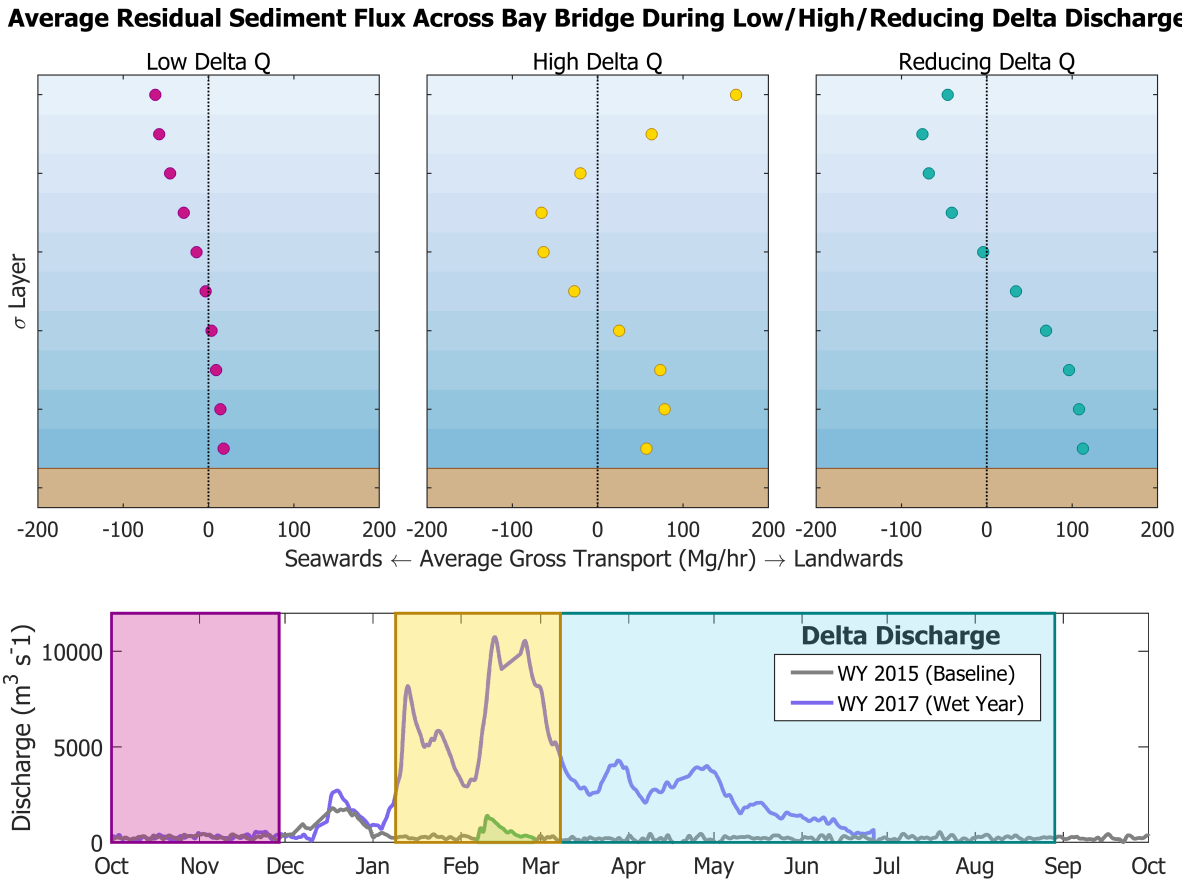

Figure 4.20: Average gross sediment flux across Bay Bridge during periods of low, high, and reducing Delta discharge. The time periods over which the averaged values were calculated are shown by corresponding colored boxes overlaid on the Delta hydrographs. The average gross fluxes for the period of low Delta discharge were based on modelled fluxes for WY 2015, and the average gross fluxes for the periods of high and reducing Delta discharge were based on modelled fluxes for WY 2017 during which the effects of freshwater discharge on density-driven circulation are more pronounced.

5

Discussion

In this chapter, the results of the model calibration and application are evaluated with consideration for the assumptions and limitations of the methodology applied. The advantages and shortcomings of the offline DELWAQ-D-FLOW coupling are discussed, and recommendations for further model improvement and research applications are proposed. In furthering our understanding of the SFB system, the DELWAQ model can serve as a tool to inform more educated, sustainable management decisions. This chapter highlights potential model applications in the context of water quality, habitat restoration, and climate change.

5.1. Modelling Fine Sediments in DELWAQ

The DELWAQ model developed and calibrated in this study provides a powerful tool to investigate how complex, spatially and temporally varying processes influence sediment transport in SFB. This study shows that an offline coupling of a D-FLOW hydrodynamics model and a DELWAQ sediment tracer model provides an efficient way to study fine sediment transport in estuarine environments where 3D circulation plays a prominent role. Here, the benefits and drawbacks of this methodology are discussed.

Pros:

- **Efficiency**: Applying the DELWAQ model to output from the D-FLOW model avoids having to recompute the computationally expensive hydrodynamics with each simulation. Running the D-FLOW model to simulate one year plus a two month spin-up period takes about 10 days, while the DELWAQ model only requires 11 hours to simulate sediment transport for the same time period.
- **WQ Applications**: Modelling suspended sediments in DELWAQ allows for easy applications in the context of water quality modelling (e.g. SPM field from DELWAQ model can be used to determine light climate for phytoplankton in DELWAQ-BLOOM model).
- **3D Capabilities**: 3D sediment dynamics is not yet implemented in Delft3D FM software.
- **Avoid Effects of Hydrodynamic Spin-Up**: By starting the DELWAQ simulation after the hydrodynamic spin-up period has ended, sediment fluxes and redistribution are not impacted by the unrealistic behavior during the hydrodynamic spin-up period.

Cons:

- **Loss of Feedback**: The offline coupling of the two models reduces the feedback between environmental and hydrodynamic forcings and sediment behavior (further discussed in Section 5.1.1). Modelling sediments online in Delft3D Flow can simulate sediment-density coupling and morphological feedback, while the offline coupling between DELWAQ and Delft3D FM Flow cannot.
- **Required Expertise**: This methodology requires the knowledge of two models, rather than just one. Linking output from the D-FLOW and DELWAQ models requires additional post-processing. The labelling of sediments and creation of cross-sections to measure sediment fluxes for an unstructured grid is not trivial, and are more easily implemented in D-FLOW

5.1.1. Modelled SSCs

While the neap-spring signal was well represented by the model, the degree to which the model captures SSC fluctuations on a sub-tidal timescale requires more attention. The direction of residual transport remained constant for all calibration parameter settings tested, likely due to the strong influence of tidal advection on SSCs and sediment transport. However, if used for other applications (e.g. phytoplankton modelling), further calibration is needed to better reproduce SSC fluctuations on shorter timescales. The modelled SSCs on the flats are higher at low water than at high water during high wind events (Figure 4.6). This is not consistent with observations by Lacy et al. (1996) or Brand et al. (2010), who found that SSCs in South Bay were higher during flood tides following wave-induced re-suspension at low water. Brand et al. (2010) concluded that sediments suspended by waves during ebb remained in the bed boundary layer on the flats, and that energy from tidal currents was needed to entrain these sediments higher in the water column. Comparisons between bed shear stresses, as determined by the near-bed velocity profile, and vertical sediment flux by Brennan et al. (2002) also suggest that sediments on the flats are restricted to the bed boundary layer during slack tide. The fact that modelled spikes in SSC on the flats correspond to low water during wind wave resuspension events indicate that this phenomena is not currently captured in the DELWAQ sediments model. Further calibration of the sediments model should focus on the phasing of SSC concentrations over the course of a tidal cycle. The tuning of the mud parameters in DELWAQ during the calibration procedure changed the magnitude of the SSC fluctuations, but did not significantly impact the phasing, so alterations to parameters in D-FLOW might also have to be explored to improve model performance, as explained in Section 5.1.1.

Bed Shear Stresses

As resuspension scales with the excess bed shear stress, further investigation into how wind and wave events are translated into bed shear stresses could help to improve the accuracy of the modelled SSC signal over shorter timescales. The coupling of the D-FLOW and DELWAQ models provides an efficient method to study sediment dynamics in SFB while accounting for the 3D effects of wind, waves, temperature, salinity, river discharge, and the tide. However, the offline coupling limits the degree to which the sediment tracer model can be calibrated, as the parameters controlling how the bed shear stresses are calculated are built into the D-FLOW model. The DELWAQ sediments model is calibrated by altering the parameters that control the vertical exchange of sediments between the bed and the water column (sediment fall velocity, w_s, critical shear stress for erosion, $\tau_{E,crit}$, and erosion rate, M). Tuning the erosion parameters and the critical shear stresses control how the DELWAQ model simulates the response of bed sediments to bed shear stresses induced by waves and currents; however there is no control over how hydrodynamic forcings (e.g. waves, currents) are translated into bed shear stresses in DELWAQ. For complete control over the behavior of the sediments in the DELWAQ model, the calibration would have to include the sensitivity of the coupled D-FLOW-DELWAQ models to changes in how the bed shear stresses are calculated.

For example, in the D-FLOW model, the wave component of the bed shear stress scales with a wave friction factor f_w, which is a function of the bed roughness length. Changes in the bed roughness in the D-FLOW model, therefore, impact the bed shear stresses that are fed into the DELWAQ sediments model and influence fine sediment settling and resuspension. Though no data on bed shear stresses is available for the time period used for calibration, Brennan et al. (2002) and T. Cheng et al. (1999) provide in-situ bed shear stress measurements in SFB that can be used for qualitative comparison. T. Cheng et al. (1999) found that the roughness length in South Bay varied over the course of the tidal cycle, which is not accounted for in the hydrodynamic model where a constant roughness length is assumed. For further details on how the bed shear stress is calculated in D-FLOW see Appendix A.

Tuning D-FLOW parameters to evaluate the impact on the DELWAQ sediments model behavior is a time consuming task, as each D-FLOW run takes about 10 days. Nonetheless it is important to consider that the behavior of sediments is not limited to the parameters set in the DELWAQ model.

D-FLOW Wind

It is important to note an error in the wind forcing of the D-FLOW model that was applied to the baseline, wet year, and barotropic simulations. There are periods ranging from one to three weeks

where the modelled wind is constant, as shown in Figure 5.1. For the periods where the wind speed fluctuates, the modelled wind accurately represents the observed diurnal wind signal and gusty wind events. For the erroneous periods with constant wind speeds, comparisons between measured and modelled SSC values are not valid.

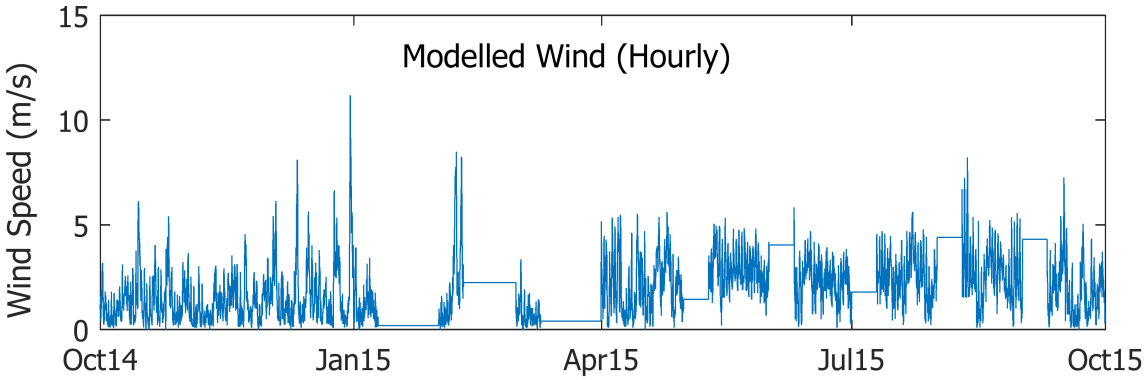

Figure 5.1: Modelled wind in D-FLOW. Periods from 1-3 weeks are incorrectly forced with constant wind speed (horizontal lines).

Sources of Error

The model does not accurately describe SPM dynamics between March and August (see Figure 3.9). As shown in Figure 5.2, the correlation between measured and modelled hourly values is twice as strong when this period is excluded from the timeseries. Possible causes for this disagreement between spikes in SSC that are measured at Dumbarton but missed by the model are discussed here.

The model simulates spikes in SSC on the East Flat at the times where SSC spikes were measured between March and August at Dumbarton. However, these modelled spikes on the east flat are not simulated seen in the model at Dumbarton. One possible explanation for this discrepancy is that the SSC fluctuations with respect to tidal phasing are not well represented. During high wind events, spikes in SSCs have been observed during high water following wind wave resuspension events on the flats (Brand et al. 2010, Lacy et al. 1996), but in the model the spikes in SSC occur at low water. Sediments suspended during ebb tide are then advected to different parts of the Bay by tidal currents. The phase shift between SSC spikes and water depth is important to reproducing the non-linear interaction between the tide and wind wave resuspension on the flats that Brand et al. (2010) identified as a controlling factor of sediment fluxes in South Bay.

The disagreement could also be an issue of fall velocity - if the fall velocity is too large, the lag time between the initiation of settling and deposition on the bed is too short for the increase in suspended sediments on the east flat to be seen in the model at Dumbarton. Another possible explanation for the temporary disagreement between observed and modelled SSCs is an error in data collection. It is possible that biological matter in the water column or algae growing on the sensor affected the measured SSC values between March and August.

σ-layers

The calibration in this study used RMSE to evalute model performance. Measured SSCs at two fixed elevations above the bed were compared to modelled SSCs at the same coordinates in the tenth (bottom) and sixth vertical layers. Since $\sigma-$ layers represent a fixed fraction of the water depth, the average height above the bed of a vertical layer varies over the course of a tidal cycle. This may skew the relationship between measured SSC values at a constant height above the bed and modelled SSC values whose height above the bed is a function of water depth and varies over each tidal cycle. The effect of depth variation on an SSC time series can be excluded by looking at modelled depth-averaged values; however, the measured vertical concentration profile of sediments would be needed to compute the corresponding measured depth-averaged values.

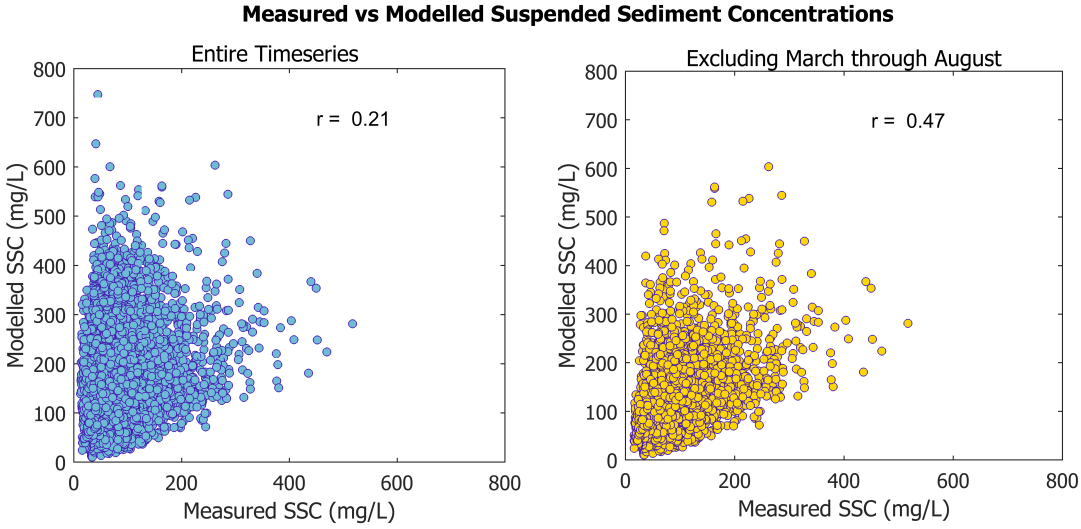

(a) Effect of the poorly simulated period between March and August. The correlation between the hourly measured and modelled values is twice as high when excluding this period.

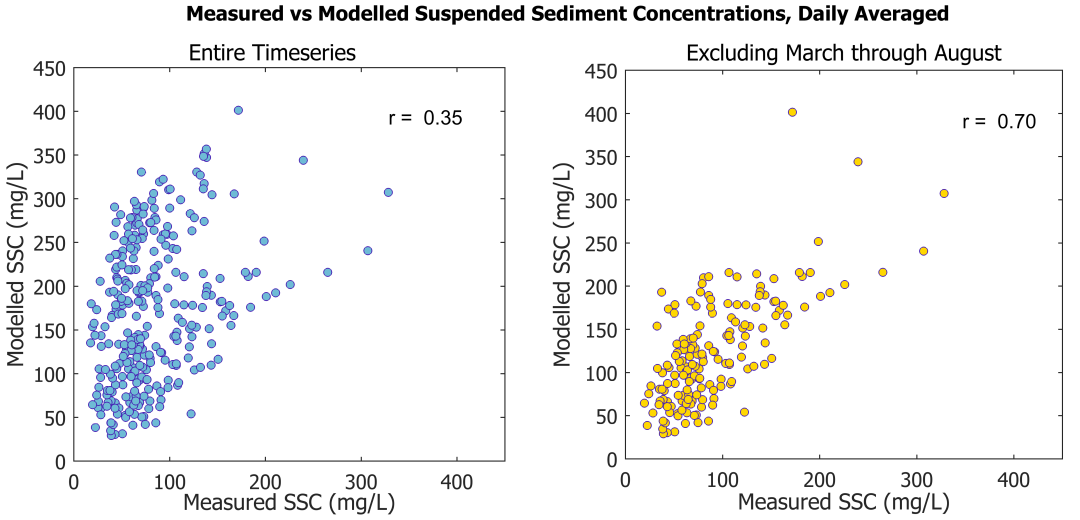

(b) Effect of the poorly simulated period between March and August for daily averaged SSC values. The correlation between the measured and modelled values is twice as high when excluding this period. The correlations are stronger between daily averaged values than between hourly values because the degree to which the model captures neap-spring SSC variations is better than that to which it captures fluctuations over the ebb-flood cycle.

Figure 5.2: Effect of the poorly simulated period between March and August on model performance.

5.1.2. Recommendations for Further Calibration & Model Improvement

To improve the DELWAQ model performance and its ability to reproduce SSC fluctuations on sub-tidal timescales, further calibration of the model is needed. As explained in Section 5.1.1, further calibration should be done to better capture the phasing between water depth fluctuations over the ebb-flood cycle and SSC fluctuations, especially during wind wave events.

Only top priority model parameters were tuned in this study. Additional model calibration could also explore model sensitivity to the number of mud fractions, the deposition efficiency (presence of a fluid mud layer), and the thickness of the buffer layer (S2). The thickness of the buffer layer was not prioritized as a calibration parameter in this study. However, further studies could alter this value (currently set at 10 cm) to calibrate the timescale of system response. This calibration could be based

on the time it takes for SPM concentrations to return to baseline after a major disturbance (personal communication, Thijs van Kessel, April 18, 2018). See van Kessel et al. (2009) and van Kessel et al. (2011) for more details on calibration methods for the buffer layer model and the impact of the thickness of the buffer layer.

Consider Larger Range of Data

The DELWAQ fine sediments model was calibrated using high-frequency USGS SSC data that was only available at one measurement station near Dumbarton Bridge during the time period simulated by the D-FLOW hydrodynamics. Good model performance in one area of South Bay, however, does not imply accurate model behavior elsewhere in the model. In South Bay, high-frequency SSC measurement stations are also located at San Mateo and Channel Marker 17 (see Figure 3.8), but the sediment data collection for these two stations ended in 2005. To perform a more thorough calibration, the D-FLOW hydrodynamics model could be adapted to simulate a period between 1992 and 2005 during which high-frequency SSC data is available at all three USGS measurement stations in South Bay). Once a robust calibration is completed, then the model can confidently be applied to different time periods. Alternatively, a comparison of data from various stations during periods where data is available could be used to qualitatively assess the DELWAQ model performance at different areas throughout the model.

Table 5.1 summarizes sources of data that could be used to further calibrate and validate the DELWAQ sediments model.

Table 5.1: Additional sources of SSC and SSF data that could be used to calibrate and validate the DELWAQ model.

Source	**Data**	**Time Periods**
Shellenbarger et al. (2013)	SSF at DMB	WY 2009 - 2011
Gartner et al. (2001)	SSC at DMB & SMB	One week in Oct. 1998 & one week in Jan. 1998 for each site
Brand et al. (2010)	SSC & SSF at two stations on East Flat near SMB	Feb. 24, 2009 - March 16, 2009
Downing-Kunz et al. (2017)	SSF at Golden Gate	One ebb and one flood tide in (a) March 2016 (b) June 2016 and (c) Feb. 2017*
Lacy et al. (1996)	SSF & SSC at location on East Flat between DMB and DMB	Nov. 23 - Dec. 15, 1993 & March 7-21, 1994
USGS R/V Polaris Cruise, Schraga & Cloern (2017)	2D SSC measurements at stations along longitudinal axis of SFB estuary taken at 1m depth intervals	Irregular; at least monthly, from 1969-2015**
USGS WQ measurements Cloern & Schraga (2017)	15-min interval SSC measurements at (a) SMB (b) DMB (c) Channel Marker 17 (d) Alcatraz stations	(a) 1992-2005 (b) 1992-present (c) 1992-2005 (d) 2003-present

*March 21-22 following storm event; June 23, 2016, during period of low Delta discharge; February 27-28, 2017 following several large storms during wet year (extreme Delta discharge). **Data from 2016-present collected by R/V Peterson; see Schraga et al. (2018).

5.1.3. Limitations of Numerical Model

Numerical models can serve as powerful tools to study complex processes, but there is a limit to the degree to which models can mimic reality. The results of the DELWAQ sediment tracer model provide new insights into sediment dynamics in San Francisco South Bay; however, these results should be

interpreted with consideration for the limitations and assumptions inherent in the model, which are described here.

Flocculation

The suspension and settling of fine sediments is influenced by a number of factors, and not all of these are accounted for in the DELWAQ model. As explained in Chapter 2, the settling of mud in the water column is related to flocculation, which determines the size and densty of suspended sediment flocs. Flocculation is complicated - it is dependent on the shear rate, presence of organic matter, pH, salinity, temperature, SSC, presence of diatoms, turbulence intensity, and the presence of sand (Manning et al. 2010, Mietta et al. 2009, Verney et al. 2009). Flocculation processes are not explicitly represented in the DELWAQ sediments model - rather the mud fractions modelled represent floc fractions. There are options in DELWAQ to include the influence of temperature and salinity on settling velocity implicitly, as described in Appendix B. As the DELWAQ model was being developed and calibrated for the first time, the adjustment of settling velocity based on salinity and temperature was not applied in this study. However, future studies could study these functions and determine whether applying them enhances the ability of the DELWAQ model to simulate sediment dynamics in South Bay.

Bed Processes

Bed erosion models don't account for the fact that the critical shear stress for erosion is dependent on the history of the sediment bed (erosion, deposition, consolidation). There is no consolidation or compaction process represented in the buffer layer bed model describing bed exchange in DELWAQ, so sediments that have remained in the buffer layer for longer periods of time are equally as likely to be resuspended for a given shear stress as those which were recently deposited.

Biological matter living in and on the bed also impacts sediment erosion, but is not represented in the model. The effects of biology on sediment dynamics vary spatially and temporally and so are difficult to represent in such a large model. Investigation into the details of bioturbation and biostabilation due to biological organisms in South Bay was out of the scope of this study.

Sediment-density Coupling

Sediment-density coupling is a phenomena in which there is feedback between sediment concentration and turbulence. Suspended sediments influence water density, which in turn influences turbulent mixing in the water column. Turbulent mixing determines the vertical sediment concentration profile. Denser water will be less mixed (meaning less upwards sediment transport), resulting in deposition (van Maren 2013). This effect is not simulated in the DELWAQ sediments model, as the vertical dispersion coefficients for each computational cell are computed by the D-FLOW model and used as input for DELWAQ.

5.2. Recommendations for Future Research

The previous section provided recommendations to improve the DELWAQ model developed in this study and summarized its main assumptions and limitations. Building on the findings and insights of this thesis, suggestions for further research and applications of the model to advance our understanding of sediment pathways in South Bay are proposed here.

5.2.1. Data Collection

Numerical models are powerful tools to study complex processes in dynamic coastal environments, but the quality of their results is limited to the degree to which they are validated with in-situ data and observations. Here, recommendations for further data collection to be used for calibration and validation are given.

SSC at River Boundaries

For WY 2017, the last 2 and a half months of the simulation are forced with SSC measurements from WY 2015 due to a lack of data. Though the river discharge rates were not high during this period, the timing between discharge and sediment concentration is important to accurately calculate the sediment loads delivered to the SFB system. More complete SSC datasets at the river boundaries represented in the model could result in more convincing estimates of sediment loads delivered to the system. The

D-FLOW model is already validated for WY 2011 and 2012 with correct tidal and wind forcings. These two WYs are representative of a ”wet” and ”dry” year (Martyr-Koller et al. 2017), so if complete SSC and discharge data for these years was available, the DELWAQ model could be applied to this period.

Although most freshwater is delivered to SFB from the Central Valley via the Delta, the sediment supply is dominated by local tributaries. Approximately 61 % of sediments entering the SFB system in recent years are delivered by over 450 tributaries draining from local watersheds. To use the DELWAQ model as a tool to estimate how sediment budgets are likely to change in upcoming years, more of these local sediment sources must be accounted for in the model. To do so, the most significant of these tributaries should be prioritized for SSC data measurements such that sediment budget calculations can be made more confidently. If the sediment contributions from these local sources were accounted for in the DELWAQ model, the model could be used to determine the impact of the growing influence of local versus far-field (Delta) sediment inputs.

Bed Shear Stresses

Although studies by T. Cheng et al. (1999) and Brennan et al. (2002) provide in-situ estimates of bed shear stresses in SFB, additional measurements on the flats and in the channel in South Bay during the time period used to calibrate and validate the D-FLOW hydrodynamics model could help tune D-FLOW parameters and improve the way that hydrodynamic forcings are translated into shear stresses.

Bed Composition

The initial condition of the bed for the DELWAQ model was created by a BCG run, during which sediments were redistributed throughout the model domain as they approach dynamic equilibrium with the hydrodynamics. The result of the BCG process generated an initial sediment distribution for the DELWAQ sediments model that was consistent with expectations and observations - mud mostly settled on the western flat (low shear stresses) and was washed out of the channel. But the composition of the bed was not compared to in-situ bed composition data. Two mud fractions characterized by different fall velocities were initialized in the model based on the findings of past modelling studies in SFB (Achete et al. (2015), Ganju & Schoellhamer (2009), van der Wegen et al. (2011)). The fall velocities of these fractions were tuned as calibration parameters, but measured floc size distributions provided by floc cameras or LISST devices could indicate whether more (or fewer) than two mud fractions are needed to represent reality.

5.2.2. Spectral Analysis

Correlations between hydrodynamic and environmental forcings and sediment responses (SSCs or sediment fluxes) can help to identify the controlling factors of sediment transport patterns in South Bay. Finding direct correlations between wind and SSC proved unsuccessful in this study. This could potentially be caused by a poor choice of the locations of observation points. Correlations between high speed wind events and SSC may be higher in even shallower areas than those analyzed in this study.

A number of forcings operating on different timescales and the interactions between them must be considered when investigating the driving forces of sediment transport. When comparing wind speed and SSC values, the SSC fluctuations are also influenced by fluctuations associated with the semidiurnal and neap-spring tidal signals. Winds blowing from different directions might impact the SPM field differently in different areas of the flat. Because the SPM climate is a function of the interaction of many processes on timescales ranging from hours to weeks, isolating one factor to evaluate its impact is a challenging task. Transform SSC and gross sediment flux data to the frequency domain by employing wavelet analysis or a fast fourier transform to decompose the signals present in the time series could reveal quantifiable relationships between forcings and sediment behavior. Applying Empirical Orthogonal Functions (EOFs) could also help to isolate and quantify the contribution of signals from different types of forcings to SSCs and sediment fluxes (Larson et al. 2003). For further information on applying spectral analysis and EOFs to understanding the driving factors of SSCs, the reader is directed to Schoellhamer (1996) and Velegrakis et al. (1997).

5.2.3. Tracer Analysis for Different Hydrodynamic Scenarios

The tracer analysis in this study only considered the baseline year hydrodynamics, but comparing how sediments move throughout the system under different hydrodynamic conditions could be a next step towards understanding the processes controlling sediment transport in South Bay. The Delta sediments simulation suggested that for WY 2015, most Delta sediments settle landwards of Carquinez Strait during the year they enter the system, and some are resuspended by pulses in subsequent years and transported seawards towards Central Bay and South Bay. It is difficult to generalize about the pathways that Delta sediments take to reach South Bay without exploring different scenarios. For example, how does this behavior change if sediments enter the system during a wet year with extreme Delta discharge rates? Do more Delta sediments reach Central and South Bay during the year they are discharged? If consecutive years of Delta pulses deposit lots of sediment in the Delta and Suisun Bay, would extreme discharge rates wash these sediments seawards? With regards to sediments from local tributaries, tracer simulations could be carried out to determine how the retention time of local sediments in South Bay changes under different hydrodynamic scenarios. These are the types of questions that could be answered by applying the sediment labels to different D-FLOW hydrodynamics.

5.2.4. Sediment Connectivity

Applying sediment connectivity concepts to study sediment transport patterns could provide a more quantitative way to describe net sediment excursion, the timescales on which this transport occurs, and what pathways sediments follow to get there. Methods such as adjacency and connectivity matrices (see Pearson et al. (2017)) could be applied to understand how sediment is shared between different areas of South Bay. In the context of sediment transport, an adjacency or connectivity matrix is a way of representing sediment pathways, with one axis representing source nodes (where sediment starts) and the other axis representing receiving nodes (where sediments end). The connectivity matrix allows for advanced analysis of sediment connectivity and the identification of sediment-sharing neighborhoods. The behavior of sediments from the east flat, the west flat, and the channel were traced and studied in this research; but, discretizing South Bay (or the entire SFB estuary) into more, smaller areas and analyzing model results within the framework of a connectivity matrix could reveal more subtle transport patterns and relationships.

The results of the tracer studies suggest that sediment entering the system from the San-Joaquin and Sacramento rivers accumulates in upper North Bay following a moderate Delta pulse with a maximum discharge rate of $2000 m^3/s$. This raises questions as to what happens to this sediment in subsequent years, and how this behavior might change with extreme discharge rates, such as those observed during WY 2017. During the baseline year, Delta sediments did not significantly contribute to residual flux across Bay Bridge relative to sediments entering from San Pablo and Central Bays; but the connectivity between the Delta and South Bay may be amplified during periods of extremely high Delta discharge. The timing between sediment deposition in North Bay (San Pablo Bay, Suisun Bay, and the Delta region) and subsequent river pulses could significantly impact sediment connectivity throughout the estuary as well. Bracken et al. (2015) provides an interesting way of studying the linkages between sediment accumulation, external forcings, and sediment connectivity in river catchments. Further research might explore these relationships and consider applying sediment connectivity principles to achieve a more concrete understanding of sediment pathways in SFB.

5.3. Model Applications

The availability and behavior of fine sediments strongly influence the ecological health and habitat potential of SFB. The improvements to the DELWAQ model made in this study (described in Section 6.1) serve as an important step towards building a tool that can be used in a predictive capacity to understand how the system will respond to changes in environmental forcings and anthropogenic developments. Here, potential applications of the DELWAQ model are discussed.

5.3.1. Habitat Restoration

In SFB, tidal wetlands are the areas most vulnerable to the harmful effects of sea level rise and increased estuarine salinity brought on by climate change. They also happen to host the majority of endemic plant species and the largest contributions to system biodiversity and primary productivity (Parker et al.

2011). The South Bay Salt Pond Restoration Project - one of the largest restoration initiatives in the United States - aims to return over 15,000 hectares of industrial salt ponds to tidal wetlands, which will restore lost marshland habitat to a diverse assemblage of wetland birds, fish, shellfish, benthic fauna, and aquatic plants (Valoppi 2018). The restoration project's success hinges on an ample supply of fine sediments to support mudflat development. Recent research has shown a trend in decreasing sediment supply to SFB due to anthropogenic developments throughout the watershed (Schoellhamer 2011). This study showed that the phase of the neap-spring tidal cycle, the nature of density-driven flows, and wind all influence net sediment transport landwards across Dumbarton Narrows. The DELWAQ model developed in this research could be used in the short-term to identify the optimal timing of dike breachings to utilize natural processes to deliver sediments to the target restoration area. One of the greatest uncertainties of the restoration project is whether or not tidal flat development will be able to keep pace with projected levels of sea level rise. On the longer term, the model could be used to predict how South Bay's sediment budget will be affected by rising water levels and other effects of climate change.

5.3.2. Climate Change

The impacts of global SLR are exacerbated in the SFB region due to local land subsidence, which raises rates of rSLR compared to global levels. The increased risk of inundation in the Bay Area could lead to saltwater intrusion, coastal erosion, and the drowning of valuable tidal and wetland habitats (Shirzaei & Bürgmann 2018). Changing precipitation patterns could change the timing and magnitude of freshwater inputs to SFB, with recent research predicting wetter springs and drier summers for SFB (Dettinger et al. 2004, Grenier & Davis 2010, Miller et al. 2004, van Rheenen et al. 2004). As density-driven circulation between South Bay and Central Bay is linked to discharge from the Delta, significant alterations to freshwater inputs to the system are likely to change the nature of these circulation patterns. The DELWAQ model developed in this research could be used to anticipate the effects of such changes on residual transport patterns and sediment budgets for different areas of the Bay.

As projections of SLR and precipitation patterns for SFB are not certain, the importance of adaptive strategic management strategies informed by scientific research is essential. The demand for resources provided by the SFB watershed to the surrounding region is often in conflict with responsible management of the SFB estuary. Freshwater diversion in the Central Valley and development in low-elevation areas in the Bay Area threaten the long-term sustainability of the estuary and influence the system's sediment budget (Parker et al. 2011). Understanding how sediment budgets will be impacted by changes in atmospheric and hydrodynamic forcings brought on by climate change is needed to inform large-scale management decisions that have the potential to prevent and mitigate harmful impacts. The DELWAQ sediment transport model could also be used to anticipate system response to management decisions to identify the most sustainable alternatives. Ongoing work is being done to adjust the D-FLOW hydrodynamics model to simulate projected future conditions.

5.3.3. Harmful Algae Blooms

The trend of decreasing sediment supply to SFB not only threatens tidal flat development. It also raises concerns about water quality in South Bay, where the magnitude and frequency of harmful algae blooms is limited by historically high turbidity levels (Ganju et al. 2008). High concentrations of SPM govern the light climate and productivity potential of photosynthesizing algae in the water column, thereby preventing phytoplankton blooms that could threaten the ecological viability of the SFB estuary. Ongoing photoplankton modelling initiatives in the SFB region seek a deeper understanding of the controlling factors of these harmful algae blooms. The DELWAQ sediments model could be coupled with DELWAQ's phytoplankton modelling BLOOM engine to incorporate the computed SPM dynamics. The chain of hydrodynamic, sediment, and phytoplankton models could allow for the investigation of linkages between hydrodynamic forcings, sediment supply, and overall water quality in the SFB system.

5.3.4. DELWAQ Model in Context: Limitations to Application

The DELWAQ model developed in this study has the potential to serve as a powerful tool to inform management decisions that could alter the long-term trajectory of the SFB system. In its current state, the model results should be interpreted with consideration for the fact that processes operating on

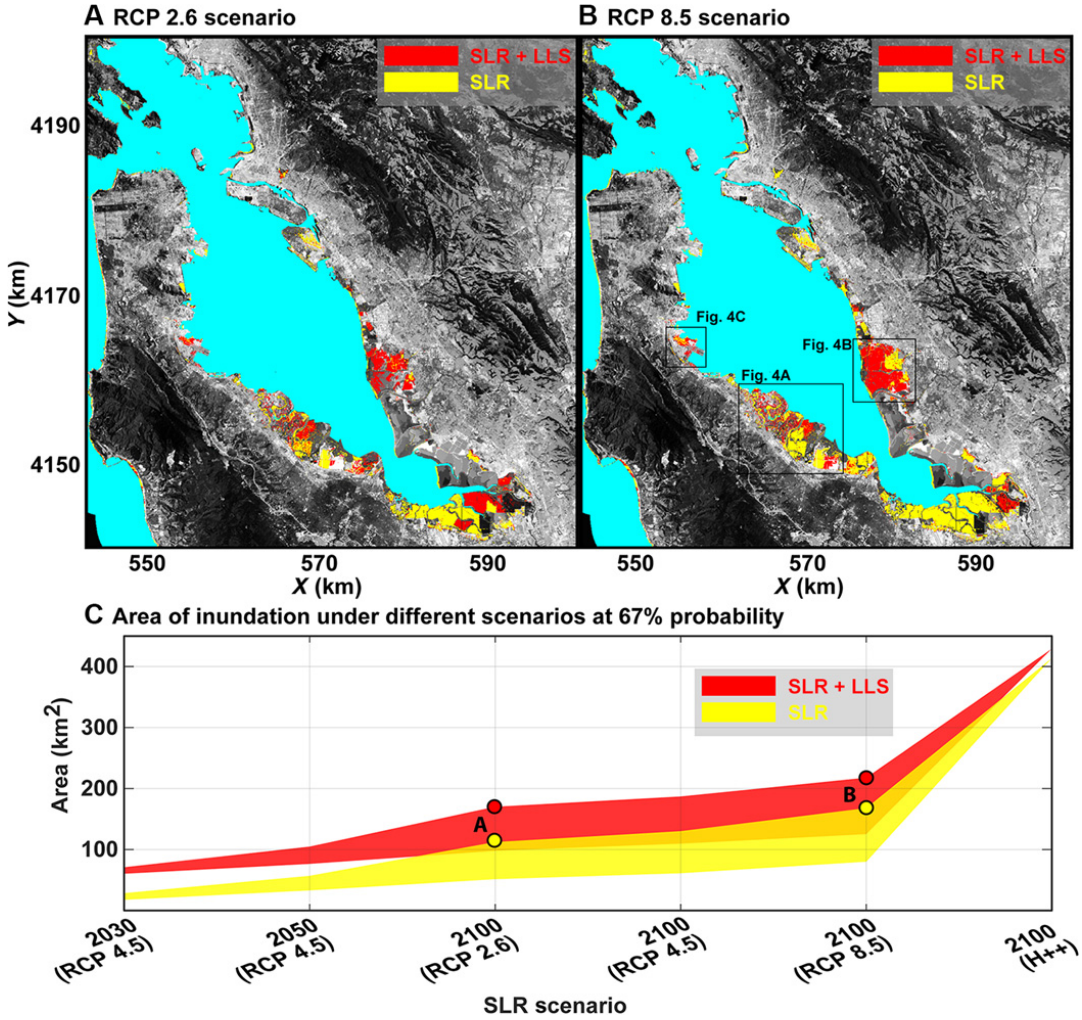

Figure 5.3: Inundation maps for different climate change predictions (RCPs) for South Bay. The yellow areas show flooding predictions based on global rates of SLR alone, and the red areas show predictions based on relative SLR, including the effects of land subsidence. Point A: area of flooding considering the SLR prediction for RCP 2.6 scenario, representing the goals of the 2015 Paris Climate Change agreement. Point B: area of flooding considering SLR prediction for RCP 8.5 scenario, with no significant effort to mitigate GHG emissions [Image: Shirzaei & Bürgmann (2018)].

shorter time scales are not well represented, and the degree to which the model simulates sediment fluxes locally has not been evaluated based on measured data. The calibration showed that large-scale patterns in sediment transport (e.g. sediment budgets for South Bay, the direction of residual transport patterns within South Bay) are largely stable regardless of alterations to parameters governing vertical sediment exchange between the bed and the water column.

As a result of this study, both horizontal transport and vertical bed exchange are included in the model, so, the primary baroclinic (estuarine circulation, tidal straining) and barotropic (tidal asymmetry, lag effects) mechanisms driving the net transport of fine material are accounted for. Since residual transport in a tidally-dominated estuary, such as SFB, is the result of unbalanced, oscillating tidal fluxes superimposed on gravitational circulation, accurate representation of the tide and the salinity gradients driving circulation patterns is important to simulating sediment transport. Confidence in the sediment behavior simulated by the DELWAQ model is therefore dependent on the accuracy with which the hydrodynamic model describes tidal currents and the salinity field.

In South Bay, wind wave resuspension plays an important role in mobilizing sediments on the flats, and the interaction between tidal currents and vertical transport influences the fate of sediments suspended by waves during ebb. Generally speaking, the relative phasing of SSC fluctuations and water depth

over the ebb-flood cycle is not well reproduced by the model; however, neap-spring SSC fluctuations are captured quite well. The accuracy with which the model needs to simulate processes on shorter temporal and spatial scales in order to reproduce larger-scale trends in sediment transport is uncertain and raises questions about the level of model complexity needed to study given processes.

Before it can be applied in an absolute, predictive sense, the model should be validated based on measured sediment flux data and SSC data at multiple locations throughout the domain. In its current state, the DELWAQ model can be used to isolate certain processes (e.g. wind, baroclinic flows, varying levels of freshwater input) to better understand the driving forces of sediment transport in SFB. It can also be used to compare relative system responses to certain changes to environmental and hydrodynamic forcings.

6

Conclusions

This thesis shows that a 3D process-based numerical model coupled with a water quality model can be used to study large-scale sediment transport patterns in complex estuarine systems, and the application of this methodology has provided new insights into sediment dynamics in SFB. This chapter highlights the scientific contributions of this research and presents the main outcomes in the context of the research questions posed to guide this study.

6.1. Advances

This work builds upon previous efforts by van Kempen (2017) to model fine sediment transport in SFB. Improvements to the previously existing model and the implications for model application are summarized here.

- **Bed Exchange**: The previous version of the DELWAQ model did not include sediment exchange between the bed and the water column. A buffer layer sediment model, with several important modifications to the classical Partheniades-Krone formulations, was implemented to describe sedimentation and erosion.
- **Initial Sediment Condition**: A BCG run was carried out to define an appropriate initial sediment bed composition and reduce the effects of model spin-up.
- **Model Calibration**: The DELWAQ model was calibrated based on high-frequency measured SSC data. The model is able to reproduce SSC fluctuations following the neap-spring tidal cycle.

By including erosion and deposition in the DELWAQ model and initializing the bed composition, the effects of wind wave resuspension and tidal asymmetry on sediment transport are now accounted for. Before bed exchange was implemented in the model, the simulated transport of fine material was not representative of reality. As a result of this study, the DELWAQ model can now be used to study sediment pathways in SFB with consideration for all of the primary mechanisms driving suspended sediment transport. It could also be adjusted and applied to study other estuarine systems characterized by fine sediments where 3D circulation patterns play a prominent role.

6.2. Findings

Four primary research questions guided this research, and the main findings are summarized here:

What are the processes controlling sediment exchange between South Bay and Central Bay?

Model results indicate that residual transport across Bay Bridge is the result of tidally-driven oscillations in gross fluxes superimposed on estuarine circulation. The nature of sediment exchange between Central Bay and South Bay at Bay Bridge is linked to horizontal salinity differences between the two, and can be characterized according to the following three scenarios:

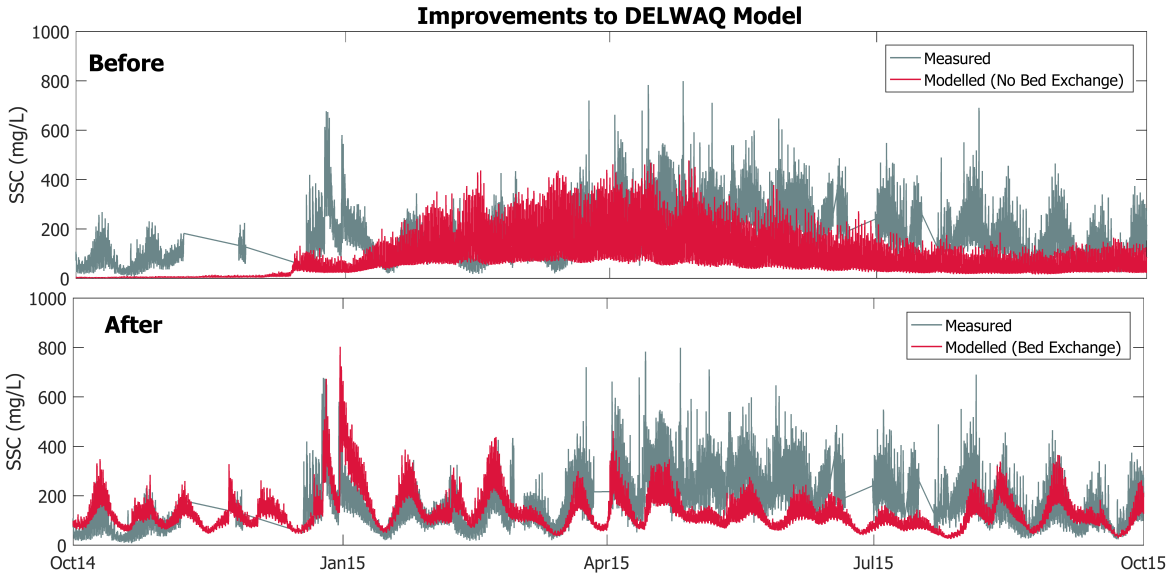

Figure 6.1: Comparison of the DELWAQ model performance before and after improvements made during this study.

1. **Low Delta Discharge:** During baseline conditions, a relatively weak salinity gradient between Central Bay and South Bay drives landwards-directed sediment flux near the bed and higher magnitude seawards-directed flux near the surface. A net export of sediment from South Bay is observed.
2. **High Delta Discharge:** Shortly after a large pulse of freshwater from the Delta reaches Central Bay, the salinity gradient along the longitudinal axis of South Bay is reversed, driving landwards-directed net flux near the surface. Residual flux near the bed is briefly (on the order of days) directed seawards before returning to landwards-directed flux. A net import of sediment into South Bay is observed.
3. **Reducing Delta Discharge:** Density-driven water exchanges during periods of high Delta Discharge freshen South Bay with respect to Central Bay, resulting in a strong salinity gradient between Central Bay and South Bay and strong estuarine circulation. Net flux near the surface is directed seawards, and net flux near the bed is directed landwards. Bottom transport dominates, resulting in net sediment import into South Bay.

A visualization of sediment flux across Bay Bridge for these three scenarios is shown in Figure 6.2. During baseline years, defined as having maximum Delta discharge <2000 m^3/s, seawards directed transport near the surface dominates, yielding a net export of sediment from South Bay. During wet years, South Bay is more likely to import sediments due to the large influx of sediments imported by density-driven circulation during and after large Delta discharge events. As the direction of transport across Bay Bridge is influenced by density-driven circulation that travels in opposing directions near the surface and near the bed, the vertical concentration profile is an important factor in determining net transport across the mouth of South Bay.

Model results suggest that the biggest contributors to sediment import into South Bay for a year similar to WY 2015 are sediments originating in San Pablo Bay, Central Bay, and Suisun Bay. Wind wave resuspension in the shallow areas of North Bay controls the amount of suspended sediments available for import into South Bay during periods of low Delta discharge.

How are sediments redistributed within South Bay, and what processes facilitate sediment exchange between the channels and the shoals?

The primary pathways landwards are through the channel and on the west flat. On the east flat, residual transport is seawards directed. Sediment circulation driven by the interaction of wind wave

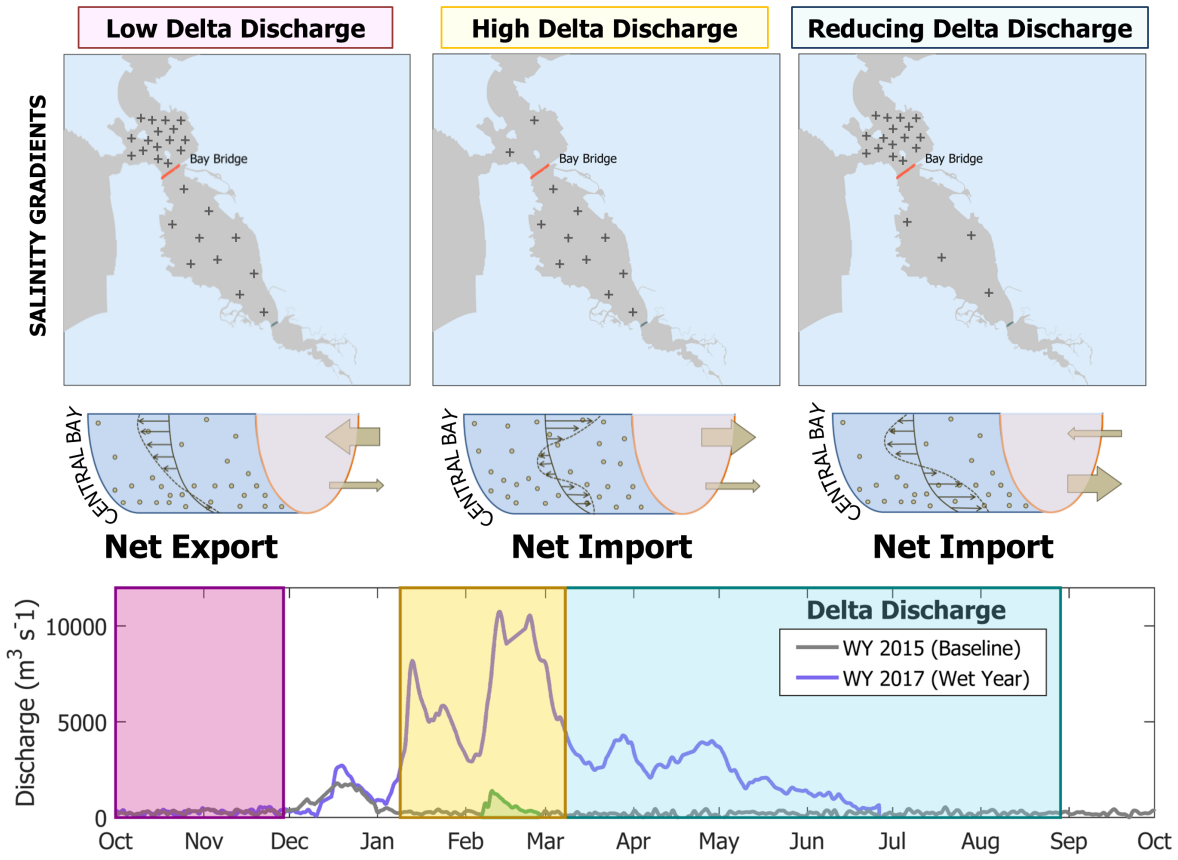

Figure 6.2: Schematic showing sediment flux at Bay Bridge corresponding to three stages of Delta discharge. **Top**: map showing salinity gradients between Central and South Bay. The '+' symbols represent salinity concentrations. **Middle**: Figures schematizing vertical sediment flux distribution at Bay Bridge cross-section. The brown arrows show the direction and relative magnitude of residual fluxes near the bed and near the surface during these periods (based on Figure 4.20). **Bottom**: Hydrographs showing rates of freshwater discharge from the Sacramento-San Joaquin Rivers and periods corresponding to low Delta discharge, high Delta discharge, and reducing Delta discharge.

resuspension and tidal currents facilitate the exchange of sediments between the channels and the shoals. Sediments that enter South Bay tend to settle on the west flat, in the dredging site in the middle of South Bay, and along the western bank of the primary channel. With the exception of Bay Bridge, the direction of residual sediment transport throughout South Bay is independent of wind, baroclinic circulation, and Delta discharge rates, suggesting that the pathways that facilitate sediment exchange within South Bay are dominated by the tide.

The amount of sediment in circulation and the magnitude of residual fluxes is related to wind wave resuspension on the flats and sediment import via Bay Bridge. Wind speed and direction, tidal phase (ebb/flood and neap spring), and water depth, collectively influence SSCs on the flats.

What pathways do sediments entering from a local tributary follow, and on what timescales does this occur?

Sediments entering South Bay directly from local tributaries enter episodically following high precipitation events. After a pulse of sediment enters the system from Alameda Creek, local sediments are gradually transported seawards across Bay Bridge and a smaller percentage travels landwards across Dumbarton Narrows. For WY 2015, the mass of Alameda sediments in South Bay following discharge events stabilized within a few months. Additional simulations where sediments from local tributaries are traced under different hydrodynamic conditions could provide insight as to how density-driven circulation impacts the retention time of local sediments in South Bay. To better represent sediment

contributions from local watersheds in the DELWAQ model, more of the local tributaries should be gauged to measure discharge rates and sediment concentrations that can be used to force model boundaries.

By which pathways do sediments from the Sacramento and San Joaquin rivers enter South Bay?

There are two primary pathways by which sediments entering the SFB estuary via the Sacramento-San Joaquin River Delta enter South Bay.

1. During periods of high Delta discharge, turbid freshwater from the Delta travels seawards and enters Central Bay. Density-driven circulation and the tide bring sediments from Central Bay into South Bay.

2. Delta sediments settle in North Bay following moderate periods of Delta outflow (<2,000 m^3/s). Delta sediments accumulate in North Bay until an extreme pulse of freshwater from the Delta (>10,000 m^3/s) resuspends these sediments and delivers them to Central Bay. Density-driven circulation and the tide then bring sediments from Central Bay into South Bay. This suggests that sediment connectivity between North Bay and South Bay is enhanced during periods of extreme Delta discharge.

In this study, the DELWAQ model was applied to investigate the governing factors of South Bay's sediment budget, the exchange of sediments between the channel and the shoals, and the pathways taken by sediments entering the system from local watersheds and the Delta. New insights provided by model results further our understanding of sediment dynamics in SFB, enabling for better predictions as to how future changes in environmental conditions and human developments might impact sediment availability in South Bay. With further validation, the model can be used as a predictive tool to understand how the dynamics of SFB might change under increasing anthropogenic pressure, rising water levels, and changing precipitation patterns. Such predictions can help to inform management strategies and policy decisions with consideration for the long-term sustainability of the estuary.

Bibliography

Achete, F., van der Wegen, M., Roelvink, D. & Jaffe, B. (2015), 'A 2D process-based model for suspended sediment dynamics: a first step towards ecological modeling', *Hydrology and Earth System Sciences* **19**, 2837 – 2857.
URL: *https://www.hydrol-earth-syst-sci.net/19/2837/2015/hess-19-2837-2015.pdf*

Alpers, C. N., Hunerlach, M. P., May, J. T. & Hothem, R. L. (2005), 'Mercury contamination from historical gold mining in California'. Publications of US Geological Survey.
URL: *https://pubs.usgs.gov/fs/2005/3014/fs2005_3014_v1.1.pdf*

Barnard, P., H. Schoellhamer, D., Jaffe, B. & Mckee, L. (2013), 'Sediment transport in the San Francisco Bay coastal system: an overview', *Marine Geology* **345**, 3–17.

Bosboom, J. & Stive, M. J. (2013), *Coastal Dynamics I, Lecture Notes for CIE4305*, Delft University of Technology.

Bracken, L. J., Turnbull, L., Wainwright, J. & Bogaart, P. (2015), 'Sediment connectivity: a framework for understanding sediment transfer at multiple scales', *Earth Surface Processes and Landforms* **40**(2), 177–188.
URL: *https://onlinelibrary.wiley.com/doi/abs/10.1002/esp.3635*

Brand, A., Lacy, J. R., Gladding, S., Holleman, R. & Stacey, M. (2015), 'Model-based interpretation of sediment concentration and vertical flux measurements in a shallow estuarine environment', *Limnology and Oceanography* **60**(2), 463–481.

Brand, A., Lacy, J. R., Hsu, K., Hoover, D., Gladding, S. & Stacey, M. T. (2010), 'Wind-enhanced resuspension in the shallow waters of South San Francisco Bay: Mechanisms and potential implications for cohesive sediment transport', *Journal of Geophysical Research: Oceans* **115**(C11), n/a–n/a.
URL: *http://dx.doi.org/10.1029/2010JC006172*

Brennan, M. L., Schoellhamer, D. H., Burau, J. & Monismith, S. G. (2002), 'Tidal asymmetry and variability of bed shear stress and sediment bed flux at a site in san francisco bay, usa', *Proceedings in Marine Science* **5**.

Burchard, H. & Schuttelaars, H. M. (2012), 'Analysis of tidal straining as driver for estuarine circulation in well-mixed estuaries', *Journal of Physical Oceanography* **42**(2), 261–271.
URL: *https://doi.org/10.1175/JPO-D-11-0110.1*

Capiella, K., Malzone, C., Smith, R. & Jaffe, B. (1999), Sedimentation and bathymetry changes in suisun bay: 1867-1990, Open file report 99-563, US Geological Survey.
URL: *https://pubs.er.usgs.gov/publication/ofr99563*

Carlson, P. R. & McCulloch, D. S. (1974), 'Aerial observations of suspended−sediment plumes in San Francisco Bay and the adjacent Pacific Ocean', *Journal of Research of the US Geological Survey* **2**(5), 519 – 526.

Cloern, J. (1987), 'Turbidity as a control on phytoplankton biomass and productivity in estuaries', *Continental Shelf Research* **7**, 1367–1381.
URL: *https://pubs.er.usgs.gov/publication/70014152*

Cloern, J. E., Alpine, A. E., Cole, B. E., Wong, R. L., Arthur, J. F. & Ball, M. D. (1983), 'River discharge controls phytoplankton dynamics in the northern San Francisco Bay estuary', *Estuarine, Coastal and Shelf Science* **16**(4), 415 – 429.
URL: *http://www.sciencedirect.com/science/article/pii/0272771483901038*

Cloern, J. & Schraga, T. (2017), Usgs measurements of water quality in san francisco bay (ca) in south San Francisco Bay: 1858-1983, US Geological Survey data release, US Geological Survey.
URL: *https://doi.org/10.5066/F7TQ5ZPR*

Conomos, T. J. (1979), Properties and circulation of San Francisco Bay waters, *in* 'San Francisco Bay: The Urbanized Estuary', Pacific Division of the American Association for the Advancement of Science, San Francisco, California, pp. 47–84.
URL: *http://downloads.ice.ucdavis.edu/sfestuary/conomos_1979/archive1019.PDF*

Conomos, T. J., Smith, R. E. & Gartner, J. W. (1985), 'Environmental setting of San Francisco Bay', *Hydrobiologia* **129**(1), 1–12.
URL: *https://doi.org/10.1007/BF00048684*

David, N., McKee, L. J., Black, F. J., Flegal, A. R., Conaway, C. H., Schoellhamer, D. H. & Ganju, N. K. (2009), 'Mercury concentrations and loads in a large river system tributary to San Francisco Bay, California, USA', *Environmental Toxicology and Chemistry* **28**(10), 2091–2100.
URL: *http://dx.doi.org/10.1897/08-482.1*

Deltares (2016*a*), *D-Water Quality Process Library Description*, Deltares. Version 5.01.

Deltares (2016*b*), *Delft3D-Flow User Manual*, Deltares. Version 1.1.

Deltares (2017), *D-Water Quality Manual*, Deltares. Version 3.15.

Dettinger, M. D., Cayan, D. R., Meyer, M. K. & Jeton, A. E. (2004), 'Simulated hydrologic responses to climate variations and change in the Merced, Carson, and American River basins, Sierra Nevada, California, 1900–2099', *Climatic Change* **62**(1), 283–317.
URL: *https://doi.org/10.1023/B:CLIM.0000013683.13346.4f*

Downing-Kunz, M., Schoellhamer, D. & Work, P. (2017), Water and suspended-sediment flux measurements at the golden gate, 2016-2017, Technical Report Contribution No. 856, SFEI & US Geological Survey. Regional Monitoring Program for Water Quality in San Francisco Bay.

Fong, S., Louie, S., Werner, I., Davis, J. & Connon, R. (2016), 'Contaminant effects on California bay-delta species and human health', *San Francisco Estuary and Watershed Science* **14**(4).

Foxgrover, A. C., Higgins, S. A., Ingraca, M. K., Jaffe, B. E. & Smith, R. E. (2004), Deposition, erosion, and bathymetric change in south San Francisco Bay: 1858-1983, Open file report 2004-1192, US Geological Survey.
URL: *https://pubs.usgs.gov/of/2004/1192/of2004-1192.pdf*

Fredsøe, J. (1984), 'Turbulent boundary layer in wave-current motion', *Journal of Hydraulic Engineering* **110**(8), 1103–1120.
URL: *https://ascelibrary.org/doi/abs/10.1061/%28ASCE%290733-9429%281984%29110%3A8%281103%29*

Fregoso, T. A., Foxgrover, A. C. & Jaffe, B. E. (2008), Sediment deposition, erosion, and bathymetric change in central San Francisco Bay: 1855–1979, Open file report 2008-1312, US Geological Survey.
URL: *https://pubs.usgs.gov/of/2008/1312/*

Fregoso, T., Wang, R.-F., Alteljevich, E. & Jaffe, B. (2017), San Francisco Bay-Delta bathymetric/topographic digital elevation model (DEM), US Geological Survey data release, US Geological Survey.
URL: *https://doi.org/10.5066/F7GH9G27*

Ganju, N. K., Knowles, N. & Schoellhamer, D. H. (2008), 'Temporal downscaling of decadal sediment load estimates to a daily interval for use in hindcast simulations', *Journal of Hydrology* **349**(3), 512 – 523.
URL: *http://www.sciencedirect.com/science/article/pii/S0022169407007068*

Ganju, N. K. & Schoellhamer, D. H. (2009), 'Calibration of an estuarine sediment transport model to sediment fluxes as an intermediate step for simulation of geomorphic evolution', *Continental Shelf Research* **29**(1), 148 – 158. Physics of Estuaries and Coastal Seas: Papers from the PECS 2006 Conference.
URL: *http://www.sciencedirect.com/science/article/pii/S0278434307002658*

Ganju, N., Schoellhamer, D., Murrell, M., Gartner, J. & Wright, S. (2007), Constancy of the relation between floc size and density in San Francisco Bay, *in* J.-Y. Maa, L. Sanford & D. Schoellhamer, eds, 'Estuarine and Coastal Fine Sediments Dynamics', Vol. 8 of *Proceedings in Marine Science*, Elsevier, pp. 75 – 91.
URL: *http://www.sciencedirect.com/science/article/pii/S1568269207800076*

Gartner, W.J., C. R., Wang, P.-F. & Richter, K. (2001), 'Laboratory and field evaluations of the LISST-100 instrument for suspended particle size determinations', **175**, 199–219.

Gatto, V. M., van Prooijen, B. C. & Wang, Z. B. (2017), 'Net sediment transport in tidal basins: quantifying the tidal barotropic mechanisms in a unified framework', *Ocean Dynamics* **67**(11), 1385–1406.
URL: *https://doi.org/10.1007/s10236-017-1099-3*

Grenier, J. & Davis, J. (2010), 'Water quality in south San Francisco Bay, California: Current condition and potential issues for the South Bay Salt Pond Restoration Project', **206**, 115–47.

Hager, S. & Schemel, L. (1996), *San Francisco Bay: The Ecosystem*, American Association for the Advancement of Science Pacific distributions, chapter Dissolved inorganic nitrogen, phosphorus, and silicon in south San Francisco Bay, I, major factors affecting distributions, pp. 189–215.

Heberger, M., Cooley, H., Gleick, P. & Herrera, P. (2009), The impacts of sea-level rise on the California coast, Report, Pacific Institute.
URL: *http://www.pacinst.org/reports/sea_level_rise*

Iglecia, M., Kuwae, T., Flynn, E., Brand, L. & Takekawa, J. (2011), 'Assessing biofilm seasonality, distribution, and composition in the southern San Francisco Bay'. South Bay Science Symposium, at Menlo Park.

Jaffe, B. E., Smith, R. E. & Foxgrover, A. C. (2007), 'Anthropogenic influence on sedimentation and intertidal mudflat change in San Pablo Bay, California: 1856-1983', *Estuarine Coastal and Shelf Science* **73**, 175–187.

Jones, C. (2008), Aquatic Transfer Facility sediment transport analysis, *in* D. Cacchione & P. Mull, eds, 'Technical Studies for the Aquatic Transfer Facility: Hamilton Wetlands Restoration Project', US Army Corps of Engineers, technical report 4, pp. 305–340.

Ketron, T., Hsu, W., McCullum, A. J., Nguyen, A., C. Remar, A., Newcomer, M., Fleming, E., Bebout, L., Bebout, B., Detweiler, A. & Skiles, J. (2011), 'Hyperspectral biofilm classification analysis for carrying capacity of migratory birds in the South Bay Salt Ponds'. AGU Fall Meeting.

Kranck, K. & Milligan, T. G. (1992), 'Characteristics of suspended particles at an 11-hour anchor station in San Francisco Bay, California', *Journal of Geophysical Research: Oceans* **97**(C7), 11373–11382.
URL: *http://dx.doi.org/10.1029/92JC00950*

Krone, R. (1979), Sedimentation in the San Francisco Bay system, *in* 'San Francisco Bay: The Urbanized Estuary', Pacific Division of the American Association for the Advancement of Science, San Francisco, California, pp. 85–96.
URL: *http://downloads.ice.ucdavis.edu/sfestuary/conomos_1979/archive1020.PDF*

Krone, R. B. (1962), *Flume studies of the transport of sediment in estuarial shoaling processes*, Hydraulic Engineering Laboratory and Sanitary Engineering Research Laboratory, Univ. of California.

Lacy, J., Schoellhamer, D. & Burau, J. (1996), 'Suspended−solids flux at a shallow-water site in south San Francisco Bay, California', pp. 3357–3362.

Larson, M., Capobianco, M., Jansen, H., Różyński, G., Southgate, H., Stive, M., Wijnberg, K. & Hulscher, S. (2003), 'Analysis and modeling of field data of coastal morphological evolution over yearly and decadal time scales. Part 1: Background and linear techniques', *Journal of coastal research* **19**(4), 760–775.

Manning, A. J., Baugh, J. V., Spearman, J. R. & Whitehouse, R. J. S. (2010), 'Flocculation settling characteristics of mud: sand mixtures', *Ocean Dynamics* **60**(2), 237–253.
URL: *https://doi.org/10.1007/s10236-009-0251-0*

Martyr-Koller, R., Kernkamp, H., van Dam, A., van der Wegen, M., Lucas, L., Knowles, N., Jaffe, B. & Fregoso, T. (2017), 'Application of an unstructured 3d finite volume numerical model to flows and salinity dynamics in the San Francisco Bay-delta', *Estuarine, Coastal and Shelf Science* **192**, 86 – 107.
URL: *http://www.sciencedirect.com/science/article/pii/S0272771416307120*

McCulloch, D., Peterson, D., Carlson, P. & Conomos, T. (1970), 'A preliminary study of the effects of water circulation in the San Francisco Bay estuary', *Geological Survey Circular* **637**, A1–A27.

McDonald, E. & Cheng, R. (1997), 'A numerical model of sediment transport applied to San Francisco Bay, California', *Journal of Marine Environmental Engineering* **4**, 1–41.

Mckee, L., Ganju, N. & H. Schoellhamer, D. (2006), 'Estimates of suspended sediment entering San Francisco Bay from the Sacramento and San Joaquin Delta, San Francisco Bay, California', **323**, 335–352.

McKee, L., Lewicki, M., Schoellhamer, D. & Ganju, N. (2013), 'Comparison of sediment supply to San Francisco Bay from watersheds draining the bay area and the central valley of California', *Marine Geology* **345**, 47 – 62.
URL: *https://ca.water.usgs.gov/pubs/2013/McKeeEtAl2013.pdf*

Metropolitan Transportation Commission (2017), Plan Bay Area 2040, Technical report, Association of Bay Area Governments.

Mietta, F., Chassagne, C., Manning, A. J. & Winterwerp, J. C. (2009), 'Influence of shear rate, organic matter content, pH and salinity on mud flocculation', *Ocean Dynamics* **59**(5), 751–763.
URL: *https://doi.org/10.1007/s10236-009-0231-4*

Miller, N. L., Bashford, K. E. & Strem, E. (2004), 'Potential impacts of climate change on California hydrology', *JAWRA Journal of the American Water Resources Association* **39**(4), 771–784.
URL: *https://onlinelibrary.wiley.com/doi/abs/10.1111/j.1752-1688.2003.tb04404.x*

Minear, J. (2010), The Downstream Geomorphic Effects of Dams: A Comprehensive and Comparative Approach, PhD thesis, UC Berkeley.

Moftakhari, H., Jay, D., Talke, S. & Schoellhamer, D. (2015), 'Estimation of historic flows and sediment loads to San Francisco Bay, 1849–2011', *Journal of Hydrology* **529**, 1247 – 1261.
URL: *http://www.sciencedirect.com/science/article/pii/S0022169415006587*

National Geophysical Data Center (2003), U.s. coastal relief model - central pacific, Digital Elevation Model, National Geophysical Data Center, NOAA.
URL: *https://www.ngdc.noaa.gov/docucomp/page?xml=NOAA/NESDIS/NGDC/MGG/DEM/iso/xml/348.xml&view=*

Nichols, F. H. (1985), 'Increased benthic grazing: An alternative explanation for low phytoplankton biomass in northern San Francisco Bay during the 1976–1977 drought', *Estuarine, Coastal and Shelf Science* **21**(3), 379 – 388.
URL: *http://www.sciencedirect.com/science/article/pii/0272771485900186*

Nichols, F., Thompson, J. & Schemel, L. (1990), 'Remarkable invasion of San Francisco Bay (California, USA) by the Asian clam Potamocorbula amurensis. II. Displacement of a former community', *Marine Ecology Progress Series* **66**(1/2), 95–101.
URL: *http://www.jstor.org/stable/24844649*

Parker, V., Callaway, J., L.M., S., Vasey, M. & Herbert, E. (2011), 'Climate change and San Francisco Bay-Delta tidal wetlands', *San Francisco Estuary and Watershed Science* **9**(3).
URL: *https://escholarship.org/uc/item/8j20685w*

Partheniades, E. (1962), A study of erosion and deposition of cohesive soils in salt water, PhD thesis, UC Berkeley.

Pearson, S., van Prooijen, B., Wang, Z. & Bak, J. (2017), Sediment connectivity and transport pathways in tidal inlets: a conceptual framework with application to ameland inlet. American Geophysical Union Fall Meeting.

Pritchard, D. & Hogg, A. J. (2003), 'Cross-shore sediment transport and the equilibrium morphology of mudflats under tidal currents', *Journal of Geophysical Research: Oceans* **108**(C10), 11.1 – 11.15.
URL: *https://agupubs.onlinelibrary.wiley.com/doi/abs/10.1029/2002JC001570*

Pubben, S. (2017), 3D mixing patterns in San Francisco South Bay, Masters thesis, TU Delft.
URL: *https://repository.tudelft.nl/islandora/object/uuid%3Ad5ca021e−8652−41f8−b91a−5c2bccdb777e*

San Francisco Estuary Institute (2017), 'SFEI Nutrients Program, ERDDAP'.
URL: *http://sfbaynutrients.sfei.org/erddap/tabledap*

Schoellhamer, D. H. (1996), 'Factors affecting suspended□solids concentrations in south San Francisco Bay, California', *Journal of Geophysical Research: Oceans* **101**(C5), 12087–12095.
URL: *https://agupubs.onlinelibrary.wiley.com/doi/abs/10.1029/96JC00747*

Schoellhamer, D. H. (2011), 'Sudden clearing of estuarine waters upon crossing the threshold from transport to supply regulation of sediment transport as an erodible sediment pool is depleted: San Francisco Bay, 1999', *Estuaries and Coasts* **34**(5), 885–899.
URL: *https://doi.org/10.1007/s12237-011-9382-x*

Schoellhamer, D. H., Mumley, T. E. & Leatherbarrow, J. E. (2007), 'Suspended sediment and sediment-associated contaminants in San Francisco Bay', *Environmental Research* **105**(1), 119 – 131. Pollutants in the San Francisco Bay Estuary.
URL: *http://www.sciencedirect.com/science/article/pii/S0013935107000424*

Schraga, T. & Cloern, J. (2017), 'Water quality measurements in San Francisco Bay by the US Geological Survey, 1969-2015', *Scientific Data* **4**.
URL: *http://dx.doi.org/10.1038/sdata.2017.98*

Schraga, T., Nejad, E., Martin, C. & Cloern, J. (2018), USGS measurements of water quality in San Francisco Bay (CA), beginning in 2016, Technical report.
URL: *https://doi.org/10.5066/F7D21WGF*

Shellenbarger, G. G., Wright, S. A. & Schoellhamer, D. H. (2013), 'A sediment budget for the southern reach in San Francisco Bay, CA: Implications for habitat restoration', *Marine Geology* **345**, 281 – 293.
URL: *http://www.sciencedirect.com/science/article/pii/S0025322713000820*

Shirzaei, M. & Bürgmann, R. (2018), 'Global climate change and local land subsidence exacerbate inundation risk to the san francisco bay area', *Science Advances* **4**(3).
URL: *http://advances.sciencemag.org/content/4/3/eaap9234*

Soulsby, R., Hamm, L., Klopman, G., Myrhaug, D., Simons, R. & Thomas, G. (1993), 'Wave-current interaction within and outside the bottom boundary layer', *Coastal Engineering* **21**(1), 41 – 69. Special Issue Coastal Morphodynamics: Processes and Modelling.
URL: *http://www.sciencedirect.com/science/article/pii/037838399390045A*

Sternberg, R., Cacchione, D., Drake, D. & Kranck, K. (1986), 'Suspended sediment transport in an estuarine tidal channel within San Francisco Bay, California', *Marine Geology* **71**(3), 237 – 258.
URL: *http://www.sciencedirect.com/science/article/pii/0025322786900721*

Swart, D. (1974), Offshore sediment transport and equilibrium beach profiles, PhD thesis, TU Delft.

T. Cheng, R., H. Ling, C. & W. Gartner, J. (1999), 'Estimates of bottom roughness length and bottom shear stress in south san francisco bay, california', **104**, 7715–7728.

Teeter, A. M. (1987), San Francisco Bay-Alcatraz disposal site erodibility, Report 3, US Army Corps of Engineers Hydraulics Laboratory.
URL: *https://ia801501.us.archive.org/7/items/DTI_ADA181837/DTIC_ADA181837.pdf*

Thompson, C., Amos, C. & Kassem, H. (2017), *Sediment Dynamics, classnotes for SOES3014*, University of Southampton.

US Geological Survey (2017), 'National water information system (NWIS) mapper'.
URL: *https://maps.waterdata.usgs.gov/mapper/index.html?state=ca*

Valoppi, L. (2018), Phase 1 studies summary of major findings of the South Bay Salt Pond Restoration Project, South San Francisco Bay, California: U.S., US Geological Survey Open-File Report 2018-1039, US Geological Survey.
URL: *https://doi.org/10.3133/ofr20181039*

van der Wegen, M., Dastgheib, A., Jaffe, B. E. & Roelvink, D. (2010), 'Bed composition generation for morphodynamic modeling: case study of San Pablo Bay in California, USA', *Ocean Dynamics* **61**(2), 173–186.
URL: *https://doi.org/10.1007/s10236-010-0314-2*

van der Wegen, M. & Jaffe, B. E. (2014), 'Processes governing decadal□scale depositional narrowing of the major tidal channel in San Pablo Bay, California, USA', *Journal of Geophysical Research: Earth Surface* **119**(5), 1136–1154.
URL: *https://agupubs.onlinelibrary.wiley.com/doi/abs/10.1002/2013JF002824*

van der Wegen, M., Jaffe, B. E. & Roelvink, J. A. (2011), 'Process-based, morphodynamic hindcast of decadal deposition patterns in San Pablo Bay, California, 1856–1887', *Journal of Geophysical Research: Earth Surface* **116**(F2), n/a–n/a.
URL: *http://dx.doi.org/10.1029/2009JF001614*

van Kempen, O. (2017), Sediment pathways in San Francisco South Bay, Masters thesis, TU Delft.
URL: *https://repository.tudelft.nl/islandora/object/uuid%3Ae219bed5−cee3−42ba−a2f8−571539b1d66f*

van Kessel, T., de Boer, G. & Boderie, P. (2009), Calibration suspended sediment model Markermeer, Report Q4612, Deltares.

van Kessel, T., Winterwerp, H., van Prooijen, B., van Ledden, M. & Borst, W. (2011), 'Modelling the seasonal dynamics of spm with a simple algorithm for the buffering of fines in a sandy seabed', *Continental Shelf Research* **31**(10, Supplement), S124 – S134. Proceedings of the 9th International Conference on Nearshore and Estuarine Cohesive Sediment Transport Processes.
URL: *http://www.sciencedirect.com/science/article/pii/S0278434310001226*

van Maren, B. (2013), An introduction to cohesive sediment transport modelling, Presentation, Deltares Community Wiki.
URL: *http://oss.deltares.nl/web/delft3d/community-wiki/-/wiki/Main/Background+theory+cohesive-fine+sediment-mud*

van Rheenen, N. T., Wood, A. W., Palmer, R. N. & Lettenmaier, D. P. (2004), 'Potential implications of PCM climate change scenarios for Sacramento–San Joaquin River Basin hydrology and water resources', *Climatic Change* **62**(1), 257–281.
URL: *https://doi.org/10.1023/B:CLIM.0000013686.97342.55*

van Rijn, L. C. (1993), *Principles of sediment transport in rivers, estuaries and coastal seas*, Amsterdam: Aqua Publications.

van Straaten, L. M. J. U. & van Kuenen, P. H. (1958), 'Tidal action as a cause of clay accumulation', *Journal of Sedimentary Research* **28**(4), 406.
URL: *http://dx.doi.org/10.1306/74D70826-2B21-11D7-8648000102C1865D*

van Straaten, L. & van Kuenen, P. (1957), 'Accumulation of fine grained sediments in the Dutch Wadden Sea', **19**.

Velegrakis, A., Gao, S., Lafite, R., Dupont, J., Huault, M., Nash, L. & Collins, M. (1997), 'Resuspension and advection processes affecting suspended particulate matter concentrations in the central English Channel', *Journal of Sea Research* **38**(1), 17 – 34.
URL: *http://www.sciencedirect.com/science/article/pii/S1385110197000415*

Verney, R., Lafite, R. & Brun-Cottan, J.-C. (2009), 'Flocculation potential of estuarine particles: The importance of environmental factors and of the spatial and seasonal variability of suspended particulate matter', *Estuaries and Coasts* **32**(4), 678–693.
URL: *https://doi.org/10.1007/s12237-009-9160-1*

Walters, R. A. (1982), 'Low-frequency variations in sea level and currents in south San Francisco Bay', *Journal of Physical Oceanography* **12**(7), 658–668.
URL: *https://doi.org/10.1175/1520-0485(1982)012<0658:LFVISL>2.0.CO;2*

Walters, R., Cheng, R. & Conomos, T. (1985), 'Time scales of circulation and mixing processes of San Francisco Bay waters', *Hydrobiologia* **129**(1), 13–36.
URL: *https://pubs.er.usgs.gov/publication/70012828*

Wells, G. P. (1962), 'The warm-water lugworms of the world (Arenicolidae, Polychaeta)', *Proceedings of the Zoological Society of London* **138**(3), 331–353.
URL: *https://onlinelibrary.wiley.com/doi/abs/10.1111/j.1469-7998.1962.tb05703.x*

Winterwerp, J. & van Prooijen, B. (2016), *Sediment Dynamics, classnotes for CIE4308*, Delft University of Technology.

Zimmerman, R. C., Reguzzoni, J. L. & Alberte, R. S. (1995), 'Eelgrass (Zostera marina l.) transplants in San Francisco Bay: Role of light availability on metabolism, growth and survival', *Aquatic Botany* **51**(1), 67 – 86.
URL: *http://www.sciencedirect.com/science/article/pii/030437709500472C*
report

Appendix A

Bed Shear Stresses

The bed shear stresses used in calculating erosion and sedimentation in DELWAQ were calculated in Pubben (2017)'s and van Kempen (2017)'s D-FLOW model. Since the bed shear control vertical sediment exchange between the bed and the water column, an overview of how they were calculated is provided here. Bed shear stresses induced by waves and by currents interact nonlinearly, thus their combined effect cannot be determined by adding the individual components ($\tau_b \neq \tau_{current} + \tau_{wave}$). Additional turbulence generated by waves is "seen" by flow as extra bottom roughness. Several complex models have been developed to characterize the bottom boundary layer under combined waves and currents. Soulsby et al. (1993) parameterized eight of these methods, thus simplifying their application to numerical modelling schemes.

$$\tau_{b,total} = Y\,(\tau_{current} + \tau_{wave}) \tag{1}$$

$$\tau_{current} = \frac{\rho \cdot g}{C_D^2} \cdot U_{flow}^2 \tag{2}$$

$$\tau_{wave} = 0.5\rho f_w \cdot U_{orb}^2 \tag{3}$$

Here, Y represents a paramaterization by Soulsby et al. (1993) of the wave-current interaction model developed by Fredsøe (1984). The friction factor is calculated according to Swart (1974):

$$f_w = \begin{cases} 0.3, & r \leq \pi/2 \\ 0.00251, \cdot exp\left(5.21 \cdot r^{-0.19}\right) & r > \pi/2 \end{cases} \tag{4}$$

with:

C_D = Manning coefficient
f_w = friction factor
$r = A/k_s$ = relative roughness height
$A = U_{orb}T/2\pi$ = semi-orbital excursion $[m]$
$k_s = 30z_0$ = Nikuradse roughness $[m]$
z_0 = roughness length [m]

The total bed shear stresses calculated by the D-FLOW model are used as input for the DELWAQ model.

Appendix B

Modelling Flocculation in DELWAQ

As explained in Chapter 3, the settling velocity of cohesive sediments cannot be directly linked to the size of individual grains due to flocculation and the influence of temporal and spatially varying water properties. In DELWAQ, the user-defined settling velocity of each fraction of sediment is adjusted to account for the dependence of flocculation on temperature, salinity, and suspended solids concentration Deltares (2016*a*).

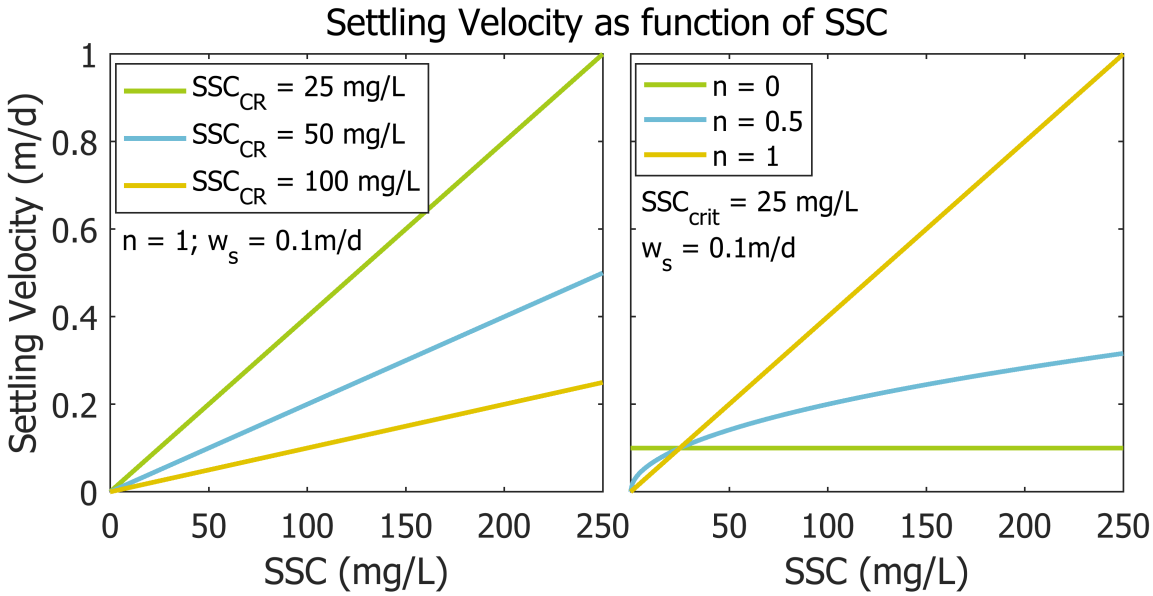

Figure 3: The dependency of settling velocity on SSC for different critical SSC values (left) and different concentration coefficients (right) in DELWAQ. The sedimentation velocity shown here is a function of only suspended solid concentration; no salinity or temperature effects are included.

The settling velocity of each fraction is calculated in DELWAQ as follows, and the dependency on salinity and sediment concentration is shown in figures 3 and 4.

$$\omega_{s,i} = f_{temp} \cdot f_{sal} \cdot f_{conc} \cdot \omega_{0,i} \tag{5}$$

$$f_{temp} = kt^{T-20} \tag{6}$$

$$f_{sal} = \frac{a_i + 1}{2} - \frac{a_i - 1}{2} \cdot \cos\left(\frac{\pi \cdot S}{S_{max}}\right) \tag{7}$$

$$f_{conc} = \left(\frac{SSC}{SSC_{cr}}\right)^{n_i} \tag{8}$$

with:

$\omega_{0,i}$ = user-defined settling velocity $[m/d]$
a_i = coefficient for flocculation enhancement $[-]$
kt = temperature coefficient for settling $[-]*$

Cs = SSC $[gm^{-3}]$
C_{crit} critical SSC $[gm^{-3}]*$
n_i = constant for concentration effect on flocculation $[-]*$
S = salinity $[PSU$ or $g/kg]$
S_{max} = maximum of salinity function $[m]$
T = water temperature $[^oC]$
i = substance index

Parameters marked with $(*)$ above can be altered by users to steer the dependency of settling velocity and flocculation on temperature and sediment concentration. For example, if n_i is less than one, this simulates a hindered settling regime, where increasing sediment concentration impedes downward settling and the fall velocity is lowered. If n_i is defined to be greater than one, this represents the case where increased sediment concentration increases the likelihood that particles will collide and aggregate. As a result, flocculation rates increase, leading to a higher fall velocity.

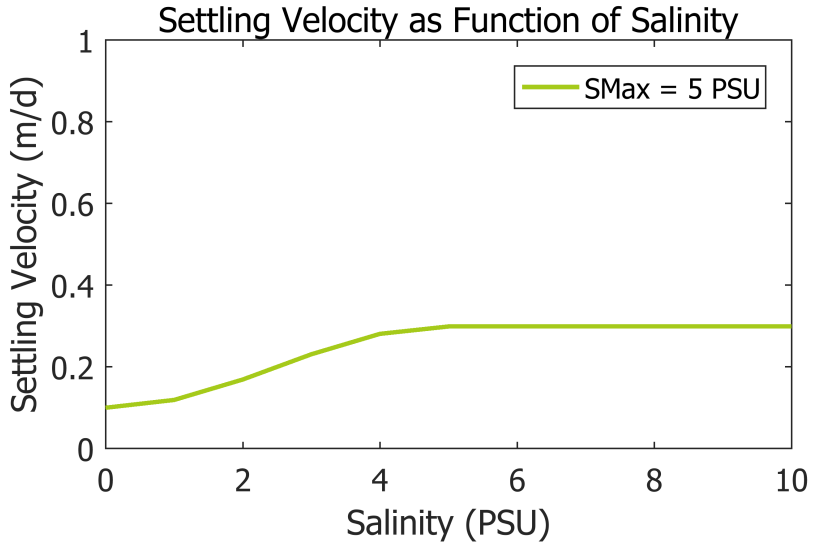

Figure 4: Settling velocity as a function of salinity only; the effect of sediment concentration and temperature are not considered.

Appendix C

Mud Parameter Sensitivity

Here, the impact of altering each parameter that was tuned during the model calibration is shown. Each plot shows the modelled SSC timeseries over one year (WY 2015) and one week in March to resolve model sensitivity on shorter timescales. In general, tuning the mud parameters impacted the magnitude of SSCs, but not the phasing of SSC fluctuations.

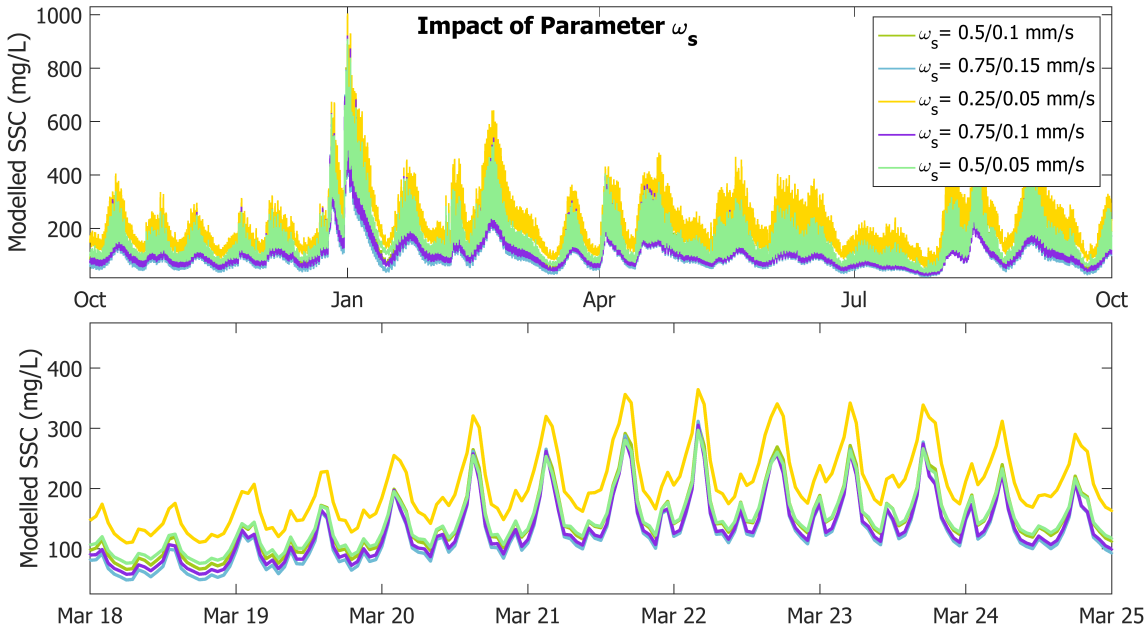

Figure 5: Model sensitivity to sediment fall velocities of both mud fractions.

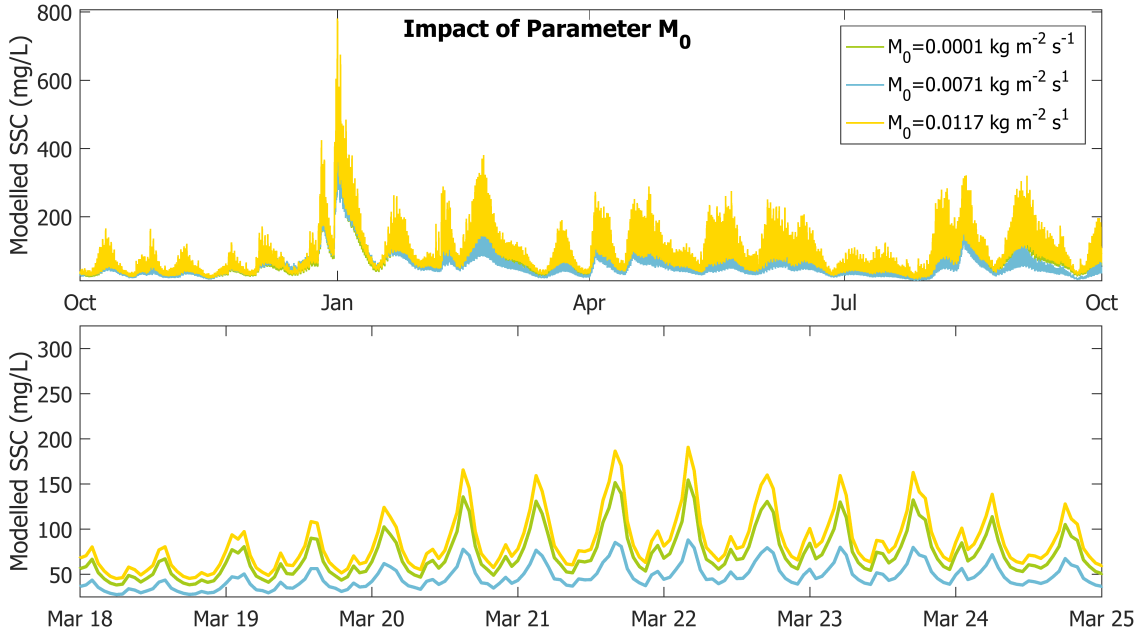

(a) Model sensitivity to zeroth order erosion parameter for the fluffy layer.

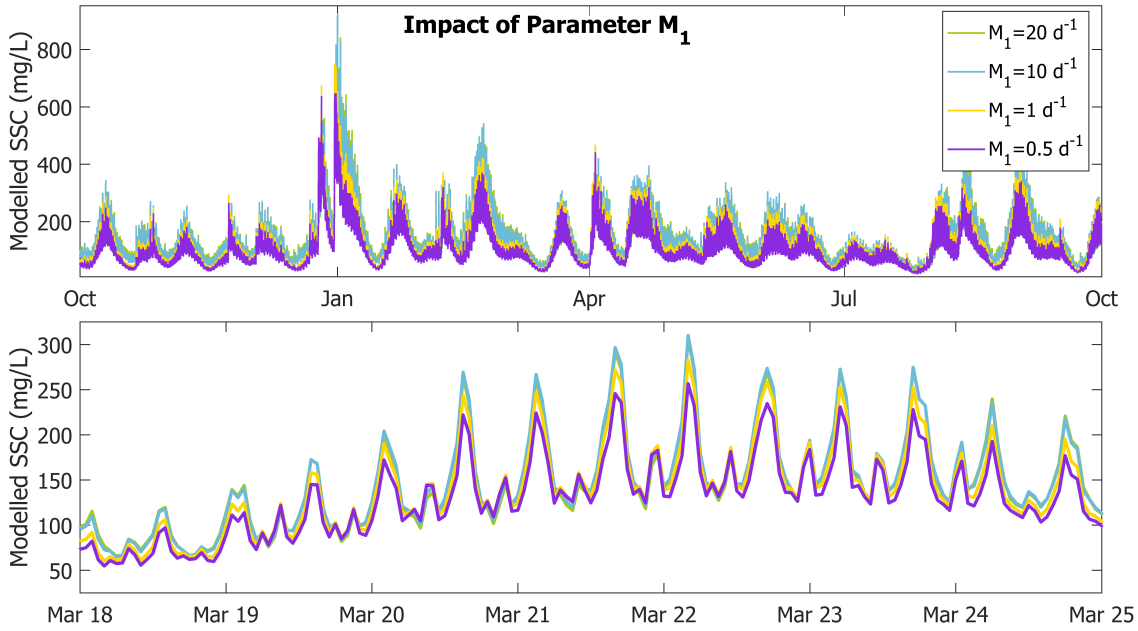

(b) Model sensitivity to first order erosion parameter for the fluffy layer.

Figure 6: Model sensitivity to parameters governing resuspension from the fluffy layer.

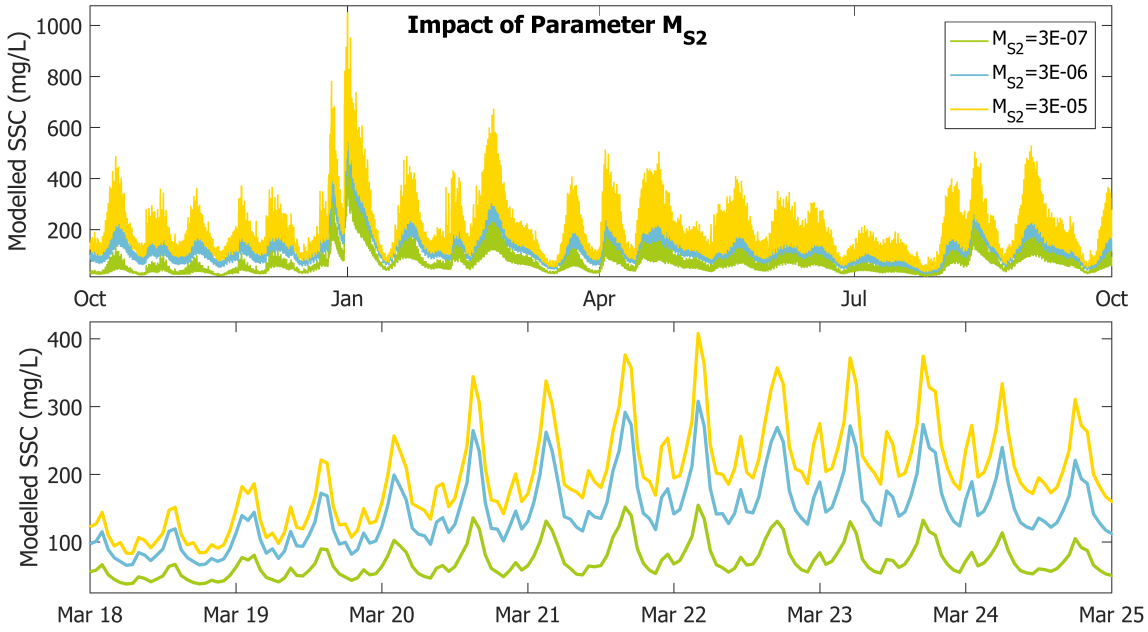

(a) Model sensitivity to erosion parameter for the buffer layer.

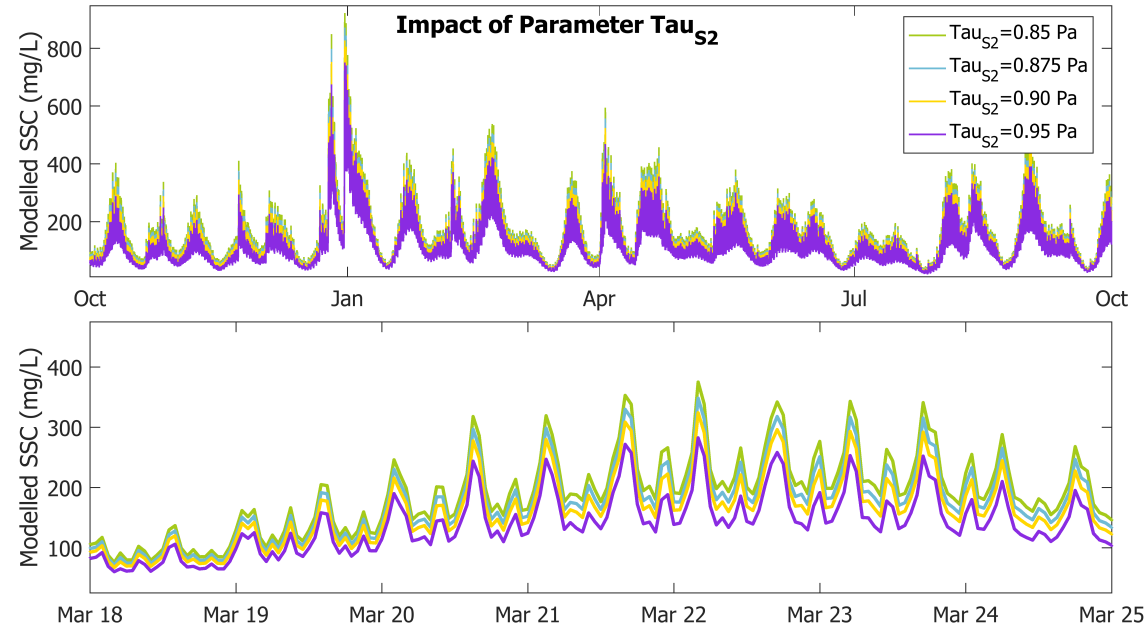

(b) Model sensitivity to critical shear stress of the buffer layer.

Figure 7: Model sensitivity to parameters governing resuspension from the buffer layer.

Appendix D

DELWAQ Cross-sections

Transects in DELWAQ are defined as continuous vertical surfaces across which fluxes are measured. Due to the nature of the unstructured model grid, the direction of positive flow is not defined positive in the same direction for each computational volume. Therefore, each transect consisted of two sub-transects: one consisting of cells defined positive in direction A→ B and the other defined positive in direction B→A. The flux for each timestep across each cross-section was calculated by taking the difference between the fluxes measured by the sub-transects corresponding to each direction.

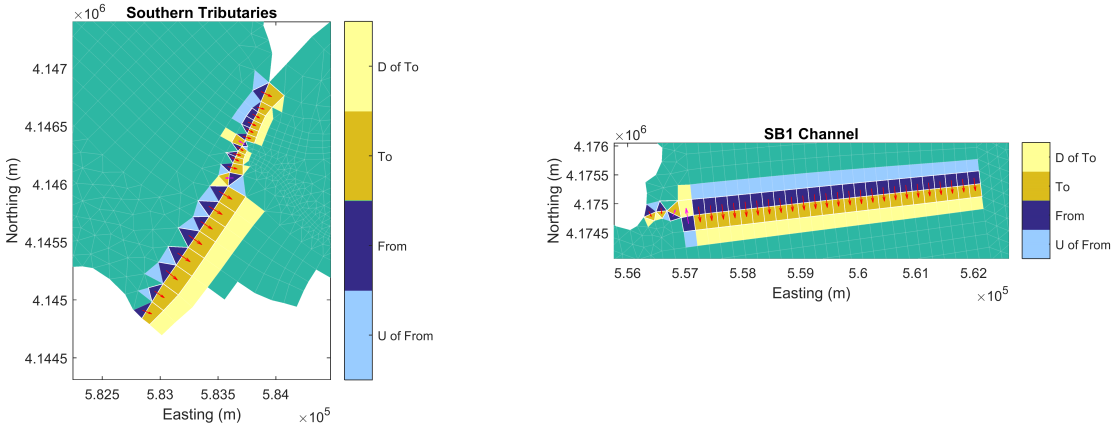

Figure 8: Visual example of how transects are created in DELWAQ. Each individual exchange surface is defined by the following 4 segments: To, From, Downstream of To (D of To), and Upstream of From (U of From).

To study sediment fluxes at different depths in the water column, for each transect a monitoring cross-section for each vertical layer was defined. As the DELWAQ model applied in this research had 10 vertical layers, and each transect needed to be defined for two directions, a total of 20 cross-sections were defined in the DELWAQ input file for each transect defined in the model. The process of creating a monitoring cross-section extending over the entire water column and calculating sediment fluxes based on model output is shown in Figure 9.

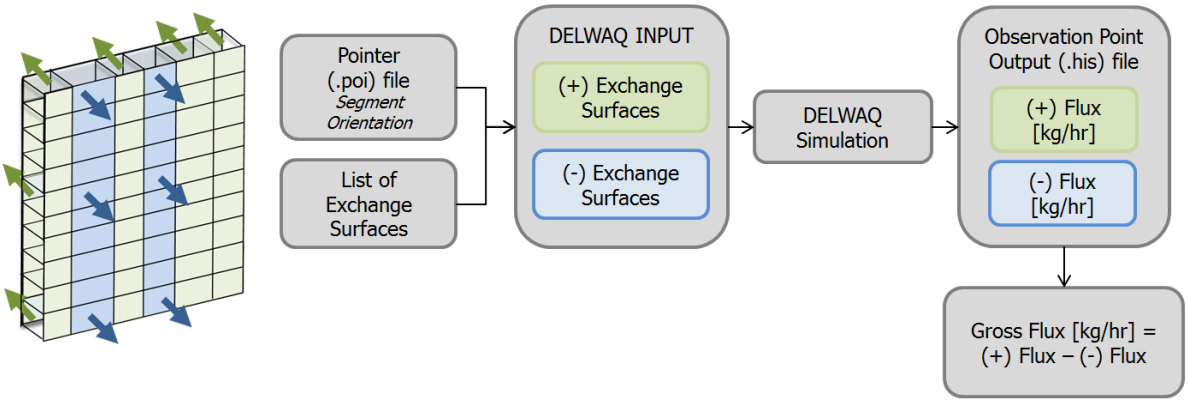

Figure 9: Simplified pre- and post-processing workflow diagram for creation of a transect and calculation of hourly sediment flux across cross-section for an unstructured grid in DELWAQ.

The pointer (.poi) file contains information on the orientation of each segment by defining the ”to,” ”upstream of to,” ”from,” and ”downstream of from” segment numbers, and is used to separate the list of exchange numbers into two sub-transects: one oriented in the arbitrarily defined (+) direction, and one oriented in the arbitrarily defined (-) direction. These are defined as two separate monitoring areas in the DELWAQ input. The DELWAQ simulation will output a .his file, containing information for each monitoring area and observation point. The difference between the (+) and (-) sediment flux for each time step is equal to the gross flux [mass/time step].